JELENA TADIC, BSc

Yeast as model to study Alzheimer's disease

Investigating A42 cytotoxicity in yeast

Master's Thesis

Graz University of Technology

Institute of Molecular Biosciences

Supevisor
Univ.-Prof. Dr.rer.nat Frank Madeo

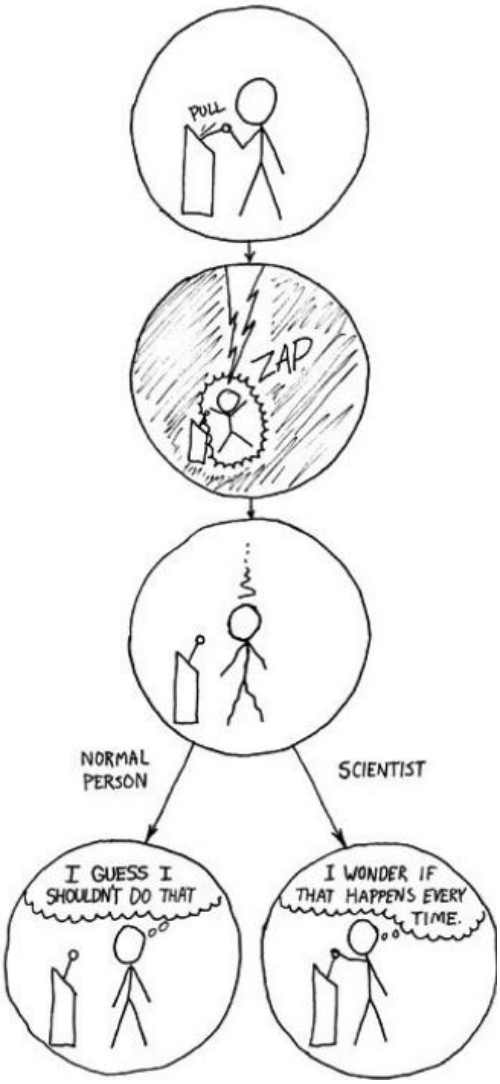

ZA MOJE RODITELJE

I declare that I have authored this thesis independently, that I have not used other than the declared sources/resources, and that I have explicitly marked all material which has been quoted literally or by content from used sources.

Graz, March 2013

Acknowledgments

First of all, I would like to thank Univ.-Prof. Dr Frank Madeo for giving me the opportunity to work in his lab group. I am glad that I had such a great professor as my supervisor.

Julia, thank you for everything you have done for me. Even though, I had so many difficulties at the beginning of my master thesis, you have never stopped trusting in me. During this work I had your full support, you were always there for me and always ready for our long discussions, which made this work even more interesting and motivating for me. Thank you for all advice and everything I have learned from you.

Of course, I want to thank you, Betti. We were the best group ever! Thank you for the precious time we spend together in the lab and your support. It was always fun working with you. We did some awesome work in the lab. I want to thank, as well you, Babsi for all your help, support and patience you gave to me and Betti. I want to thank all of my "Perlen" for the great time we spent. You made my every single day spent in the lab. I will never forget our salad sessions, pizza nights, poker nights, zotter and all the fun we had outside of the walls of our institute. Thank you my dear friends, Lena, Kathi, Marion, Jutta, Schatz, Hipster, Betti and of course Tobi for all of our crazy and special moments. I want to thank, of course all lab members of Madeo and Fröhlich group, it was great working with you. Thank you Lukas, Slaven, Andi, Brini, Alex, Vera, Didac, Patrick… for all your support and fun we had. I also want to thank Dirk Mossmann and Chris Meisinger for giving me the opportunity to work with them in Freiburg and for giving me the chance for improving my practical skills. I want to thank all members of Pfanner and Meisinger lab group who made my stay in Freiburg unforgettable and more easy than expected.

I want to thank you Chris, for everything you have done for me, for motivating me, for supporting me, for being there for me in bad and good times. I would not have come so far without you.

Posebno se zahvaljujem svima vama sto ste me podrzali u Grazu, a posebno svojim prijicama iz Banja Luke. Cito, Tico, Tina, Leno, Darko, Ogi hvala vam za podrusku i jer ste sve ove godine uvijek bili tu za mene.

Naravno, najvece hvala za mamu, tatu, Natasu, bake i dede. Hvala vam sto ste bili uz mene, za svu ljubav sto ste mi pruzili, sto ste me podrzali u svemu i nikad prestali da vjerujete u mene.

Abstract

Alzheimer´s disease (AD) is an age-associated neurodegenerative disorder with over 36 million people worldwide affected. It is associated with brain shrinkage due to neuronal cell death which is reflected by gradual changes in behavior and intellect, as well as loss of memory. The two pathological hallmarks are the extracellular plaques and intracellular neurofibrillary tangles. The plaques are mainly consisted of the amyloid-beta (Aβ) peptides which vary in length. Beside the extracellular plaques, intracellular Aβ became the focal point of AD and cell death research. Recent studies demonstrate that intracellular Aβ genesis and accumulation to soluble oligomeric species are crucial events in AD development and progress. Referring cell death pathways and key players, the mitochondria are an important component of the AD pathogenesis. It has been shown, that Aβ is able to trigger dysfunction of the mitochondria by interaction with mitochondrial proteins, leading to elevation of ROS (reactive oxygen species) levels or disorganization of the respiratory chain.

In our work we used yeast as a model for aging post mitotic neurons. Aim of this study was to investigate the pathogenic pathways associated with Aβ using our developed AD yeast model.

We could show that Aβ causes toxicity in yeast by accumulation of ROS. Further, a screen of potential key players in Aβ mediated toxicity revealed a few proteins, which are mainly part of mitochondrial transport, respiration and chaperon network. We investigated two chaperons and could show that they influence Aβ aggregation and its translocation. Further, we could detect Aβ oligomers at mitochondria suggesting this to be the crucial trigger to start the death cascade. With our work we were able to confirm some of the known aspects of AD as well as to show new findings. Our work may yield results leading to better understanding of molecular mechanisms of Aβ related toxicity at least with respect to the involved cell death pathways.

Kurzzusammenfassung

Morbus Alzheimer (MA) ist eine altersbedingte neurodegenerative Erkrankung, die mehr als 36 Millionen Menschen weltweit betrifft. MA ist gekennzeichnet durch Hirnmassenverringerung durch Absterben von neuronalen Zellen. Dies führt zu schrittweisen Veränderung im Verhalten und Intellekt des Betroffenen sowie dem Verlust des Gedächtnisses. Extrazelluläre Plaques und intrazelluläre Neurofibrillen sind pathologische Kennzeichen von MA. Die Plaques bestehen hauptsächlich aus dem Amyloid-Beta Peptid (Aβ), das in seiner Länge variieren kann. Abgesehen von den extrazellulären Plaques sind die intrazellulären A-Beta Peptide der Mittelpunkt der MA- und Zelltodforschung geworden. Neuere Publikationen zeigen, dass die Entstehung von Aβ und die Akkumulation von löslichen oligomeren Aβ Spezies entscheidende Ereignisse in der MA Entwicklung sind. Mitochondrien sind eine wichtige Komponente der Pathogenese bei MA. Aβ ist in der Lage, durch Interaktion mit mitochondrialen Proteinen eine Dysfunktion der Mitochondrien auszulösen. Dies kann zu einer Erhöhung von ROS (reaktiven Sauerstoffspezies) oder einer Desorganisation der Atmungskette führen.

Wir haben die Hefe als Modell für Alterungsstudien an post-mitotischen Neuronen genutzt. Ziel dieser Studie war es, die pathogenen Wege, die mit Aβ in Verbindung stehen, in dem von uns entwickelten MA-Hefe-Modell zu untersuchen.

Wir konnten zeigen, dass Aβ durch die Akkumulation von ROS eine Toxizität in Hefe hervorruft. Zusätzlich wurde ein Screen von Deletionsstämmen durchgeführt. Mit Hilfe dieses Screens konnten die Proteine, die mit der Aβ vermittelten Toxizität in Verbindung stehen, identifiziert werden. Die meisten identifizierten Proteine sind am mitochondrialen Transport oder dem Hitzeschock response beteiligt. Es wurde beobachtet, dass zwei identifizierte Proteine des Hitzeschock responses die Aggregation von Aβ und seine Translokation beeinflussen können. Weiters konnten wir Aβ-Oligomere an Mitochondrien erkennen, wodurch wahrscheinlich die Zelltodkaskade ausgelöst wird. Mit unserer Arbeit konnten wir einige der bekannten Aspekte von MA bestätigen und zusätzlich neue Erkenntnisse gewinnen. Unsere Arbeit kann zum besseren Verständniss der molekularen Mechanismen der Aβ induzierten Toxizität beitragen.

Contents

1. Introduction

1.1 Programmed cell death (PCD) – under control

Programmed cell death (PCD) is highly regulated process of an active cell suicide. The cell is able to react to any change in the endogenous or exogenous conditions which can force the cell to make a molecular decision to adapt and survive or to simply die in a favor to the whole organism or even a cell population. This process is highly evolutionary conserved, observed not only in multicellular organism (*C. elegans*, *Drosophila melanogaster,* Mouse) but also in unicellular organism such as *Saccharomyces cerevisiae*. Programmed cell death is observed in embryonic development, autoimmunity, tumor tissues, in some neurodegenerative diseases and some other pathological conditions. This phenomenon was for the first time recognized as a regular process during ontogenesis by Gluecksmann in 1951 [Baehrecke, 2002; Ring *et al*., 2012; Eisenberg *et al.* 2010, Glueckmann, 1951].

Important discoveries concerning genetic regulation of organ development and programmed cell death in worms were made by H. Robert Horvitz, Sydney Brenner and John E. Sulston. For their outstanding contribution to science, they were awarded with Nobel Prize in Physiology and Medicine in 2002 [Brenner, 1972; Sulston and Horvitz, 1976; Ellis and Horvitz, 1986].

Apoptosis and necrosis were for the first time in detail described by Kerr, Wyllie and Currie in the article published in 1972. Since then the apoptosis was used as a general term for describing PCD for decades. Researches and the science community were more interested in controlled mode of cell death than an "accidental" type of cell death such as necrosis or some other alternative modes [Kerr, Wyllie and Currie, 1972].

In 1973, Schweichel and Merker classified three major modes of programmed cell death during embryonic development in three different types. The apoptosis was classified as a Type I cell death and as a type II cell death was classified autophagic death. In that time less analyzed alternative cell death modes were classified as type III cell death defined as nonlysosomal vesiculate degradation. Nowadays, cell death type III is recognized as a programmed necrosis [Schweichel and Merker, 1973].

PCD programs are genetically defined and manifested by different phenotypes. PCD phenotypes can be apoptotic like apoptosis or non-apoptotic like programmed necrosis or autophagic cell death.

These phenotypes are often overlapping which results hard distinguishing between the modes of the cell death [Ludvico, Madeo and Silva, 2005].

There are many ways of classifying cell death types such as morphologically, activation via the mitochondria or independent of this organelle, enzymological criteria (caspase independent or caspase depended) or immunological characteristics [Kroemer et al, 2009].

Nomenclature Committee on Cell Death (NCCD) is updating the recent discoveries in this field of research and is using novel data and new information to classify the programmed cell death modes. Through the unified classification of different programmed cell death modes, researches could be able to communicate easily which could accelerate discovery processes in this field. There are already three rounds of recommendations for the classification from 2005, 2009 and 2012 published in *Cell Death and Differentiation.* In 2005, Kroemer tried to answer the complicated question: "When is a cell dead". It is important to define an irreversible phase "point-of-no-return" in cells and thus, distinguish death cells from dying cells. Kroemer postulate three criteria on a morphological basis which refer to this irreversible phase. The cell is in a point-of-no-return phase only if: 1. the cell loose the integrity of plasma membrane; 2. the cell, including the nucleus undergo complete fragmentation into apoptotic bodies; 3. the corpse is engulfed by an adjacent cell *in vivo* [Kroemer *et al*, 2009; Kroemer *et al*, 2005; Wloch-Salamon and Bem, 2012].

In 2012, the recommendations for the classification were extended by including biochemical and molecular characteristics to avoid misinterpretations due to morphological overlapping characteristics between different modes. The new NCCD classification defined the cell death routines by series of precise, measurable biochemical features. These include extrinsic apoptosis, caspase-dependent or –independent intrinsic apoptosis, regulated necrosis, autophagic cell death, mitotic catastrophe and other cell death modalities, such as anoikis, entosis, parthanatos, pyroptosis, netosis and cornification [Galluzzi *et al.* 2012].

1.1.1 Apoptosis

The term "apoptosis" was suggested by Kerr, Wyllie and Currie in 1972 to describe controlled cell deletion followed by specific morphologies of cell death. In Greek this term is describing "falling off" of leaves from the tree [Kerr, Wyllie and Currie, 1972].

Apoptosis is a type of programmed cell death and it is a highly regulated process which requires energy input. Apoptosis takes part in tumor suppression, autoimmune diseases or removal of damaged and potentially dangerous cells, such as cells infected by viruses. Moreover, this is a

natural process which takes part in forming and deleting structures during development, as well as a crucial process for controlling cell numbers [Baehrecke, 2002]. Additionally, apoptosis is observed in neurodegenerative diseases, AIDS as well as ischemic stroke which are result of abnormalities in apoptosis regulation. This type of cell suicide is quick and efficient without inducing any immune response. Reason for that are membrane-bound fragments which prevent spillage of intracellular contents within intercellular space [Madeo *et al*, 1997; Wloch-Salamon and Bem, 2012; Woodle and Kulkarni, 1998].

Kerr, Wyllie and Currie described apoptosis morphologically as a process divided in few important steps, which consider cell and nuclear condensation, fragmentation into membrane-bound fragments and uptake of apoptotic bodies by other cells which are able to perform a lysis of these fragments [Kerr, Wyllie and Currie, 1972]. Following years more morphological characteristics were observed, such as ROS accumulations [Yang *et al*., 1998], DNA cleavage between nucleosomes [Wyllie, 1980] or exposure of phosphatidylserine on the cell surface important for the macrophage uptake [*Martin et al*., 1995].

However, during investigation of DNA changes in different epithelial cell lines, which demonstrated clear apoptotic characteristics, the typical DNA ladders of DNA fragmentations were not always observed [Oberhammer *et al*., 1993]. This was clear evidence that there are distinct subtypes of apoptosis which are morphologically similar, but however triggered by different biochemical routes. For instance, apoptosis can be either induced by extracellular stress signals, (extrinsic apoptosis) which can be sensed by specific transmembrane receptors [Mehlen and Bredesen, 2011] or through intracellular stress conditions (intrinsic apoptosis) such as DNA damage, oxidative stress or cytosolic Ca^{2+} overload or accumulation of unfolded protein in ER. Similar to DNA degradation, caspase activity is also not strictly required for execution of cell death pathway [Lockshin and Zakeri, 2002]. Therefore, intrinsic apoptosis can be based on caspase-dependent or caspase-independent mechanism [Galluzzi *et al.* 2012].

1.1.1.1 Apoptosis in mammals

Apoptosis regulation can differ depending on tissues, development state or organism. This program is regulated by diverse proteins such as caspases, Bcl-2 family proteins, several nucleases or effector proteins released by mitochondria. Caspases are one of the most important key players in apoptosis induction which are evolutionary conserved and possess an active-site cysteine. They cleave their substrates always after aspartate residues and there are more than 100 reported caspase substrates

such as key cellular proteins. Proteins in Bcl-2 family have pro- or anti-apoptotic activities and they contain one or more Bcl-2 homology (BH) domains. The anti-apoptotic proteins include Bcl-2 like 1 (Bcl-XL), Bcl-2 like 2 (Bcl-w), Bcl-2 related protein A1 (Bfl-1) and myeloid cell leukemia-1 (Mcl-1). These proteins contain mostly BH domains 1-4.The pro-apoptotic proteins such as Bax and Bak contain BH 1-3 domains. BH-3 only proteins are also pro-apoptotic proteins which cause activation of Bax and Bak at mitochondria and can be activated by DNA damage, oncogene activation or some other noxious stimuli. Mitochondria have a central role in induction of apoptosis and can release some pro-apoptotic proteins such as cytochrome c, AIF or Smac/DIABLO.

As already mentioned, there are various pathways for induction of cell destruction. Extrinsic apoptosis can be regulated through binding of lethal ligands to death-receptor super family receptors. One of these ligands is CD95L which can bind to the death receptor CD95. As a result, CD95 recruit pro-caspase-8 and FAS-associated protein with death domain (FADD). This complex is called death inducing signaling complex (DISC). The activation of caspase-8 can be inhibited by c-FLIP, degenerate caspase homologue. As a result of caspase-8 activation, the caspase cascade is induced. The caspase 3 is activated by Caspase-8 and apoptosome (Cytochrom c, Apaf-1, dATP and Pro-caspase-9), which is able to execute apoptosis by caspase-activated DNase (CAD) or by cleavage of some other apoptotic substrates. Second pathway influenced by activated caspase 8 involves stimulation of the mitochondrial outer membrane permeabilization (MOMP) by cleaving the BH3-only protein BID. Together with pro-apoptotic protein Bax, which is regulated by p53, BID promotes cytochrome c mitochondrial exit. This pathway can be inhibited by Bcl-XL protein. Cytochrome c is able together with Apaf-1 and pro-caspase-9 to build apoptosome which is involved as already mentioned in caspase 3-activation. The caspase 3-activation through BID is a cross-talk between death-receptor- and mitochondrial pathway, extrinsic- and intrinsic pathway, respectively.

The mitochondria are a central control mechanism during intrinsic apoptosis. As a consequence of cell reaction to intracellular stress, MOMP occurs. MOMP influences mitochondrial transmembrane potential dissipation, as well as an arrest of mitochondrial ATP synthesis. Reactive oxygen species (ROS) production is also affected and it comes to the over generation of ROS. Some of the proteins which are normally confined within the mitochondrial intermembrane space can exit the mitochondria such as, cytochrome c, IAP binding protein (DIABLO), HTRA2, apoptosis inducing factor (AIF) and endonuclease G (ENDOG). DIABLO and HTRA2 are able to degrade some of the inhibitor of apoptosis proteins. AIF and ENDOG are responsible for DNA degradation and they are able to enter nucleus. Secondly they function in caspase-independent manner. The overview of the pathways can be seen in the Figure 1.1 [Galluzzi *et al*., 2012; Brunelle and Letai, 2009; Hengartner, 2002].

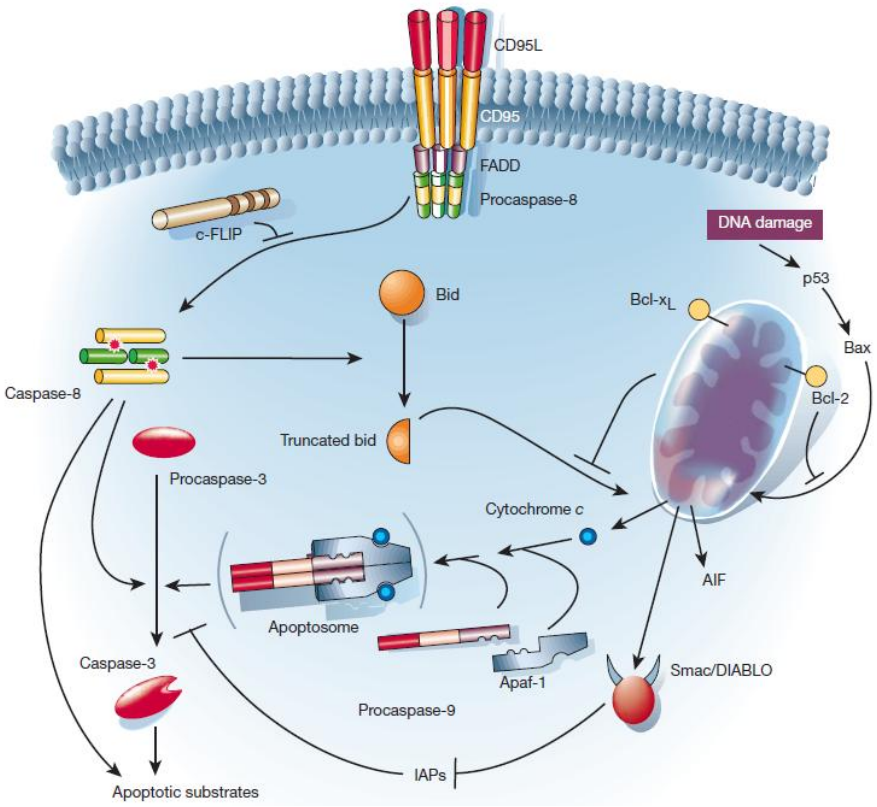

Figure 1.1; Two major apoptotic pathways in mammalian cells. Extrinic and intrinsic apoptosis. Extrinic apoptosis is regulated through extracellular signals which are sensed by cell death receptors, such as CD95. After detection of the signal a ligand CD95L binds to CD95 and recruits pro-caspase-8 and FAS-associated protein with death domain (FADD). Caspase-8 is activated and caspase cascade is induced. Initially, the caspase 3 is activated by Caspase-8 and Apoptosome (Cytochrom c, Apaf-1, dATP and Pro-caspase-9) which is an executor caspase of apoptosis. Caspase 8 also influences stimulation of the mitochondrial outer membrane permeabilization (MOMP) by cleaving a protein BID. BID and a pro-apoptotic protein, Bax promote cytochrome c mitochondrial exit. This pathway can be inhibited by Bcl-XL protein. Cytochrome c can regulate the caspase-3 activation by creating an apoptosome together with Apaf-1 and pro-caspase-9. Intrinsic apoptosis is a consequence of a cell reaction to intracellular stress. Consequently, the MOMP, mitochondrial transmembrane potential dissipation, ROS overproduction and arrest of mitochondrial ATP synthesis occur. Additionally, diverse molecules can exit the mitochondria such as, cytochrome c, IAP binding protein (DIABLO), HTRA2, apoptosis inducing factor (AIF) and endonuclease G (ENDOG). The activation of caspase 3 is a cross-talk between these two pathways [Hengartner, 2002].

1.1.1.2 Apoptosis in Yeast

Apoptosis is an evolutionary conserved process present in higher organism, C. *elegans*, plant kingdom [Pennell and Lamb, 1997], unicellular eukaryotes [Madeo, 1997] or even bacteria [Lewis, 2000]. In multicellular organisms, possessing this process gives many advantages such as elimination

of dangerous or damaged cells or forming and deleting structures during tissue development or embryogenesis. Function of apoptosis in unicellular organism is not yet clear. However, there are some evidences and physiological scenarios of the yeast apoptosis which could explain possible evolutionary advantages for this unicellular organism [Buettner *et a*l., 2006].

It was demonstrated that the yeast can induce apoptosis to eliminate infertile cells, due to the fact that the successful mating can prevent apoptosis and that during failed mating, mating-type pheromones can induce apoptosis. Through this evolutionary decision, the yeast favors diploid state over haploid state for better adaptive possibilities [Severin and Hyman, 2002]. Similarly, it was shown that the apoptosis can be induced after successful mating to ensure that only cells with genetic recombination which are more adaptive to environment, survive [Ahn, *et al*, 2005b]. *S. cerevisiae* is able to form biofilms in laboratory as well as in natural environment. In such circumstances, apoptosis removes selectively the oldest cells from the population. In this way, survival of the clone or younger cells is enabled. The oldest cells after apoptosis do not consume the nutrients which are spared for the younger cells. Additionally, it was determined that the older cells through dying release substances which promote survival of the younger cells [Fabrizio *et al*., 2004]. These and many other scenarios reveal why yeast cells can undergo apoptosis [Buettner *et a*l., 2006].

Madeo described for the first time yeast apoptosis in *S. cerevisiae* in 1997 by analyzing a yeast mutant *CDC48* which showed several apoptotic morphologies such as externalization of phosphatidylserine, DNA fragmentation, chromatin condensation or potential apoptotic bodies [Madeo *et a*l., 1997]. Since then many yeast orthologues of mammalian apoptotic proteins were described. Novel discoveries using yeast as a model improved understanding in cell death pathways as well as in its regulation on proteosomal, mitochondrial or epigenetically level.

A yeast metacaspase YCA1 was identified to be involved in oxidative stress-induced cell death by Madeo in 2002. YCA1 overexpression lead to cell death followed by apoptotic markers and a deletion of the same protein rescued the cells from apoptosis during a chronological aging [Madeo *et a*l., 2002]. Metacaspases are caspase-releated family together with caspases and paracaspases [Uren *et a*l., 2000]. Even though these proteins do not share the same cleavage specificity, a shared functional substrate cleaved by metacaspases and caspase-3 was identified by Bozhkov. Therefore, yeast possesses an ortholog of mammalian caspases [Carmona-Gutierrez *et a*l., 2010].

Nevertheless, a yeast cell death can be induced independently of YCA1 in caspase-independent manner. Yeast caspase-independent apoptosis can be induced by apoptosis-inducing factor Aif1p, a

yeast ortholog of mammalian AIF or Nuc1p, a yeast ortholog of mammalian EndoG [Wissing *et a*l., 2004; Buettner *et a*l., 2007; Carmona-Gutierrez *et a*l., 2010].

Another yeast homolog of the proapoptotic mammalian HtrA2/Omi, which was described is a nuclear mediator of apoptosis Nma111p. In contrast to Htr2A/Omi which is localized in mitochondria in mammalian cells, Nma111p is localized in the nucleus in yeast cells. This protease is able to cleave the yeast inhibitor-of-apoptosis, Bir1p. Additionally, Nma111p deletion reduces cell death [Fahrenkrog *et a*l., 2004].

In addition, in 2011, it was reported that yeast genome encodes a BH3 domain containing protein (Ybh3). It was suggested, that this protein regulates mitochondrial pathway of apoptosis, similar like proteins with BH3 domain in eukaryotes [Büttner *et al.,* 2011].

Some other mediators of yeast cell death were uncovered, such as Ndi1p, Nde1p, Dnm1p, Ste20p or Mmi1p. These proteins are involved in mitochondrion-associated induction of cell death, histone H2B phosphorylation or mitochondrial fragmentation [Carmona-Gutierrez *et a*l., 2010].

Small signaling molecules such as ROS, NO and ammonia are also essential components of apoptotic cell death network. ROS play a central role in most of the apoptotic known pathways and it accumulates in yeast cells after apoptotic induction [Madeo *et a*l., 1999]. The network of the known apoptotic pathways in yeast can be seen in the Figure 1.3.

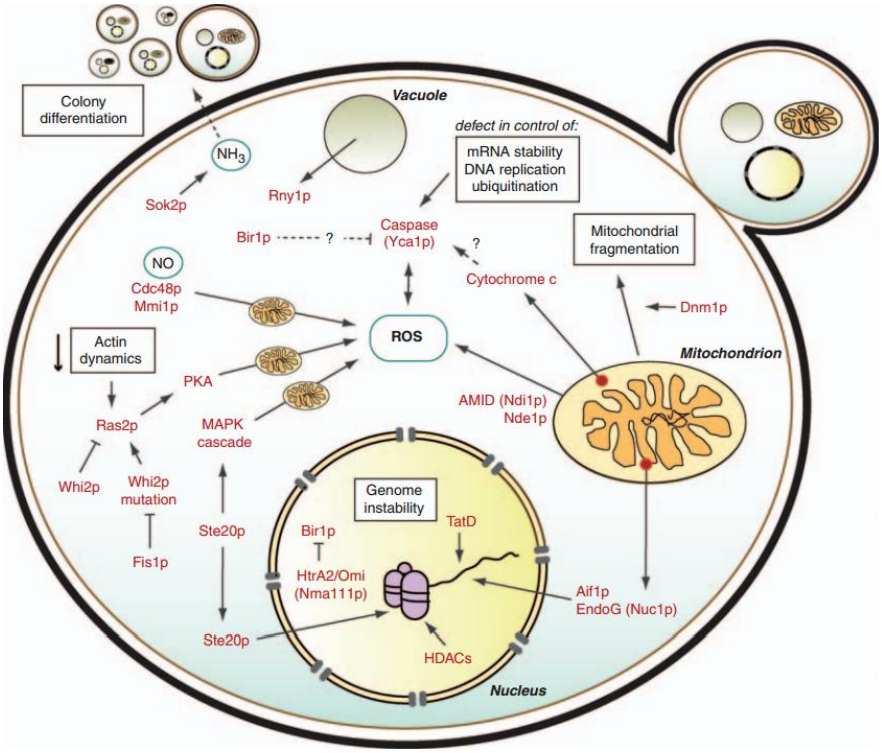

Figure 1.2 Yeast apoptosis pathways. Crucial yeast cell death regulators involve metacaspase (Yca1p), nuclear mediator of apoptosis (Nma111p), apoptosis inducing factor (Aif1p), NADH dehydrogenase (Ndi1p, human homolog AMID), Nde1p, a yeast homolog of dynamin related protein-1 (Drp1), a yeast homolog of EndoG (Nuc1p). In addition, small signaling molecules take part in yeast apoptosis, such as ROS, NO and ammonia [Carmona-Gutierrez *et a*l., 2010].

1.1.1 Necrosis

Since the first description of programmed cell death, necrosis was considered as an accidental "chaotic" cell death mode [Kerr, Wyllie and Currie, 1972]. Described for the first time in detail in 1988 by Walker, necrosis was morphologically characterized by swelling of the organelles, plasma membrane rupture and increase of the cell volume, also called oncosis [Walker *et a*l., 1988]. During necrosis, cells also release factors which can stimulate an immune response. Contrarily, apoptosis is a well-organized and "clean" process, without spillage of the cell material into the extracellular space. However, recently, in programmed cell death research, a new chapter was opened. New data are accumulating based on hypothesis that necrosis might be regulated on a certain level. It was observed that genetic manipulation of some proteins prevented or enhanced necrotic cell death. It was also shown that multiple factors can trigger necrosis. Not only is the induction of necrosis possible through brutal chemical or physical torture, but it also occurs during normal physiological conditions, such as mammalian development or adult tissue homeostasis. This type of cell mode death also occurs in some pathological conditions such as ischemia, neurodegeneration (Alzheimer's disease, Huntington's disease or Parkinson's disease) or infection [Syntichaki and Tavernarakis, 2003]. Acetic acid and H_20_2, well known cell death inducers, induce apoptosis in low concentrations but in higher concentrations trigger rather the necrotic cell death [Ludvico *et a*l., 2001]. When caspases are inhibited, the ligation tumor necrosis factor receptor 1 leads to so called necrosome assembly which has a pronecrotic function. This complex contains receptor-interacting protein kinases 1 and 3 (RIP1 and RIP3). Other important necrosis regulators and key players were found using diverse programmed necrosis model organisms, such as *C. elegans*, *D. discoideum* or *S. cerevisiae* [Galluzzi, 2011]. Some of the first genetic evidences that specific cystein proteases, calpains and cathepsins, are involved in necrosis were discovered in *C. elegans* [Syntichaki *et a*l., 2002]. In mammals calpains are responsible for lysosomal membrane permeabilization upon Ca^{2+} overload stimulating CathD release. Yeast homolog is a Cpl1p, a calpain-like cystein protease which is able to activate Rim101p. Cathepsins, lysosomal proteases are involved in some necrotic scenarios. Their yeast homolog is Pep4p, a vacuolar aspartyl protease. Using *C. elegans* as a model system,

specific ion channel proteins, also called degenerins, DEG-1 and MEC-4 were characterized. Through the constitutively activation of these ion channels it comes to Ca^{2+} overload and necrotic degeneration of specific groups of neurons. Furthermore, during yeast necrosis some biological changes were observed, such as mitochondrial outer membrane permeabilization, dissipation of mitochondrial potential, ATP depletion as well as over generation of ROS. In addition, the cells release Nhp6Ap from the nucleus, a yeast homolog of mammalian high mobility group box-1 protein (HMGB1). Peroxisomal and vacuolar functions can inhibit yeast necrosis, due to their roles maintaining intracellular pH and ROS homeostasis [Galluzzi, 2011; Eisenberg *et a*l., 2010; Scaffidi *et a*l., 2002].

1.2 Alzheimer's disease

Aging is one of the greatest risk factors for neurodegenerative diseases. Life expectancy dramatically increased in the last century. Therefore, people are achieving the age at which neurodegenerative disorders occur frequently. One of the most common forms of dementia is Alzheimer's disease (AD). The neuropathological characteristics in the brain of Alzheimer's patients are neuron loss in the regions that are responsible for storing and cognition, as well as neurotransmitter depletion, oxidative stress, neuroinflammation, synaptic changes and the deposition of two types of protein aggregates. In early stage, this disorder is characterized by loss of short term memory and disorientation. As the disease progress, patients are not able to make judgment, communicate, take care of themselves or reason clearly. Additionally, they show aggression, mood swings, problems with attention, trouble with language and long-term memory loss. In the last stage of disease it comes to malnutrition, brain death or organ failure which can lead to the death of the afflicted person [Prasansukllab and Tencomnao, 2013, Zahs and Ashe, 2013].

This defect was for the first time described by Dr. Alois Alzheimer in 1906. The patient, Auguste D., was showing changes in her personality, disorientation and symptoms of memory loss. After her death, her brain was pathologically examined by Alzheimer. Brain preparations exhibited the characteristics of what is nowadays known as Alzheimer's disease. These features include neuronal loss, extracellular amyloid plaques and intracellular neurofibrillary tangles [Alzheimer *et al*., 1907].

Currently, there are several diseases caused by accumulation of amyloid deposits in the various tissues, such as to Alzheimer's disease, Parkinson's disease, Huntington's disease, secondary amyloidosis and type II diabetes. The common features of these diseases are misfolding of proteins, aggregation and precipitation of otherwise normal proteins.

Nowadays, 10 % of the population over 65 years and 50 % of the population over 85 years suffer from this neurodegenerative disorder, an estimated 24 to 35 million people worldwide. The number of afflicted person is increasing rapidly and by 2050, 1 of 85 will be living with this disease because of the prolongation of life span. Depending on age, duration and course there are 2 types of AD, early- or late-onset. A small proportion (<10 %) of AD patients have early-onset AD (EOAD) which is believed to be dominantly inherited. Other risks of AD include smoking, stroke, depression, arthritis, diabetes, estrogen supplements or heart diseases. Mediterranean diet, intellectual stimulation and exercise are decreasing the risk of the AD [Prasansukllab and Tencomnao, 2013; Zhang *et al*., 2011, Ridge *et al.,* 2013].

At the present moment it is only partly possible to treat the symptoms of Alzheimer's disease. Currently, there are no drugs available for an effective treatment for the causes.

1.2.1 Amyloidosis and Alzheimer's disease (AD)

The two major AD pathological hallmarks described by A. Alzheimer are located in vulnerable brain regions, cortex and hippocampus. The intracellular neurofibrillary tangles (NFTs) consist of hyperphosphorylated twisted filaments of the microtubule-associated protein tau. The extracellular plaques are deposits of different sized amyloid-β peptides (Aβ). Amyloid plaques contain also other substances, such as proteoglycans, inflammatory molecules, serum-related molecules, metal ions, apolipoprotein, proteases or antioxidants. The Aβ-peptide was for the first time characterized and identified in 1984 [Glenner and Wong, 1984]. The Aβ production is mediated by proteolysis of an amyloid precursor protein (APP), which can be proteolyzed by two pathways, amyloidogenic- and non-amyloidogenic pathway. The resulting APP metabolites may have different functions and can vary in the length. Most of the full-length produced amyloid peptides contain 40 amino acids, A40. A small portion of derived Aβ-peptides, contain 42 amino acids and they are more aggregation prone than the A40-peptides. The proteolysis takes place in endoplasmic reticulum, where most of A42 is generated, in trans-golgi network, where most of the A40 is generated and in endosomal/lysosomal system where is Aβ in smaller-scale produced. Beside the extracellular plaques, intracellular Aβ became the focal point of AD and cell death research. Recent studies demonstrate that intracellular Aβ genesis and accumulation to soluble oligomeric species are crucial events in AD development and progress [Shirwany *et al*., 2007; Zhang *et al*., 2011; La Ferla, *et al*., 2007].

1.2.2 Amyloid-β peptide metabolism

APP is a transmembrane protein with a large extracellular domain and a short cytoplasmic tail, highly expressed in the brain and concentrated at neuronal synapses. The gene encoding APP is located on human chromosome 21 and its protein contains 695-770 amino acids. It has been hypothesized that APP has an important role in neuroprotection and can regulate cell-cell interactions or cell growth. Different groups or complexes of the enzymes take part in the proteolysis, such as α-, β- and γ-secretases [Prasansukllab and Tencomnao, 2013, Zhang *et al*., 2011].

In non-amyloidogenic pathway, α-secretase cleaves APP in two fragments, C-terminal fragment which contains 83 amino acids and large N-terminal domain sAPPα which is excreted into the extracellular medium and has neuroprotective function. The resulting C-terminal fragment (83 amino acids) is cleaved by the γ-secretase, creating a short fragment, p3. Due to the fact that α–secretase cleaves the Aβ domain, Aβ production is prevented. On the contrary, β- and γ- secretases take part in alternative cleavage pathway, in amyloidogenic pathway leading to Aβ formation. β-secretase is a β-site amyloid precursor protein (APP) cleaving enzyme, BACE and the γ-secretase is a complex of presenilin (PS, PS1 and PS2) , nicastrin , stabilization factor APH -1 (anterior pharynx defective I) and PEN -2 (presenilin enhancer 2) [Zhang *et al*., 2011]. The β-secretase cleaves APP at the 99th amino acid position from the C –terminus. This results a 99 amino acid long C-terminal fragment (C99) which remains in the membrane and an N-terminus fragment, sAPPβ. γ -secretase proteolyzes C99 producing an intact Aß peptide containing 42 amino acids and untoxic C57 fragment. In addition, γ -secretase can proteolyze C99 to Aß peptide containing 40 amino acids and untoxic C59 fragment (Figure 1.3) [La Ferla, *et al*., 2007; Zhang *et al*., 2011].

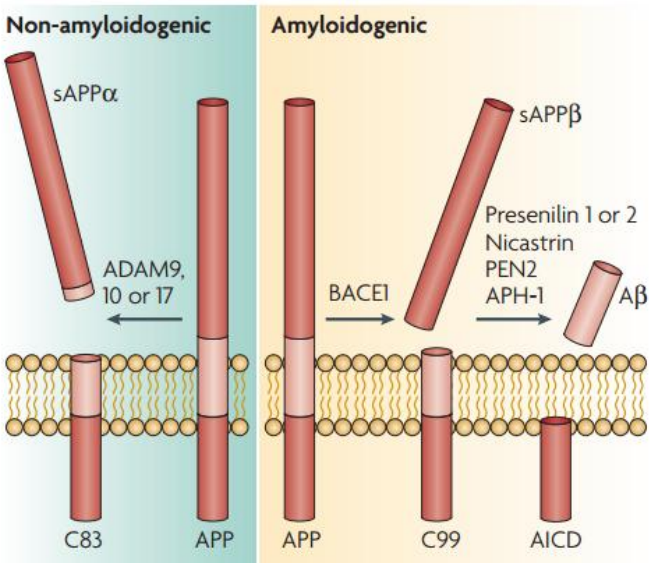

Figure 1.3. APP proteolysis. The Aβ peptide is generated by amyloid precursor protein (APP) proteolysis. APP is a transmembrane protein consisting of 695-770 amino acids, proteolyzed in two pathways. In the non-

amyloidogenic pathway, the formation of Aβ is prevented, and the first cleavage is performed by α –secretase. This protein belongs to the metaloproteases family, ADAM family, respectively. A –secretase cleavage results formation of two fragments, sAPPα and a smaller C-terminal domain. C83 is additionally cleaved by γ-secretase, generating p3 domain. Aβ is generated through the amyloidogenic pathway. In amyloidogenic pathway the APP is cleaved by a β-secretase (BACE1) in the first step. This cleavage results in two fragments, N-terminal sAPPβ and C99, which remains in the membrane and is processed by the γ-secretase complex again. In the last step γ-secretase generate non toxic C57 fragment which remains in the membrane and intact Aβ which can vary in the length [La Ferla, *et al*., 2007].

It is known that mutations in three genes of the APPs, PS1s (chromosome 14) and PS2s (chromosome 1) cause EOAD which is inherited in an autosomal dominant pattern. More than 200 mutations of these genes were identified. Studies done on EOAD showed that in patients carrying these mutations, more A42 is produced. Through accumulation of these evidences, it was suggested that A42, which is hydrophobic and more prone to aggregate, is the primary pathogenic agent in the AD. For instance, it was found that the patients with Down syndrome carry an extra copy of amyloid precursor protein APP, due to third copy of chromosome 21. As a result, A42 production is 1.5-fold greater than in normal controls and individuals with this disease show AD symptoms [Masters *et al*., 1985; Saido, 2013; Ridge *et al*., 2013].

It has been demonstrated that the APP is processed in the brains of both, young and old individuals. However, the accumulation of Aβ peptides in brains of the young individuals is prevented. This indicates that these peptides are produced in brain in normal conditions, but under strict regulation. The Aβ is rapidly catalized before it can aggregate. Amount of produced Aβ peptides is regulated by APP proteolysis as well as its clearance and degradation [Saido, 2013]. These peptides are present in the blood 10-fold greater than in interstitial fluid of the brain or CSF of healthy individuals and the levels of Aβ peptides in plasma are increasing with the age. The Aβ influx into brain is controlled trough the blood-brain-barrier (BBB). Aging can affect structural and functional changes in the walls of blood vessels. As a result these peptides can cross the defective BBB and bind selectively to neurons in brain [Clifford *et al*., 2007, Prasansukllab and Tencomnao, 2013]. It has been also demonstrated that A42 and A40 can be degraded by a peptidase, neprilysin which is exclusively expressed in neurons, and on this way control Aβ clearance [Saido, 2013; Zhang *et al*., 2011; Giuffrida *et al*., 2009].

1.2.3 Assembly of Amyloid oligomers

To date there has been little agreement on Aβ peptide function after its generation. It was suggested that low levels of the Aβ monomers could play an important role at the synapse and its structural-functional plasticity and that Aβ monomer can increase hippocampal long-term potentiation and enhances memory [Giuffrida *et al*., 2009; Saido, 2013]. It was demonstrated that A42 is not toxic in rate cortical neurons and it can increase expression of antiapoptotic protein Bcl-2. Additionally, it is suggested that the monomers can activate phasphatidylinositol-3-kinase pathway, which plays an important role in survival of neurons.

However, after the Aβ is liberated it can rapidly form oligomers, protofibrils and fibrils, which are associated with AD, due to imbalance in the production and clearance of these peptides. Normally, in healthy individuals, shortly after its generation, Aβ is catabolized before it can deposit. Both, A40 and A42 can oligomerize, however via distinct pathways. Due to the hydrophobic C-terminal, A42 forms faster fibrils than A40. Soluble A40 peptides exist as monomers, dimers, trimers and tetramers. On the other hand A42 can additionally form spherical pentamers and hexamers, so called paranuclei due to Ile41. Tetramer structures of A42 and A40 differ in its form. A42 tetramer is more "open" and can add more monomers or dimers, to form pentamers or hexamers. A40 tetramer structure is closed and does not allow any addition of mono- or dimmer. A42 oligomerize itself rapidly into paranuclei where C-terminal of each monomer is oriented to the center of the oligomer. Hexamers (A42)x6 can build dodacamer ((A42)x6)x2, a 56kDa soluble amyloid assembly. However, 18-mer ((A42)x6)x3 is absent, which indicates that addition of next hexamer is slow and energetically unlikely. For that reason more ((A42)x6)x2 accumulates and an adds more monomers to form fibrils. There are also some evidences that the dimers are basic building blocks of AD associated fibrils. The oligomerization pathways are presented in Figure 1.4 [Kirkitadze and Kowalska, 2005; O'Nuallain *et al*., 2010; Bitain *et al*., 2002; Berstein *et al*., 2009; Ahmed *et al*., 2010].

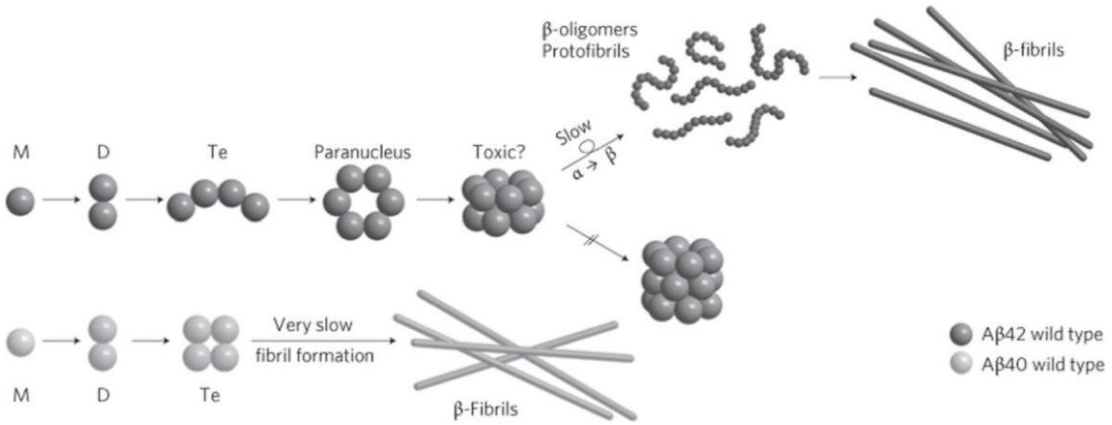

Figure 1.4. Assembly of A42 and A40 peptides to oligomers and fibrils. The amyloid peptides monomers assemble quickly to soluble low-molecular weight oligomers. However, A42 can form paranuclei, hexamers and pentamers, due to open tetramer structure. Contrarily, A40 forms more stable closed tetrames which do not allow any addition of monomer or dimmer. A42 paranuclei assemble further into larger beads structures, dodacamers which can generate protofibrils. Final step of the A42 and A40 assembly generates fibrils [Berstein *et al*., 2009].

It was demonstrated that A42-oligomerization was influenced and prevented by substitutions at positions Phe19 or Ala21. On the contrary, A40-oligomerization was sensitive to the substitutions of Glu22 and Asp23. Therefore, oligomerization of these peptides is controlled by different specific regions of the sequence. These low-n oligomers varying sizes are SDS-stable, such as dimers, trimers, tetramers or dodacamers and can be detected by western blotting through various anti-Aß antibodies in APP transgenic mouse brain and human brain.

Despite the small difference (last two amino acids) between the two peptides, A42 and A40 show different clinical, biological and biophysical behavior. The concentration of secreted A42 is 10% of the secreted A40. The A42 shows stronger neurotoxicity compared with A40. As a consequence of oligomer formation, protofibrils and fibrils can be formed. Assembly of monomers and forming paranuclei are reversible, as well as forming of protofibrils. However, assembly to fibrils is rather irreversible. Fibrillization pathway is dependent on Aβ concentration, pH, time and properties of the solution. It was observed that form of the monomeric Aβ, paranuclei and large oligomers is mainly helical or unordered. Contrarily, protofibrils exhibit β-sheet/β-turn. Since both of the peptides form protofibrils, it is suggested, that the main difference between A40 and A42 is the pathway which generates the oligomers. Recent studies also suggested that Aβ can be post-transcriptional modified, which can promote its aggregation. These include isomerization, racemization, pyroglutamination or phosphorylation. It was demonstrated that the modified Aβ show higher toxicity than unmodified

peptides [Kirkitadze and Kowalska, 2005; Kumar and Walter *et al*., 2011; Bitain *et al*., 2002; Ahmed *et al*., 2010].

Since last decade, more evidences are accumulating that small and soluble Aß oligomers show neurotoxic activities and not the mature Aß fibrils or amyloid plaques, as it was considered. It is suggested that Aß oligomers can harm cultured neurons and impair synaptic function as well as memory. It was shown, by Walsh and his colleagues, that the cerebral microinjection of cell medium containing oligomers, in absence of Aß monomers and Aß fibrils, inhibited hippocampal long-term potentiation in rats [Walsh *et al*., 2002]. It was also suggested that these oligomers activate glycogen synthase kinase-3β (GSK-3β) thereby influencing signaling pathway involved in phosphorylation of tau and APP processing in AD brains [Takashima *et al.,* 1998]. In addition, Aß oligomers activate microglia to induce neuroinflammation through processing of IL-1β, a pro-inflammatory cytokine in AD [Parajuli *et al.*, 2013]. Evidence have been demonstrated that the Aß deposits from the extracellular space also play an important role in AD, in particular as an alternative Aß source. The cells are able to internalize the Aß peptides via different receptors, for instance α7 nicotinic acetylcholine receptor or passive diffusion. Dependent on lipid composition of the membrane and a peptide structure and conformation of the Aß, these peptides might induce membrane disruption and form membrane channels. Due to the membrane disruption, a pass of ions is enabled, thereby altering cellular homeostasis [O'Nuallain *et al*., 2010; Yip and McLaurin, 2001; Shirwany *et al*., 2007; Haass and Selkoe, 2007; Bayer and Wirths, 2010].

One of the approaches for designing AD therapeutics would be to determine the pathophysiological function of each Aß oligomer in the brain. Amyloid-ß oligomers, in cerebrospinal fluid, are already suggested to be a biomarker for AD [Hölttä *et al*., 2007].

1.2.4 Chaperones and Alzheimer's disease (AD)

In recent two decades, numbers of studies are accumulating, which demonstrate a link between AD and chaperones. Molecular chaperones mainly belong to heat shock proteins (HSP), as a part of the heat shock response (HSR), a highly conserved program. Function of these proteins is primarily to protect damaged proteins from aggregation through refolding or targeting them for degradation. Additionally they take part in translocation of proteins. There are many different groups and subgroups of chaperons, depending on their location, size or function.

Class of cytosolic heat shock protein 70 (Hsp70) in *S. cerevisiae* includes Ssa, Ssb, Sse and Ssz1 families. There are four genes encoding proteins of the Ssa family, namely *SSA1*, *SSA2*, *SSA3* and

SSA4. The ssa1 and ssa2 proteins share most of the functions, such as protein folding, translocation and they are constitutively expressed as well as induced under stress. Deletion of these two genes can activate heat shock factor 1 (Hsf1), which regulates HSP expression. Ssa3 and Ssa4 can be only expressed under the stress and they cannot complement the Ssa1 and Ssa2 function. Hsp40, so called J-proteins induce the Hsp70 ATPase activity, while accelerating a conformational change for ATP hydrolysis. The most studied cytosolic Hsp40 is Ydj1, which is able together with Ssa to induce activity of Hsp90-dependent clients. It was demonstrated that Hsp70 protein family modulates transport to the mitochondria and the ER. Additionally, it was shown that Ydj1 is required also for this transport. Due to farnesylated C-terminus, Ydj1 can take part in translocation process of the proteins and additionally can bind to the membranes [Verghese *et al*., 2012; Caplan *et al*., 1992].

It was shown that different classes of neurons do not share the same expression profile of constitutively expressed Hsps. The Hsc70 and Hsp27 show higher levels in neurons of spinal cord than in neurons of substantia nigra or neurons of the hippocampus and entorhinal cortex. This expression profile correlates with the neurodegenerative disorders [Chan and Brown, 2006]. However, the expression of Hsps differs in healthy and aged brains. Few scientists published that levels of Hsc70 and Hsp70 are increased or unchanged in aged brains compared to healthy brains. Levels of Hsp90 were however decreased in aged brains. It was hypothesized that the chaperones during aging could act as “sick chaperons” and be target of proteotoxic damage. Due to increase of chaperone potential targets, a phenomenon called “chaperone overload” appears and the capacity of the chaperones is saturated [Nardai *et al*., 2002].

In addition, it was demonstrated that some of the chaperones are up-regulated in the AD brains. αB-crystallin and Hsp27 are up-regulated in astrocytes which are surrounded by senile plaques and neurofibrillary tangles. Hsp20, HspB2 and HspB8 can be found colocalized to Aβ in senile plaques and cerebrovascular amyloid angiopathy [Wilhelmus *et al*., 2007]. Significant higher levels of Hsp72 and Hsp73 were found in postmortem cortical tissues from AD brains. It was suggested that the induction of these proteins associates with AD [Perez *et al*., 1991]. Moreover, it was shown that some chaperones can interact with intracellular amyloid peptides, such as Hsp70 and some members of αB-crystallin proteins (Hsp16s). There is a possibility that these proteins play an important role in early stages of the AD and Aβ metabolism [Fonte *et al*., 2002]. Mild heat shock can induce expression of Hsps and promote cellular survival. One study showed that induced heat shock in neurons makes the neurons even more vulnerable to Aβ treatment. However, overexpression of few chaperones protected the neurons against the Aβ toxicity. After Hsp27 overexpression in cortical neurons, the Aβ toxicity was reduced, the cells had better survival and Hsp27 prevented

decrease in mitochondrial size induced by Aβ treatment [King *et al*., 2009]. Alzheimer's disease-related phenotypes were also suppressed by over-expression of Hsp70 in Alzheimer's disease mouse model [Hoshino *et al*., 2011]. Additionally, chaperone-deficient mice models showed behavioral defects [Ojha *et al*., 2011]. The influence of chaperones on the Aβ aggregation and assembly was examined *in vitro*. It was observed that the Hsp70 and Hsp40 in combination can partially inhibit the aggregation of Aβ. Hsp70 also blocked aggregation, however, not efficient as the combination of those two chaperones. The Aβ peptides assembled into small roughly circular structures and some short fibrils, instead of amyloid fibrils. Hsp40 alone could not block the amyloid aggregation. It was also shown that the ATPase activity is required for chaperones to block the aggregation of the peptides. Treatment of the amyloid fibrils with the combination of Hsp40/Hsp70 and Hsp90 exhibited minor changes in the length of the fibrils. The fibrils tended to be shorter. In contrast, the combination of Hsp40/Hsp70 and Hsp90 could recognize and degrade small Aβ oligomers. Nevertheless, the combination of Hsp40 and Hsp70 did not measurably influence the early assembly of Aβ. This study suggested that if the early Aβ structures are formed, presence of the chaperones can inhibit further fibrilisation [Evans *et al*., 2011]. Carnini and her colleagues were analyzing Hsp40 in the presence of the Aβ in different cell lines. Transient transfection of Hsp40 in CAD cells could decrease the Aβ levels in cells. However, in hippocampal neurons Hsp40 increased the Aβ levels. Hsp40 could potentially protect the toxic Aβ which could result with the acceleration of the disease. This could be explained by the fact that the expression of Hsp40 and the expression network in general of other chaperones vary in different cell lines [Carnini *et al*., 2012]. Few others studies were also examining if chaperones can affect Aβ oligomerization. Due to the fact that a human prefoldin has been found expressed in the human brains and it take part in *de novo* protein folding, archaeal prefoldin was investigate if it can form the Aβ oligomers. During the fibrillization of Aβ in the presence of this prefoldin the aggregation was inhibited and toxic oligomers which could induce apoptosis were observed [Sakono *et al*., 2008]. However, few years later, the same scientific group performed the same experiments using human prefoldin. Higher Aβ oligomeres were observed again and the fibrillization process was inhibited, however, these oligomeres were not toxic for the cells [Sörgjerd *et al*., 2013]. αB-crystallin can inhibit generation of Aβ fibrils, as well and produce protofibrils which are also toxic for the neurons. It was also reported that the Hsp90 can modulate the early amyloid assembly of α-synuclein, a Parkinson-related protein in ATP-dependent manner [Falsone *et al*., 2009]. Yet, the cells are trying to protect themselves against age-onset proteotoxicity. The cells developed two pathways, namely, HSF-1 pathway which controls disaggregation and the DAF-16 pathway which give arise to generation of larger Aβ oligomeres which are nontoxic. It was shown that the RNAi of DAF-16 and HSF-1 increased the number of the paralyzed *C.elegans* which

expressed Aβ. Furthermore, these two pathways function in opposing activities [Cohen *et al*., 2006]. Another way how the cells utilize chaperones to protect themselves is activation of micoglial clearance by activating the Hsp90 [Takata *et al*., 2003].

1.2.5 Role of the mitochondria in Alzheimer's disease (AD)

Mitochondria are one of the most important cell organelles, associated with generating of the cell energy, coordinated with metabolic processes such as oxidative phosphorylation or tricarboxylic acid cycle. Mitochondria can also produce harmful substances such as, reactive oxygen species (ROS), which can influence mtDNA mutations, lipid peroxidation or reduce mitochondrial number. Mitochondria are essential for the neurons and they are enriched at the synapses. They can be found in the neurons in very high number, where they provide the energy for the cells and are essential for the normal function of the brain.

More evidences are accumulating supporting the hypothesis that the intracellular Aβ can negatively influence the mitochondria and impair its function. It was shown that the Aβ can be imported by the mitochondria, independently of mitochondrial membrane potential and located in mitochondrial cristae, shown *in vivo* and *in vitro* [Petersen *et al*., 2010]. The Aβ import machinery is connected to the translocase of the outer membrane (TOM) and translocase of the inner membrane (TIM), as shown in isolated rats mitochondria. Due to the C-hydrophobic terminal of Aβ, it was suggested that the Aβ is binds hydrophobically to the import receptors. However, this uptake is dependent of the Aβ length, hydrophobicity, as well as helix potential of the peptide. Since the Aβ could be inserted in the mitochondrial inner membrane after the import, a respiratory chain complex IV could be inhibited [Kish, et al. 1992]. The insertion of Aβ could be shown in neurons of postmortem brain specimens of AD patients as well as in neurons of brain in mouse model organism. Nevertheless, it was also demonstrated that APP can be colocalized to the mitochondria. Novel findings showed that APP can be associated to TOM40 and TIM23 in AD patient brains. Therefore, it was proposed that the Aβ could also be generated in mitochondria [Hansson Petersen *et al*., 2010; Pagani and Eckert, 2010; Reddy, 2009].

Mitochondria have a great pool of the proteins which are potential targets of Aβ peptides. It was reported that Aβ can colocalize with a heat shock protein Hsp60 in mitochondria matrix, not only in mouse but also in human brain samples. Aβ may block mitochondrial translocation of nuclear-encoded proteins, impair mitochondrial dynamics or induce apoptosis activated by mitochondrial substrates. Impaired mitochondria produce less ATP and disturb Ca^{2+} homeostasis which can alter neuronal function. Oligomeric Aβ influences Ca^{2+} homeostasis and promotes the excess of

intracellular Ca^{2+}. Through the Ca^{2+} accumulation the mitochondrial permeability transition pore is opened and in this way the mitochondrial structure is damaged. Consequently, alternation of mitochondrial dynamics induces synaptic failure which leads to the cell death and the neurodegeneration. Yet a mechanism by which is Aβ transported to the mitochondria is still unknown [Bayer and Wirths, 2010; Pagani and Eckert, 2010; Reddy, 2009].

In recent years, there has been an increasing interest in elucidating the link between Aβ and mitochondria. A study from 2011, demonstrated that some cells in AD patient's brain are resistant to A42 mediated toxicity and cell death, due to the fact that they switched their metabolism to aerobic glycolysis by which they avoided respiration [Newington *et al.*, 2011]. Warburg effect has been observed and described using cancer cell. Most of the cancer cells produce energy by glycolysis followed by lactic acid fermentation, which contrast to the most of the normal cells which use lower rate of glycolysis followed by oxidation of pyrivate in mitochondria.

1.3 Yeast as a model

Saccharomyces cerevisiae, bakers' yeast, is a unicellular eukaryotic organism and share many cellular mechanism with other eukaryotic cells. As an established model organism, *S. cerevisiae* is used in fundamental and applied research. It offers an attractive cellular system to investigate eukaryotic cell processes in molecular and cellular biology research. Yeast is an adjustable organism whose growth and division can be controlled by changing the environmental conditions very easily. In 1996 the whole yeast genome sequence was published and shortly after a human genome and yeast genome was compared. During this study, it was uncovered that 30% of the genes involved in human diseases have yeast orthologs. Since then, yeast databases have been efficiently updating and nowadays there are number of easily accessible databases on the web dealing with yeast genome, proteome, yeast mutant collections, as well as yeast phenotypic and expression analysis. Due to the fact that the yeast is easy to handle and can be simply genetically manipulated, this model organism became a leading organism to study pathways involved in human diseases and aging. Furthermore, yeast is an excellent experimental tool for investigation of protein-protein interactions, DNA replication, recombination, cell division, vesicular trafficking or stress-induced signal transduction. In addition, yeast is also used for expression of non-homologous human disease-related proteins. In this manner, "humanized yeast" offers to scientific community a promising tool for investigation of novel medical compounds and potential drugs [Mager and Winderickx, 2005].

Very important breakthrough in yeast research was the discovery of the apoptosis in yeast in 1997, by Madeo. Since then, yeast became very convenient tool for apoptosis and cell death research and new key players involved in this pathway in yeast were reported [Madeo *et al*., 1997; Madeo *et al*., 2002]. Additionally, yeast has two lifespans, namely, replicative and chronological lifespan. Replicative lifespan is measured by a number of daughter cells produced by a mother cell. In contrast, chronological lifespan is length of time how long non-dividing cells in stationary phase can survive and maintain their viability. The stationary phase starts when yeast grows into post-diauxic state and switch to the mitochondrial respiratory mode after depletion of glucoses in the media. Cells start using the ethanol which is generated during fermentation and slow the metabolic rates. In addition the stress-resistance pathways are up-regulated during the chronological aging. Aging is a process in which cells try to maintain the balance between available resources and competing priorities of somatic maintenance and reproduction. Longevity is a length of time in which cells remain alive and do not die through any extrinsic cause. The mitochondrial dysfunction is one of the consequences of the aging. This manifestation is followed by increased ROS generation, which contributes to oxidation damage of cell lipids, proteins or DNA. It has been suggested that the oxidative stress is a factor that determine the survival of stationary yeast [Piper, 2006].

It has been demonstrated, that ROS can induce apoptosis and is associated with aging not only in yeast but also in other organisms. The oxidative damage theory indicates that the aging is due to accumulations of cell damage induced by ROS levels in the cells. ROS induces damages in aerobic cells, which indicates that this process is highly conserved. Furthermore, Ludvico described that low doses of acetic acid as an external stress can induce apoptosis and elevate ROS levels in the cells. Yeast stationary phase during chronological aging can be used as a model for investigating factors that might influence the aging of post mitotic tissues in higher organism [Madeo et al., 2002; Longo et al., 2012; MacLean, 2000; Ludvico et al., 2001].

1.3.1 Yeast as a model to study neurodegenerative diseases (ND)

Even though yeast lacks a nervous system, data maintained by humanized yeast in recent years are demonstrating that yeast provides useful pool of information considering neurodegenerative disorders. The molecular signaling pathways involved in protein folding, cellular trafficking and secretion, as well as other proteins involved in human ND are functionally conserved in yeast. Neurodegenerative disorders are characterized by protein misfolding and intracellular and/or extracellular deposits in the patients' brains. Misfolded proteins tend to aggregate into fibrils which are pathological hallmarks of ND, such as Alzheimer's disease, Parkinson's disease or Huntington's

disease. Yeast prions also tend to accumulate into proteolytic-degradation resistant aggregates. The misfolded form of the prion protein can stimulate misfolded transformation of the normal prion form. The conversion of these proteins leads to specific phenotypes, [*PSI*$^{+}$], which can be non-chromosomally inherited. The maintenance of this phenotype is Hsp40 and Hsp70 dependent, as well as Hsp104 which is responsible for [*PSI*$^{+}$] inheritance [Vishnevskaya *et al*., 2007; Bharadwaj *et al*., 2010].

Besides misfolded proteins and aggregations patterns, oxidative stress plays also a crucial role in neuronal death. Due to the fact that human brain consumes 20% of our body oxygen, high ROS levels are accumulated in the brains. Evolutionary, cells were able to develop a system which offers them a protection against evaluated ROS levels, such as adaptive response to oxidative stress or expression of antioxidant molecules. Excessive production of ROS can impair the cellular redox balance and induce cellular damage. The mitochondria are essential to the neurons due to high demand for energy. As mitochondria are thought to be one of the main ROS source in the cell, it was suggested that the neurodegenerative disease are also mitochondrial diseases [Pimentel *et al*., 2012].

Many different humanized yeast models were developed to investigate ND. Huntington's disease yeast models express mainly polyQ N-terminal peptides of human Huntigtin protein (Htt) as fusion or tagged proteins. Expression of α-synuclein in yeast, a protein responsible for Parkinson's disease, induces synthesis of heat shock proteins and probably induces apoptosis. 4850 yeast strains expressing mutated Htt and α-synuclein were analyzed. It was revealed that toxicity of these diseases is mediated by different pathways and conserved proteins. It was suggested that the most of the 52 proteins, which enhance Htt toxicity belong to the groups of proteins responsible for response to stress, protein folding and ubiquitin-dependent protein catabolism. In contrast, most of the 86 proteins which could enhance α-synuclein toxicity were linked to the lipid metabolism and vesicle-mediated transport. Various humanized yeast models of Alzheimer's disease were developed. Most of them deal with tau phosphorylation-conformation-aggregation cascade, APP processing or Aβ oligomerization. These models have a great value for the ND research due to elucidation of the links between oxidative stress, dysfunction of mitochondria and induction of cell death via protein-misfolding [Vishnevskaya *et al*., 2007; Winderickx *et al*., 2008; Willingham *al*., 2003].

1.3.2 Yeast as a model to study Alzheimer's disease (AD)

Yeast as model offers us many advantages, for instance the experiments performed in yeast are inexpensive and convenient, in addition, potential inhibitors of Aß oligomerization that are cytotoxic can be immediately eliminated due to inhibition of the cell growth. Potential drugs have to cross the blood-brain barrier, which can be tested by uptake of these compounds to the yeast cells. This system also offers identification of indirect compounds as well, such as inhibitors of the chaperons. Using these eukaryotic cells, large screens of potential drugs are possible in very short period of time [Prozoor and Macreadie, 2013].

There have been many approaches to generate an AD suitable yeast model. One small group of researchers was trying to modulate yeast cells to express tau protein which could together with Aß lead to development of AD. Two human tau isoforms of six that could be expressed in yeast do not impair yeast growth. However, expression resulted in similar characteristics of those in neuronal cell in AD, such as aggregation. The phosphorylation pathway can also be investigated and many orthologs of tau phosphatases and kinases have been recognized [Prozoor and Macreadie, 2013]. On the other hand many groups are putting an effort in generation of AD yeast model for investigation of APP processing and Aß toxicity. One of the first studies, dealing with AD yeast models tried to express the human APP in yeast to analyze its processing. Via these models it was found that yeast expresses at least two proteins which have α-secretase activity such as in neurons that is able to cleave APP and prevent building of Aß. Deletion of the genes encoding the aspartyl proteases in yeast acting in the late Golgi, Yap3 and Mkc7 could decrease α-secretase activity [Zhang *et al*., 1997]. No proteins with β- or γ-secretase activity were detected in yeast. However, using yeast many BACE1 (β-secretase) inhibitors were discovered and function of each γ-secretase component could be investigated. In contrast, it was shown that *Pichia pastoris* could express proteins with β- and γ-secretase activity [Bharadwaj *et al*., 2010].

Bharadwaj and his colleagues tested the toxicity of Aβ oligomers and its fibrils. These peptides were added to the diluted cell suspension of *Candida glabrata* in required concentrations. Using cell survival assays, it could be shown that the Aβ oligomers caused 70% loss of the cell viability, whereas Aβ fibrils did not influenced cell survival [Bhardwaj *et al*., 2008].

Due to the fact that yeast does not have APP homologous or corresponding secretases that could cleave the APP, Caine and his associates expressed A42, C- and N-terminally fused with green fluorescent protein (GFP), in yeast. They showed that expressing the native A42 without a fusion is is not stable in the yeast cell, as it may be degraded as fast as it is produced. GFP on one hand stables

A42 in yeast and on the other has enabled the visualization and localization of the fusion construct. It has been found that A42 is colocalized to lipid particles as punctuate patterns. Using this model Caine also demonstrated activation of the heat shock response which could arise from A42 inducing ROS levels and production of misfolded proteins [Caine *et al*., 2007].

Broad range of Aβ oligomerization studies in yeast were carried out. Using two-hybrid system, it was reported that Aβ is able to build dimers *in vivo* [Hughes *et al*., 1996]. Additionally, SDS-stable low-n oligomers were also detectable in a yeast reporter system, where A42 was fused to MRF. MRF is a Sup35 translational termination factor Sup35 without N-terminal domain. N-domain of Sup35 is responsible for yeast prion phenotype [*PSI*$^{+}$]. The translational termination activity and *ade1-14* nonsense allele were used for the assay. In this manner the oligomerized Aβ-MRF construct could be distinguish from the non-oligomerized Aβ-MRF mutants which contained mutations in the Aβ regions which are responsible for oligomerization. Via this system it could be also shown that disruption of yeast chaperone Hsp104 decreased the oligomerization of the fusion protein. In yeast, disaggregation of the toxic intermediates is orchestrated by Hsp104, Hsp70/Hsp40, Hsp42 and Hsp26. On the contrary, guanidine which inhibits ATPase activity of Hsp104 increased oligomerization of the same fusion protein [Bagriantsev and Liebman, 2010]. In the next study, the same research group used this model for identification of nontoxic inhibitors of A42 oligomerization via yeast high-throughput screen. Park and his colleagues tested 12 800 compounds and revealed two compounds, AO-11 and AO-15, which were able to inhibit the oligomerization. However, AO-11 and AO-15 also had influence on the large aggregates [Park *et al*., 2010]. Furthermore, another research group fused Aβ to maltose binding protein and also detected low-n-oligomers of the protein construct such as, dimers, trimers, tetramers or hexamers. It could be also shown that this MBP-Aβ construct can induce cell death in yeast, as well as in neuronal cells [Caine *et al*., 2011]. Treush et al. developed a yeast model expressing A42 fused to an ER-targeting signal to the N-terminus. After the cleavage of the signal sequence in ER, A42 should be transited to secretory pathway. This model also revealed broad range of oligomer species. Using this model a screen for genetic modifiers of A42 toxicity was done, which identified 23 suppressors and 17 enhancers, from which 12 had homologues in human. The identified proteins were mostly linked to clathrin-mediated endocytosis or functionally associated to cytoskeleton [Treush *et al*., 2011]. Two years later a new yeast model was established expressing A42 fused to GFP with a linker sequence in-between and mating factor α sequence secretion signal. Expression of this construct decreased yeast cell viability compared to its controls. Deletion of the gene encoding for the Hsp104 restored the viability even though Hsp104 is a cytosolic chaperone and MFα-A42-GFP associates to secretory pathway. It was

suggested that Hsp104 mediates the A42 toxicity by production of smaller more toxic intermediates by disaggregation [D'Angelo *et al*., 2013].

1.3.3 Current state of the research

A new AD yeast model expressing human A42 or A40 fused to enhanced green fluorescent protein (EGFP) was established in our lab, by Dr. Julia Ring and Mag. Mirjana Jovisic. As control-constructs, cells expressing EGFP only (WT ev) and cells expressing a fusion protein EGFP-C57 were used. C57 is a nontoxic intermediate of the last step of APP processing, generated from the C-terminal fragment of C99, whereas A42 is N-terminal. A linker between the N-terminal EGFP and A42 was essential for proper folding of GFP and toxicity of A42. Expression of these constructs was carried out with GAL10 promotor and it was induced due to shift from minimal medium with 2% glucose to minimal medium with 2% galactose after 16 hours of yeast growth. It could be shown that heterologous EGFP-A42 expression induces age-dependent oxidative stress, as well as the cell death compared to controls. An increase of the ROS levels in chronologically aged cultures mediated by A42 was observed, as well as A42-induced cell death which was demonstrated by markers for necrosis. As expected cells expressing EGFP-A40 showed toxicity, however less than EGFP-A42, as A42 is more prone to aggregate (Figure 1.5).

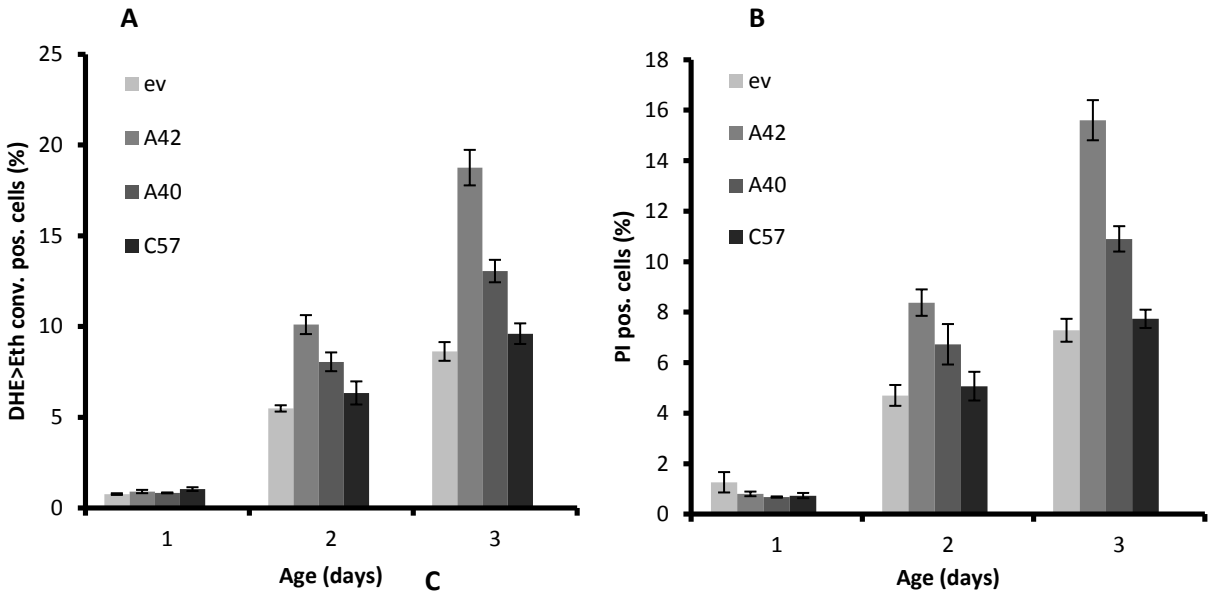

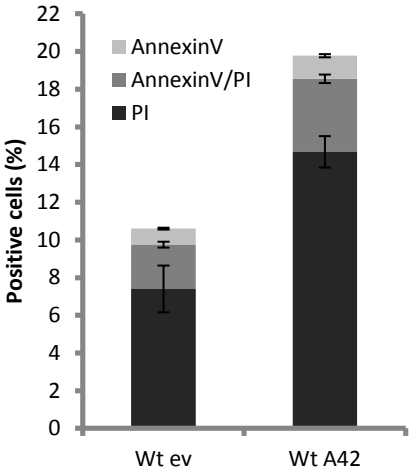

Figure 1.5. A42 induces cell death in yeast. A ROS levels on day 2 and 3 of chronological aging compared to controls were two-fold higher in yeast cells expressing A42. ROS levels were quantified by conversation of DHE to Eth and measured by flow cytometer. **B** PI staining determined cells which lost their viability and their membrane integrity. Two-fold bigger fraction of the cells expressing A42 was stained with PI compared to corresponding controls. **C** Quantifying phosphatidylserine externalization, which is apoptotic marker and membrane integrity which is necrotic marker, it was shown that A42 induces necrotic cell death compared to ev. Data represent mean +/- S.E. of four independent experiments performed at the same time. Unpublished data Julia Ring.

Furthermore, a screen of over 150 deletions mutants was carried out. The identified proteins that could mediate A42 toxicity were linked to respiratory processes and mitochondria as well, as heat-shock response. These players were elucidated by calculating the ratio between ROS positive cells expressing A42 and its vector control, which was frequently on day two 2-fold. The strains which showed 1.3-fold or lower were treated as potential hits (Figure 1.6).

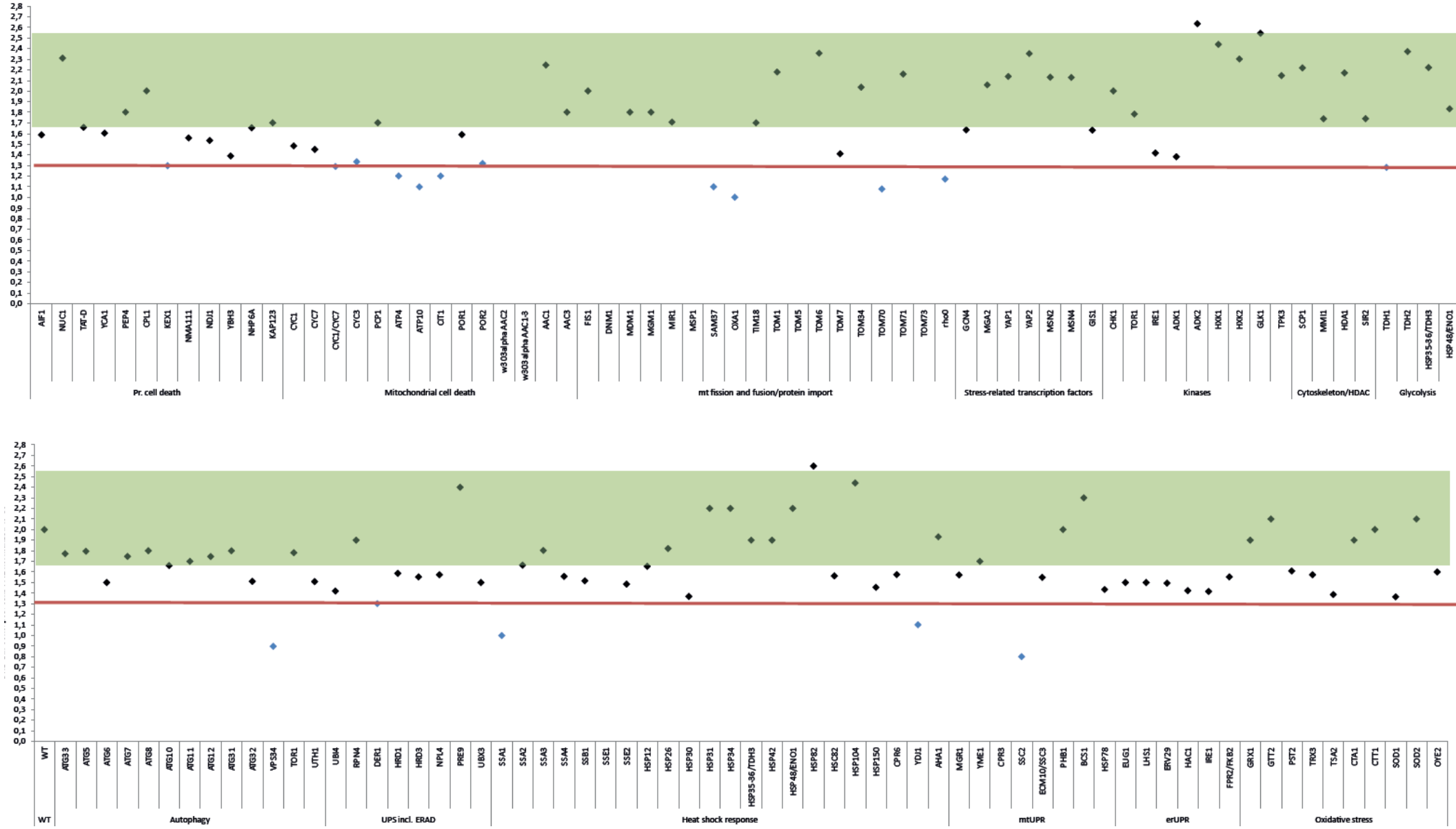

Figure 1.6. A screen of 157 deletion strains revealed 17 genes coding for proteins which are involved in A42-mediated cytotoxicity in yeast.

1.4 Aims of the project

The overall aim of the project is to analyze impact of APP peptide, A42, expressed in yeast BY4741 on cell viability and to elucidate portential key players and pathways involved in A42 meadiated cytotoxicity. During my work on this project, we additionally investigated oligomerization and aggregation properties of A42 linked to cytotoxicity. For that reason, A42 mutants which are not able to oligomerize or aggregate were compared to A42. The main focus of my work in this project was to closely analyze elucidated proteins from deletion mutant screen. These include two chaperones, Ssa1p and Ydj1p, two mitochondrial proteins, Tom70p and Oxa1p and a respiratory deficient strain, Rho0. Since the screen of knock out strains revealed two chaperones which influenced A42 cytotoxicity, our goal was to investigate impact of these proteins on A42 aggregation and localization. Furthermore, due to difficulties in growth and protein expression of two respiratory deficient strains, new inoculation scheme was developed and our aim was to repeat investigation of Rho0 and *OXA1* deletion strain using new scheme.

ROS accumulation within cells was determined by DHE staining and FACS analysis. The localization studies were performed by cellular fractionation and fluorescence microscope. Cellular fractionation and oligomerization studies were performed in laboratory of Chris Meisinger, at the “Institute of biochemistry and molecular biology” in Freiburg.

During this work, new insights concerning key players and cell pathways involved in toxicity of intracellular A42 using yeast as a model system for human neurons were revealed.

2. Materials

All of the materials which were used in this work are listed in this chapter, including materials used at the "Institute of Molecular Biosciences" in Graz and "Institute of biochemistry and molecular biology" in Freiburg.

2.1 Strains and Plasmids

The experiments were carried out in BY4741 (MATa *his3Δ1 leu2Δ0 met15Δ0 ura3Δ0*), *Saccharomyces cerevisiae,* which were obtained from Euroscarf. All the strains that have been using during this work can be seen in the Table 2.1.

Table 2.1. Strains used during the project:

Strain	Genotype	Plasmid	Origin
BY4741	MATa *his3Δ1 leu2Δ0 met15Δ0 ura3Δ0*		Euroscarf
BY4741	MATa *his3Δ1 leu2Δ0 met15Δ0 ura3Δ0*	pESC-his + EGFP	Julia Ring
BY4741	MATa *his3Δ1 leu2Δ0 met15Δ0 ura3Δ0*	pESC-his + EGFP + A42	Julia Ring
BY4741	MATa *his3Δ1 leu2Δ0 met15Δ0 ura3Δ0*	pESC-his + EGFP + A40	Julia Ring
BY4741	MATa *his3Δ1 leu2Δ0 met15Δ0 ura3Δ0*	pESC-his + EGFP + C57	Julia Ring
BY4741	MATa *his3Δ1 leu2Δ0 met15Δ0 ura3Δ0*	pESC-his+EGFP + A42m2	This work
BY4741	MATa *his3Δ1 leu2Δ0 met15Δ0 ura3Δ0*	pESC-his+EGFP + A42m1	This work
BY4741 *ssa1Δ*	BY4741 *ssa1Δ::KanMX*	pESC-his + EGFP	Julia Ring
BY4741 *ssa1Δ*	BY4741 *ssa1Δ::KanMX*	pESC-his + EGFP + A42	Julia Ring
BY4741 *ssa2Δ*	BY4741 *ssa2Δ::KanMX*	pESC-his + EGFP	Julia Ring
BY4741 *ssa2Δ*	BY4741 *ssa2Δ::KanMX*	pESC-his + EGFP + A42	Julia Ring

BY4741 *ssa3Δ*	BY4741 *ssa3Δ::KanMX*	pESC-his + EGFP	Julia Ring
BY4741 *ssa3Δ*	BY4741 *ssa3Δ::KanMX*	pESC-his + EGFP + A42	Julia Ring
BY4741 *ssa4Δ*	BY4741 *ssa4Δ::KanMX*	pESC-his + EGFP	Julia Ring
BY4741 *ssa4Δ*	BY4741 *ssa4Δ::KanMX*	pESC-his + EGFP + A42	Julia Ring
BY4741 *ydj1Δ*	BY4741 *ydj1Δ::KanMX*	pESC-his + EGFP	Julia Ring
BY4741 *ydj1Δ*	BY4741 *ydj1Δ::KanMX*	pESC-his + EGFP + A42	Julia Ring
BY4741 *tom70Δ*	BY4741 *tom70Δ::KanMX*	pESC-his + EGFP	Julia Ring
BY4741 *tom70Δ*	BY4741 *tom70Δ::KanMX*	pESC-his + EGFP + A42	Julia Ring
BY4741 *oxa1Δ*	BY4741 *oxa1Δ::KanMX*	pESC-his + EGFP	Julia Ring
BY4741 *oxa1Δ*	BY4741 *oxa1Δ::KanMX*	pESC-his + EGFP + A42	Julia Ring
BY4741 *oxa1Δ*	BY4741 *oxa1Δ::KanMX*	pESC-his + EGFP + C57	Julia Ring
BY4741 (rho0)	MATa *his3Δ1 leu2Δ0 met15Δ0 ura3Δ0*	pESC-his + EGFP	Julia Ring
BY4741 (rho0)	MATa *his3Δ1 leu2Δ0 met15Δ0 ura3Δ0*	pESC-his + EGFP + A42	Julia Ring
BY4741 (rho0)	MATa *his3Δ1 leu2Δ0 met15Δ0 ura3Δ0*	pESC-his + EGFP + C57	Julia Ring
BY4741	MATa *his3Δ1 leu2Δ0 met15Δ0 ura3Δ0*	pESC-his + EGFP; pESC-ura	Julia Ring
BY4741	MATa *his3Δ1 leu2Δ0 met15Δ0 ura3Δ0*	pESC-his + EGFP + A42; pESC-ura	Julia Ring
BY4741	MATa *his3Δ1 leu2Δ0 met15Δ0 ura3Δ0*	pESC-his + EGFP; pESC-ura + YDJ1	Julia Ring
BY4741	MATa *his3Δ1 leu2Δ0 met15Δ0 ura3Δ0*	pESC-his + EGFP + A42;	Julia Ring

		pESC-ura + YDJ1	
BY4741 ydj1Δ	BY4741 ydj1Δ::KanMX	pESC-his + EGFP; pESC-ura	Julia Ring
BY4741 ydj1Δ	BY4741 ydj1Δ::KanMX	pESC-his + EGFP + A42; pESC-ura	Julia Ring
BY4741 ydj1Δ	BY4741 ydj1Δ::KanMX	pESC-his + EGFP; pESC-ura + YDJ1	Julia Ring
BY4741 ydj1Δ	BY4741 ydj1Δ::KanMX	pESC-his + EGFP + A42; pESC-ura + YDJ1	Julia Ring

pESC-his plasmid was used in this work for the expression of few fusion constructs. This plasmid is obtained from Agilent Technologies. The features of the pESC-his plasmid are presented in Figure 2.1. The fusion constructs are listed in the Table 2.2 and can be seen in Figure 2.3. pESC-ura plasmid was used to overexpress YDJ1 (Figure 2.2).

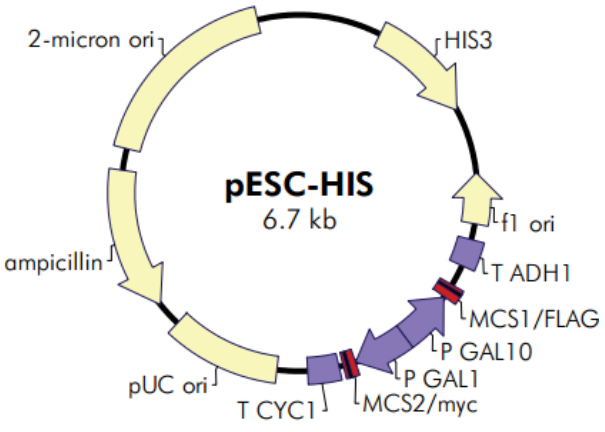

Figure 2.1 The pESC-HIS vector. This vector has many features, such as *HIS3* selection marker, multiple cloning site 1 and 2, FLAG tag, ampicillin resistance, c-

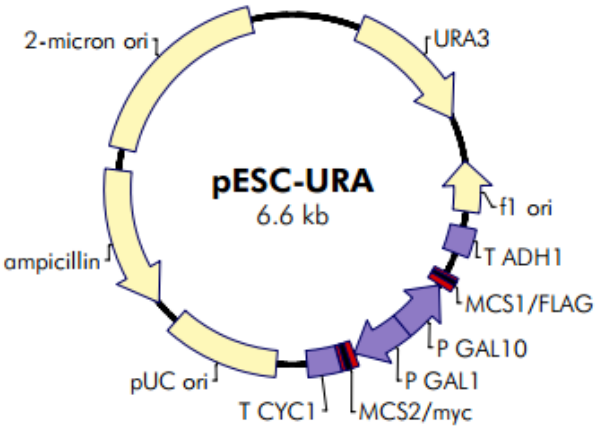

Figure 2.2. The pESC-URA vector. Features of this vector are as *URA3* selection marker, multiple cloning site 1 and 2, FLAG tag, ampicillin resistance, c-myc tag, yeast

myc tag, yeast *GAL1/GAL10* promoter and etc. *GAL1/GAL10* promoter and etc.

Table 2.2 The pESC-his vector constructs used in this work

Vector	Insert	Features	Origin
pESC-his cFLAG		HIS-marker, GAL10 promoter, C-terminal FLAG-tag	Stratagen
pESC-his EGFP		HIS-marker, GAL10 promotor, N-terminal EGFP tag, Stop-codon in the MCS1	Julia Ring
pESC-his EGFP_G		HIS-marker, GAL10 promotor, N-terminal EGFP tag, no Stop-codon in the MCS1, used for cloning	Julia Ring
pESC-his EGFP_G	A42	HIS-marker, GAL10 promotor, N-terminal EGFP tag, A42 Insert in the	Julia Ring
pESC-his EGFP_G	A40	HIS-marker, GAL10 promotor, N-terminal EGFP tag, A40 Insert in the MCS1	Julia Ring
pESC-his EGFP_G	C57	HIS-marker, GAL10 promotor, N-terminal EGFP tag, C57 Insert in the MCS1	Julia Ring
pESC-his EGFP_G	A42m1	HIS-marker, GAL10 promotor, N-terminal EGFP tag, A42m1 Insert in the MCS1	This work
pESC-his EGFP_G	A42m2	HIS-marker, GAL10 promotor, N-terminal EGFP tag, A42m2 Insert in the MCS1	This work

Figure 2.3 pESC-his fusion constructs cloned into the MSC1. A42m1 and A42m2 were obtained from Sei-Kyoung Park, Department of Biochemistry and Molecular biology, University of Nevada. pCUP1::A42 F19, 20T/I31MRF as A42m2MRF; pCUP1::A42 F19, 20T MRF as A42m1MRF;

For the cloning of these constructs into the pESC-his plasmid, primers were designed and produced by MWG Biotech. The primer sequences can be seen in Table 2.3.

Table 2.3 List of used primers and their sequences:

Primer	Sequences 5' → 3'
EGFP sense	ATCTGAATTCATGTCTAAAGGTGAAGAATTATTCAC
EGFP antisense	ATCTGAATTCTTTGTACAATTCATCCATACCATG
A42, A40, A42m1, A42m2 sense	ATCTACTAGTATGGATGCAGAATTCCGACATGAC
A42, A40, A42m1, A42m2 antisense	ATCTATCGATTTACGCTATGACAACACCGCCC
C57 sense	ATCTACTAGTATGACAGTGATCGTCATCACCTTG
C57 antisense	ATCTATCGATTTAGTTCTGCATCTGCTCAAAGAAC

2.2 Growth media

2.2.1 Preparation of culture media

For the preparation of the liquid and plate cultivation media, double distilled water was used. For the plate cultivation media, 2% of agar was additionally added. The ingredients were obtained from Becton Dickinson and Company (USA) and AppliChem (Germany). The autoclaving was done by systec autoclave (program 8). The antibiotics were added after the autoclaving the media and before use. 10x amino acids stocks which were used for minimal media were autoclaved and stored at -20°C and added to the media before use or pouring plates. At the "Institute of biochemistry and molecular biology" in Freiburg amino acids were added before autoclaving.

2.2.2 Growth media for E.coli strains

E.coli strains were cultivated in Luria Bertani medium (LB). For the selection of *E.coli* strains carrying the plasmid, 100mg/ml of Ampicillin was added to the media before the cultivation of the *E.coli* culture. Components of the LB medium can be seen in the Table 2.4.

Table 2.5. LB Medium used for the cultivation of the *E.coli* culture

Medium	Ingredients
Luria Bertani Medium (LB)	0.5% Yeast Extract
	0.5% Natriumchlorid
	1% Bacto-Trypton
	(Plates: 2% Agar)
	(Selection: 100mg/ml Ampicillin)

2.2.3 Growth media for *S. cerevisiae*

S. cerevisiae strains were cultivated in full media or minimal media containing different carbon sources, such as glucose or galactose. Full media contained all the amino acids, adenine and uracil, while minimal media were lacking one or more depending on the plasmid yeast is carrying. The media used for the cultivation of the yeast culture are listed in the Table 2.6 and 2.7.

Table 2.6. List of the components of the full media used in this work for the cultivation of yeast cultures

Medium	Ingredients
Yeast Peptone Dextrose (YPD)	1% Yeast Extract
Full medium	2% Bacto-Peptone
	4% Glucose
	(Plates: 2% Agar)

Table 2.7 List of the components of the minimal media used in this work for the cultivation of yeast cultures at both institutes

Media used at the "Institute of Molecular Biosciences" in Graz

Medium	Ingredients
Synthetic Medium Dextrose (SMD)	0,17% Yeast Nitrogen Base
Minimal medium	0,5% Ammonium sulfate
	2% Glucose

	320mg/l Uracil
	200mg/l Leucine
	80mg/l Histidine
	30mg/l Adenine
	30mg/l all other amino acids
Synthetic Medium Galactose (SMG)	0,17% Yeast Nitrogen Base
Minimal medium	0,5% Ammonium sulfate
	2% Galactose
	320mg/l Uracil
	200mg/l Leucine
	80mg/l Histidine
	30mg/l Adenine
	30mg/l all other amino acids

Media used at the "Institute of biochemistry and molecular biology" in Freiburg

Medium	**Ingredients**
Synthetic Medium Dextrose (SMD)	0,67% Yeast Nitrogen Base
Minimal medium	2% Glucose
	0,8g/l CSM mix-Histidin (-Uracil)
Synthetic Medium Galactose (SMG)	0,67% Yeast Nitrogen Base
Minimal medium	2% Galactose
	0,8g/l CSM mix-Histidin (-Uracil)

2.3 Cultivation and storage

2.3.1 Incubation of liquid cultures

Liquid cultures of *E. coli* strains were incubated in a shaker at 37°C and 145 rpm until the desired density of cells was reached. Liquid cultures of *S. cerevisiae* strains were incubated in a shaker at 28°C and 145 rpm until the desired density of cells was reached. At the "Institute of biochemistry and molecular biology" in Freiburg *S. cerevisiae* strains were incubated in at 30°C.

2.3.2 Incubation of plate cultures

Plate cultures of *E. coli strains* were incubated for one day at 37°C and stored at 4°C for up to one month. Plate cultures of *S. cerevisiae* strains were incubated for two or more days at 28°C (30°C) and stored at 4°C for up to one month.

2.3.3 Long-time storage of cultures

For the storage in tubes, 750µl of the overnight culture was mixed with 750µl 50% glycerol and stored at -70°C. For the storage in ELISA plates, 125µl of the overnight culture was mixed with 125µl 50% glycerol and stored at -70°C.

2.4 Laboratory equipment

The Equipment which was used in this work at both institutes is listed in following table.

Table 2.8. Equipment used during this work

Equipment used at the "Institute of Molecular Biosciences" in Graz

CASY cell counter	Schärfe System, Germany
BD FACSAria™ Flow Cytometer	BD Biosciences, USA
LemnaTec Colony Counter	Lemna Tec
Fluorescence microscope	Zeiss, Germany
Pipettes	Eppendorf AG, Germany; Socorex, Swiss

Tips	Eppendorf AG, Germany
Reaction tubes	Eppendorf AG, Germany
Minispin centrifuge	Heraeus, Germany
RC5C centrifuge	Sorvall Instruments
5403 centrifuge	Eppendorf AG, Germany
Electroporator	Eppendorf AG, Germany
Shaker for liquid cultures	Infors AG, Swiss
Autoclaves	Systec
Vortex	Kika Labortechnik, Austria
Freezer	Thermo Forma, USA
Incubator	Heraeus Instruments, Germany
pH meter	inoLab
Thermocycler	Thermo Hybaid
Scales	Sartorius, Germany
Electrophoreseboard for agarose gels	Thermo EC
Agarose gel documentation system	Biozym Diagnostic
UV transilluminator	UVP Inc.
Tecan	Tecan, Austria
Spectrophotometer	Hitachi

Additional equipment used at the "Institute of biochemistry and molecular biology" in Freiburg

ImageQuant LAS 4000	GE Healthcare Life Sciences
NuPage Xcell4 SureLock™ Midi-Cell	Life Technologies
4-12% NuPAGE Novex Bis-Tris Gels	Life Technologies
Semi dry blotting system	GALILEO bioscience

2.5 Chemicals

All the kits, substances and chemicals used for various assays and experiments in this work, at the "Institute of Molecular Biosciences" in Graz and the "Institute of biochemistry and molecular biology" in Freiburg, are listed in this chapter and can be seen in Table 2.9.

Table 2.9. Used kits, substances, enzymes and chemicals in this work

Used kits, substances, enzymes and chemicals at the "Institute of Molecular Biosciences" in Graz	
Yeast extract	Becton, Dickinson and Company, USA
Bacto-pepton	Becton, Dickinson and Company, USA
Bacto-trypton	Becton, Dickinson and Company, USA
Yeast nitrogen base	Becton, Dickinson and Company, USA
Agar	Becton, Dickinson and Company, USA
Amino acids	AppliChem., Germany
GeneJET™ Plasmid Miniprep Kit	Fermentas
GeneJET™ Gel Extraction Kit	Fermentas
GeneJET™ PCR Purification Kit	Fermentas
Restriction enzymes	Fermentas
Primer	MWG Biotech, Germany

Taq Pilymerase	Finnzymes
Lambda DNA/EcoRI+HindIII Marker	Fermentas
DHE	Sigma
PI	Roche, Germany
Sorbitol	Fluka BioChemika
Microscope Slide	BRAND GMBH + CO KG, Germany
Other chemicals	ROTH, Germany; FLUKA Chemie, Swiss; SIGMA, USA

Additional substances used at the "Institute of biochemistry and molecular biology" in Freiburg

NaOH	ROTH
SDS	SERVA
Glycerol	SIGMA ALDRICH
TRIS	MP Biomedicals
β-mercaptoethanol	ROTH
K2HPO4	ROTH
KH2PO4	ROTH
Zymolase	SEIKAGAKU
EDTA	Calbiochem
Proteinase Inhibitor	ROCHE
Starta Clean	Agilent
MOPS	SIGMA
ProteinaseK	ROCHE

ECL	GE Healthcare
MES	ROTH
Acrylamid	ROTH

In addition at the "Institute of biochemistry and molecular biology" in Freiburg, for the fibrilisation assay, synthetic A40 and A42 peptides were used. A40 was obtained from SIGMA and A42 was obtained from Bachem. The antibodies used for the detection of the proteins are listed in the Table 2.10.

Table 2.10. Used antibodies in this work

Used antibodies at the "Institute of Molecular Biosciences" in Graz	
GFP (mouse)	Roche
α-mouse POD	Sigma
Used antibodies at the "Institute of biochemistry and molecular biology" in Freiburg	
α-Amyloid beta	Milipore
α-Amyloid beta	Covance
α-GFP	Novus Biologicals
α-Ssa1	Gramsch
α-Ydj1	Gramsch
α-Pgk1	Gramsch
α-Sss1	Gramsch
α-Tom22	Gramsch
α-Sec61	Gramsch
α-Kar2	Gramsch
α-Ssc1	Gramsch

α-Jackson	Sigma
α-Mouse	Sigma

2.6 Solution and buffers

The ingredients of solutions and buffers used in this work at both institutes are listed in this chapter and can be seen in the Table 2.10.

Table 2.10. Solutions used in this work

"Institute of Molecular Biosciences" in Graz

Solution	**Components**
Agarose gel electrophoresis	
Loading Buffer	Brominephenolblue in 87% glycerin
TAE	40 mM Tris/Acetat
	1 mM EDTA, pH 8.0
Agarase Gel	1% Agarose in TAE
	0,001% ethidiumbromide
Yeast transformation	
10xTE	100 mM Tris pH 7.5
	10 mM EDTA
10xLiAc	1 M LiAC
50% PEG	50 % Polyethylenglykol 3350
Carrier-DNA (ssDNA)	Hering sperm DNA (10 mg/ml)
DHE staining	
PBS buffer	25 mM potassium phosphate buffer

	0.9% NaCl (w/v)
	pH 7.0
DHE (2.5 mg/ml)	1:1000 dilution in PBS buffer
Stress agents	
10 M potassium acetate	0,084 g potassium acetate
	6.4 ml 100% glacial acetic acid
	filled up to 10 ml with ddH_2O

Additional solutions – "Institute of biochemistry and molecular biology" in Freiburg

Solution	**Components**
SDS Page and Western blotting	
Running gel	390 mM Tris/HCl pH 8,8
	0,01 % SDS
	12,5 % Acrylamide
	0,6 % ammonium peroxydisulfate
	0,1 % N,N,N‘,N‘-Tetramethylethylenediamine
Stacking gel	60 mM Tris/HCl pH 6,8
	0,1 % SDS
	5 % Acrylamide
	1 % ammonium peroxydisulfate
	0,2 % N,N,N‘,N‘-Tetramethylethylenediamine
Cell lysis	
Laemmli buffer	2g SDS

	10% Glycerol
	0,727g Tris
	pH 6,8 HCl
	0,02g bromophenol blue
	5% β-Mercaptoethanol
	filled up to 100 ml with ddH_2O
Cellular fractionation	
DTT buffer	100mM Tris pH 9,4/H_2SO_4
	10mM DTT
Sorbitol buffer	2,4M
Zymolase buffer	1,2M Sorbitol
	20mM Kpi
	0.5%(w/v) Zymolase per strain
Kpi	1M K_2HPO_4 (basic)
	1M KH_2PO_4 (acidic)
	Titration of the basic solution with the acidic solution to pH 7,4
Homogenization buffer	0,6M Sorbitol
	10mM Tris pH 6,4
	1mM EDTA
	1mM PMSF

	Filled up to 1500 ml with H_2O
PMSF	0,2M in Ethanol
SEM buffer	85,58g Saccharose
	0,372g EDTA
	2,1g MOPS
	pH 6 with KOH

3. Methods

In this chapter all of the methods used at the both institutes are listed and described.

3.1 Molecular cloning

3.1.1 Polymerase chain reaction

Polymerase chain reaction (PCR) is a method in molecular biology which is used for the amplification of wanted DNA *in vitro*. Essential for this reaction are DNA template, dNTPs, DNA polymerase, two primers, DNA polymerase buffer, as well as water (ddH_20). The total volume which is required for the reaction is between 20µl and 50µl. PCR program starts initialization step, with DNA denaturation at 95°C for 5 minutes. The cycling begins with the denaturation at 95°C for one minute and primer annealing which is 2 degrees lower than Tm (temperature melting) of the two primers. The next step of cycling is performed at the 72°C. This step is required for the elongation, in which the DNA polymerase synthesizes new DNA strands complementary to the DNA template. This temperature is dependent on the optimum of the used DNA polymerase. The DNA polymerase links the 5'-phosphate group of the dNTPs with the 3'-hydroxyl group of the synthesized DNA strand. After the last cycle the elongation temperature is hold for further 10 minutes to ensure the completion of started DNA synthesis. At the end of the program the temperature is lowered to 4°C. PCR reactions can be stored at 4°C.

3.1.2 Agarose gel electrophoresis

Agarose gel electrophoresis is a method used for the separation and analysis of the DNA and its fragments, based on size and charge of the DNA. Used gel in this work was 1% agarose gel. The agarose was solved in 1xTAE buffer to get the 1% solution and heated up in the microwave for 2-3 minutes to melt the agarose. After cooling down the gel solution, it is poured into the gel chamber, where ethidiumbromid (0,001%) is added. Air bubbles were removed using comb, which is afterwards used for forming of the wells. After 20-30 minutes the gel is polymerized and is ready for use. The samples, which contain 1 x loading dye, can be 44immers into the wells. For the quantification of the DNA samples, a DNA marker Lambda DNA EcoRI/HindIII is also loaded into the gel. The electrophoresis is carried out in 0.5 x TAE buffer at 90 Volt. The gel was evaluated using UV to visualize the DNA bands. The Lambda DNA EcoRI/HindIII standard can be seen in the Figure 3.1.

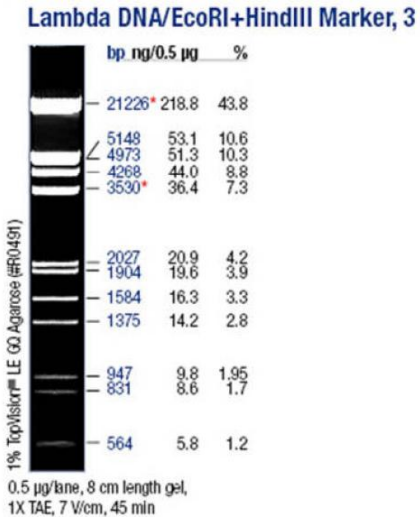

Figure 3.1. The Lambda DNA/EcoRI+HindIII marker. DNA marker used as standard for the agarose gel electrophoresis in this work.

3.1.3 Purification of the PCR product

The purification of the PCR product was performed using "PCR clean up kit" by Fermentas. The instructions were given from the producer.

3.1.4 Restriction digest

Restriction enzymes are able to cleave the double stranded DNA at the specific DNA sequences or near the recognized sequence. These enzymes are primarily isolated from bacteria. ClaI and SpeI were used for the PCR product and pESC-his_nGFP_G vector digest. Both of the enzymes work in Buffer Tango. The reaction lasted for 4h at 37°C and was stopped at 80°C for 20 minutes.

3.1.5 Gel extraction of DNA

The DNA from the gel can be purified using the "Gel Extraction Kit" by Fermentas, following the instructions of the producer. In this work the whole volume of the digest mix was loaded to the gel electrophoresis and exposed to UV light. The wanted bands were cut from the gel with a scalpel.

3.1.6 Ligation

For the efficient ligation, 1:3 ratio of vector to insert is required after the determination of the fragment concentrations in the gel. This reaction is performed using T4 DNA Ligase, which is combined with the ddH2O, digested plasmid and PCR products, as well as the ligase buffer. The reaction was performed over night at 16°C. The inactivation of the ligase was done by heat-shock for 15 minutes at 65°C. The ligation mixture has to be desalted for 30-60 minutes before the *E.coli* transformation. This process was done using little filters floating on ddH_2O.

3.1.7 E.coli XL-1 transformation

E.coli transformation is a process of the DNA transfer into the bacteria cells. Competent bacteria cells are essential for this process due to transfer of the DNA. XL-1 competent *E.coli* cells (40µl) were used in this work for this experiment. After the cells were slowly defrosted on ice, they were 45immers into electroporation cuvettes together with the plasmid DNA and placed into the electroporator. The electro shock was at 1750V after which 1ml of LB medium was added to the cells. The regeneration of the cells was 30 minutes at 37°C. Finally the cells were platted onto LB plates containing 100µl/ml ampicillin. The ampicillin is essential for the selection of *E. coli* cells that carry a plasmid. The plates were incubated for 1 day at 37°C.

3.1.8 Colony PCR

After the DNA transformation, the colonies from the LB-ampicillin plates were picked up and the clones were verified using PCR colony method. At the same time chosen colonies were streaked out on a new plate. After the PCR reaction was finished, PCR products were analyzed using agarose gel electrophoresis.

3.1.9 Yeast transformation

Aim of this method is to transfer the DNA into yeast cells. 3ml of the yeast culture is cultivated over night in required media depending if the cells already contain another plasmid. The following day, the cells are diluted to OD_{600} → 0.2 in 50 ml of the final volume. The culture is cultivated next 4-5h to OD_{600} → 0.6-0.8. The cells are centrifuged by 3500rpm for 3 minutes and washed with 10ml ddH_2O. The centrifugation step is repeated and the cells are washed with 1xLithium Acetate/0.5xTE. The cells are third time centrifuged and the pellets are resuspended in 300µl 1xLithium Acetate/0.5xTE and incubated for 30 minutes at 28°C. During this time the carrier DNA was prepared for 10 minutes at 95°C and then 10 minutes on ice. 5µl Carrier-DNA, 1µg Plasmid-DNA and 300µl 40%PEG/1xLiAc/1xTE were added to 50µl of the cells and vortexed for 30 seconds. After an incubation of 30 minutes at 28°C the cells were heat-shocked for 20 minutes at 42°C and centrifuged for 15 seconds at 10 000 rpm. The cells were resuspended in 100µl ddH2O and plated on the corresponding selection SMD agar plates. The plates were incubated for two or more days at 28°C.

3.1.10 Plasmid isolation

The plasmid isolation from the *E.coli* was performed using "Plasmid Isolation Kit" by Fermentas by following the instructions of the producers. Electrophoresis gel is run to verify isolated plasmids and their concentration.

3.2 Sequencing

Sequencing is done by MWG Biotech AG, Sequencing Department, Germany. For the sequencing procedure, 2µg DNA has to be solved in 20µl 5 mM Tris/HCl (pH 8.0).

3.3 Fluorescence microscopy

For the microcopy procedure, aliquots of the yeast culture are centrifuged for 1 minute at 10 000rpm and ca. 2µl is applied to microscope slides, which are covered with a cover glass and examined under the fluorescence microscope. The green fluorescence of the EGFP tag was observed with an EGFP filter.

3.4 Whole yeast Extracts (WCE)

The whole yeast extracts experiments which were done at the "Institute of biochemistry and molecular biology" in Freiburg were performed using this protocol:

For the standard whole yeast extract (1xWCE) OD_{600}→ 2.5 cells have to been harvested and solve in 150µl 1xLaemmli buffer. WCE can also be higher concentrated, depending on the amount of the protein that is needed for the antibody detection. The cells are harvested at 4000 rpm and for 5 minute at room temperature (RT). The supernatant is discarded and the pellet is resuspended in 0.1M NaOH (200µl per 2.5 OD_{600}). The next step is incubation for 5 minutes at 1400 rpm and RT. The extract is again centrifuged and supernatant discarded. The pellet is resuspend in 150µl 1xLaemmli buffer/5% β-mercaptoethanol. In the next step the extract is incubated for 10 minutes at 1400rpm and RT. The last step is the centrifugation of the extract at the 14000 rpm and RT for 1 minute. The extract is than ready for the loading on the polyacrylamide gel.

3.5 Cellular fractionation

The cellular fractionation experiments were performed at the "Institute of biochemistry and molecular biology" in Freiburg.

For the cellular fractionation, 5ml of the yeast cells were inoculated overnight in required media and the following day 70OD of yeast cells were harvested at 4000rpm at 5 minutes and RT. The pellets are resuspended with ddH_2O and transferred to 2ml tubes and again centrifuged. The supernatant is discarded and the pellets are resuspended in 2ml DTT reduction buffer, after which the cells are incubated for 10 minutes at 1000rpm and 30°C, to break the disulfide bonds within cell wall proteins. In the next step cells are centrifuged again and resuspended in 1ml zymolase buffer without zymolase. After the cells were harvested again, zymolase buffer was added again to cells with zymolase (5mg/strain solved in 100µl zymolase buffer) to generate spheroplasts. The cells are incubated for 45 minutes at 1000rpm and 30°C. After the incubation, generation of the spheroplasts is checked under the

microscope. Spheroplastas appear as spherical cells with bright halos. The next step is spinning down the spheroplastas for 5 minutes at 1500g. Zymolases and other contaminating proteases and enzymes are removed by washing the cells with 1ml 1.2M sorbitol. All the following steps are performed at 4°C. The spheroplasts are harvested for 5 minutes at 1500g and 4°C and resuspended in 2ml homogenization buffer with 1mM PMSF and 1xPIs, after which the spheroplasts were dounced 20 times in cooled glass-Teflon potter on ice. The samples were subjected to a cleaning spin (300g, 4°C, 5 minutes) to remove unlyzed cells, nuclei and larger aggregates. To prevent contamination the supernatant fractions with the pellet only 80% of the supernatants were harvested. Half of the supernatant is saved for further processing as post nuclear supernatant (PNS). The other half of the supernatant is further centrifuged (13000g, 4°C, 15 minutes) to generate the mitochondrial pellet (P13 fraction) and supernatant, the microsome/ER fraction and cytoplasm (S100 and P100). After the centrifugation step the supernatant is carefully transferred into ultracentrifuge tube. However due to preventing P13 contamination in ER fraction, small volume of supernatant above the pellet remains in the tube and it is centrifuged again (13000g, 4°C, 30 seconds) and the rest of the supernatant is discarded away. The P13 (mitochondria) pellet is resuspended in 1ml SEM buffer and carefully homogenized with a glass-Teflon potter on ice and subjected to centrifugation (13000g, 4°C, 10 minutes). The supernatant is discarded and 200µl of 1xLaemmli/5% β-mercaptoethanol/1xPIs is added to pellet and incubated for 10 minutes at 25°C and 1400rpm. The mitochondrial fraction is after this step ready for the loading into gel. At the same time the S100/P100 fraction is centrifuged at 100 000g for 1 hour at 4°C. After the centrifugation the supernatant is removed to new tube as cytoplasm fraction (S100). To prevent ER contamination in S100 small amount of supernatant above the pellet remains and it is centrifuged again (30s, 13 000g, 4°C). After the centrifuge, the rests of supernatant is discarded. Remained pellet is P100 fraction which is resuspended in 200µl 1xLaemmli/5% β-mercaptoethanol/1xPIs and incubated for 10 minutes at 25°C and 1400rpm. After this step P100 fraction is ready for the loading into gel. The PNS and S100 fractions are processed further. 60µl of StrataCleanResin is added to samples and incubated for 20 minutes at RT and 1400rpm. After the incubation the fractions are spinned down for 1 minute, at 14000rpm and RT. The supernatant is discarded and the pellets of S100/PNS fractions are resuspended in 200µl 1xLaemmli/5% β-mercaptoethanol/1xPIs and incubated for 10 minutes at 25°C and 1400rpm. Last step is centrifugation at 14 000rpm and RT for 1 minute. The samples are ready for loading the gel.

3.6 Mitochondrial isolation

The mitochondrial isolation experiments were performed at the "Institute of biochemistry and molecular biology" in Freiburg.

For the cellular fractionation, 5ml of the yeast cells were inoculated overnight in required media and the following day 70OD of yeast cells were harvested at 4000rpm at 5 minutes and RT. The pellets are resuspended with ddH_2O and transferred to 2ml tubes and again centrifuged. The supernatant is discarded and the pellets are resuspended in 2ml DTT reduction buffer, after which the cells are incubated for 10 minutes at 1000rpm and 30°C, to break the disulfide bonds within cell wall proteins. In the next step cells are centrifuged again and resuspended in 1ml zymolase buffer without zymolase. After the cells were harvested again, zymolase buffer was added again to cells with zymolase (5mg/strain solved in 100µl zymolase buffer) to generate spheroplasts. The cells are incubated for 45 minutes at 1000rpm and 30°C. After the incubation, generation of the spheroplasts is checked under the microscope. Spheroplastas appear as spherical cells with bright halos. The next step is spinning down the spheroplastas for 5 minutes at 1500g. Zymolases and other contaminating proteases and enzymes are removed by washing the cells with 1ml 1.2M sorbitol. All the following steps are performed at 4°C. The spheroplasts are harvested for 5 minutes at 1500g and 4°C and resuspended in 1ml homogenization buffer with 1mM PMSF and 1xPIs, after which the spheroplasts were dounced 20 times in cooled glass-Teflon potter on ice. The samples were subjected to a cleaning spin (300g, 4°C, 5 minutes) to remove unlyzed cells, nuclei and larger aggregates. To prevent contamination the supernatant fractions with the pellet only 80% of the supernatants were harvested and transferred in new tube and the cleaning spin is repeated and supernatant is transferred to new tube. For the generation of P13 fraction is centrifuged for 10 minutes at 13 000g and 4°C. The supernatant is discarded and the P13 pellet is resuspended in 1ml SEM and treated with 10 strokes on the ice with a glass-Teflon potter. The fraction is centrifuged for 5 minutes, at 4000rpm and 4°C. Supernatant is transferred to new tube and centrifuged for 10 minutes at 14 000rpm and 4°C and supernatant is discarded. Pellet is resuspended in SEM buffer depended on the desirable mitochondria concentration.

3.7 SDS Assay

The SDS Assay experiments were performed at the "Institute of biochemistry and molecular biology" in Freiburg.

To test whether our yeast system can generate SDS-stable oligomers, SDS assays were performed. To perform this assay, 5ml yeast cells were inoculated over night and on the following day 10OD of cells was harvested (4000rpm, 5 minutes, RT). Pellets are resuspended in 0.1M NaOH and incubated for 5 minutes at 1400rpm and RT. The cells are equally divided into new tubes and centrifuged (4000rpm, 5

minutes, RT) and the supernatant is discarded. The pellets are resuspended 1x Laemmli/2%SDS (10OD/240µl). One half is incubated for 7 minutes at 1400rpm and RT, the other half 5 minutes at 1400rpm and 95°C. The samples are centrifuged for 1 minute, at 14000rpm and RT and loaded into the gels.

3.8 Fibrillization Assay

The Fibrillization Assay experiments were performed at the "Institute of biochemistry and molecular biology" in Freiburg.

The synthetic A42 and A40 are diluted with 1xPBS to the final concentration of 50µM. 20µl of synthetic peptides are incubated for 24 hours, at 1000rpm and 37°C. To the samples 100µl 1x Laemmli without β-mercaptoethanol is added and the samples are incubated for 10 minutes at 1400rpm and 25°C and then loaded into the gels. The controls, non-fibrillated peptides were also generated. To 20µl of synthetic peptides (50µM), 100µl 1x Laemmli/5%β-mercaptoethanol is added and the samples are incubated for 5 minutes at 1400rpm and 95°C and then loaded into the gels.

3.9 Polyacrylamide gel electrophoresis and Western Blotting

Western blotting experiments were performed at the "Institute of biochemistry and molecular biology" in Freiburg.

One-dimensional vertical SDS polyacrylamide or NuPage gel electrophoresis was performed to separate proteins according to their molecular weight under denaturing conditions. Separation of proteins loaded to the SDS gels was performed at 25mA and of proteins loaded to the 4%-12% Bis-Tris NuPage gels was performed at 400mM. After the gel electrophoresis proteins were transferred to Polyvinylidendifluorid (PVDF) membranes using semi dry transfer method. Before use, PVDF membranes were activated with methanol. Whatman paper has to be equilibrated in blotting buffer (20mM Tris base, 150mM glycine, 20% (v/v) methanol, 0.08% (w/v)) and placed on the anode electrode. The activated membrane is placed on the Whatman paper. Further the gel is placed on the membrane together with three additional sheets of Whatman paper. The cathode electrode is placed on the top and the electrotransfer was performed at 250mA for 2.5h. The visualization of protein marker bands was carried out by reversible staining of the membrane with Coomassie blue stainer (0.5% (w/v) coomassie brilliant blue R-250, 10% (v/v) acetic acid, 40% (v/v) ethanol). The membranes were destained using destaining buffer (50% (v/v) methanol, 10% (v/v) acetic acid) and methanol. The membranes were ready for the blocking and immunodecoration. After western blotting membranes were incubated for 60 minutes with TBS

(150mM NaCl, 10mM Tris-HCl, pH7.5)/5% (w/v) milk power to block nonspecific binding sites. The membranes are then incubated with the primary antibody over night at 4°C. The membranes are then washed five times for 45 minutes in TBST (0.1% Tween20, 150mM NaCl, 10mM Tris-HCl pH 7.5). After the washing step, membranes are ready for the incubation with the secondary antibody coupled with horseradish peroxidase for 1.5h at RT. The membrane are washed five times for 45 minutes at RT and then treated with chemiluminescence solution (ECL, or ECL prime). The signals were detected using LAS-4000 system and processed by the Multi Gauge software.

3.10 Chronological aging scheme

Chronological aging experiments were performed using 96 deep well plates or 100ml flasks. In this work two inoculation scheme were used. The inoculation scheme 2 was used for respiratory deficient strains, rho0 and *oxa1Δ.* The illustrated scheme 1 and scheme 2 can be seen in Figure 3.2.

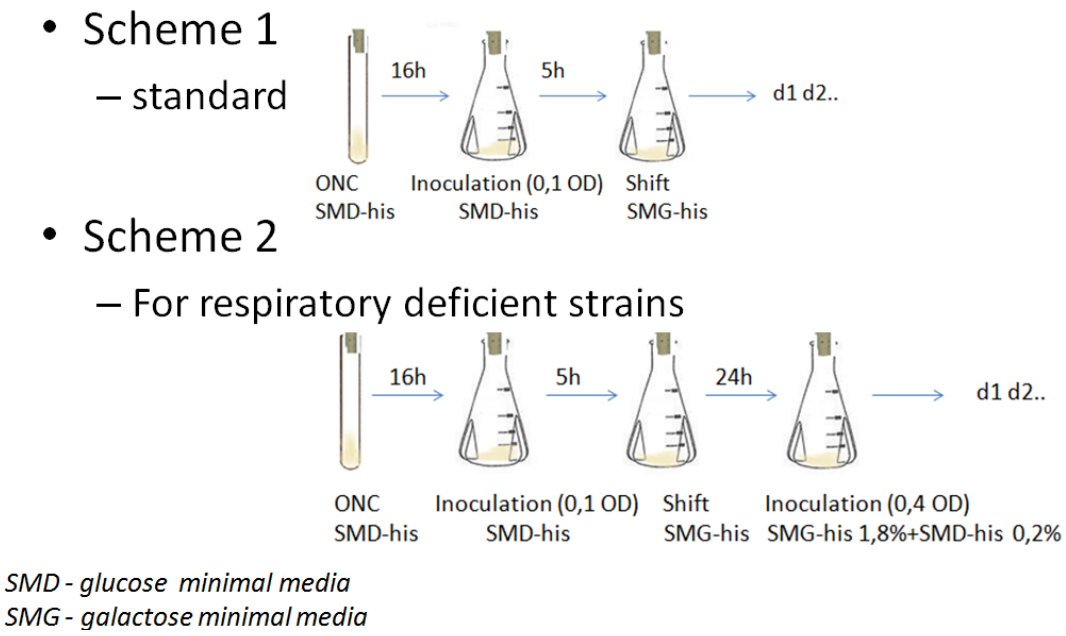

Figure 3.2. Inoculation scheme used in this work. The Inoculation scheme 1 is a standard scheme used for most of the strains. The inoculation scheme 2 was used for the respiratory deficient strains.

3.10.1 Chronological aging experiments in 96 deep well plates

For most of the experiments 96 deep well plates were used. For the aging in 96 deep well plates, ONCs were prepared by inoculation of 200µl of corresponding media with a yeast colony. The plates were incubated in deep well shaker at 28°C and 145rpm overnight for 20 hours. The following day, a new 96 well plate was prepared and filed with fresh glucose medium (SMD) in which 5µl of overnight culture was inoculated. Depending on the strain, inoculation of 6µl-10µl overnight culture is also possible. The cells are further inoculated for 5h and than were harvested (5 minutes, 4000rpm, RT). The medium was replaced by galactose medium (SMG) due to activation of the transformed peptide expression. The following day, was the day 1 of the aging in inoculation scheme 1. One additional step was performed in inoculation scheme 2. After 24h hours of incubation of the cells with SMG medium, OD_{600} of the cells was measured by TECAN. The cells were then inoculated with SMG 1.8% + SMD 0.2% fresh medium to $0.4OD_{600}$.

3.10.2 Chronological aging experiments in 100ml flasks

For the aging experiments in 100ml flasks ONCs were prepared by inoculation of 3ml of the corresponding SMD medium with a yeast colony and incubated in a shaker at 28°C and 145 rpm over night for 16 hours. The following day 100ml flasks with 10 to 15ml SMD medium were inoculated with the ONCs to an OD_{600} = 0.1. The cultures were incubated following 5 hours, after which cells were harvested for 5 minutes at 4000rpm and RT. After centrifugation, SMD medium was replaced with SMG medium. One additional step was performed in inoculation scheme 2. After 24h hours of incubation of the cells with SMG medium, OD_{600} of the cells was measured. The cells were then inoculated with SMG 1.8% + SMD 0.2% fresh medium to $0.4OD_{600}$.

3.11 DHE staining

Dihydroethidium (DHE) is substance which is used for measuring the ROS levels in cells, as an early apoptotic cell death marker. DHE can be converted to Ethidium in presence of the ROS. This conversion can be measured via flow cytometry analysis (FACS). 1.0×10^7 cells are harvested (5 minutes, 4000rpm, RT) and the pellets were resuspended in 250µl 1xPBS/DHE solution and incubated for 5 minutes in the dark. The centrifugation step was repeated and the pellet was resuspended in 250µl 1xPBS. The cells were ready for the quantification via FACS. For each measurement, 30 000 cells were analyzed.

3.12 Stress experiments with acetic acid

For the stress experiments 96 deep well plates were used. Cell cultures were inoculated and 16h after the cells were transformed to galactose medium, acetic acid is added in required concentrations (100mM, 120mM 140mM and 160mM). The cells were incubated next 4h, after which DHE staining was performed. Cell cultures which were inoculated following the scheme 2, were treated with acidic acid 16h after second inoculation with SMG 1.8% + SMD 0.2% medium.

4. Results

4.1 Human A42 cytotoxicity in wild type yeast BY4741

4.1.1 Heterologous expression of human A42 leads to decreased viability and increased ROS levels in yeast BY4741 during chronological aging and acetic acid treatment

The first goal of this work was to reproduce the former results of heterologous expression of human A42 in wild type (WT) yeast BY4741 like already described in 1.3.3. The experiments were carried out in 96 deep well plates and 100 ml baffled flasks. As already mentioned chronologically aging yeast is used as a model for postmitotic human cells, such as neurons. In this work, ROS levels, as a stress and early cell death marker, were quantified by DHE-staining, as described in 3.12.

Acetic acid can be used as cell death stimuli in yeast research. Human cells are exposed lifelong to stress conditions which makes acetic acid helpful tool for stress condition mimicry and inducer of cell death. Acetic acid was added to cells after 16 hours of EGFP-A42 expression and the ROS levels were measured after 4 hours of treatment. A42 expressing cells were compared to cells harboring the corresponding empty vector (ev) expressing EGFP only.

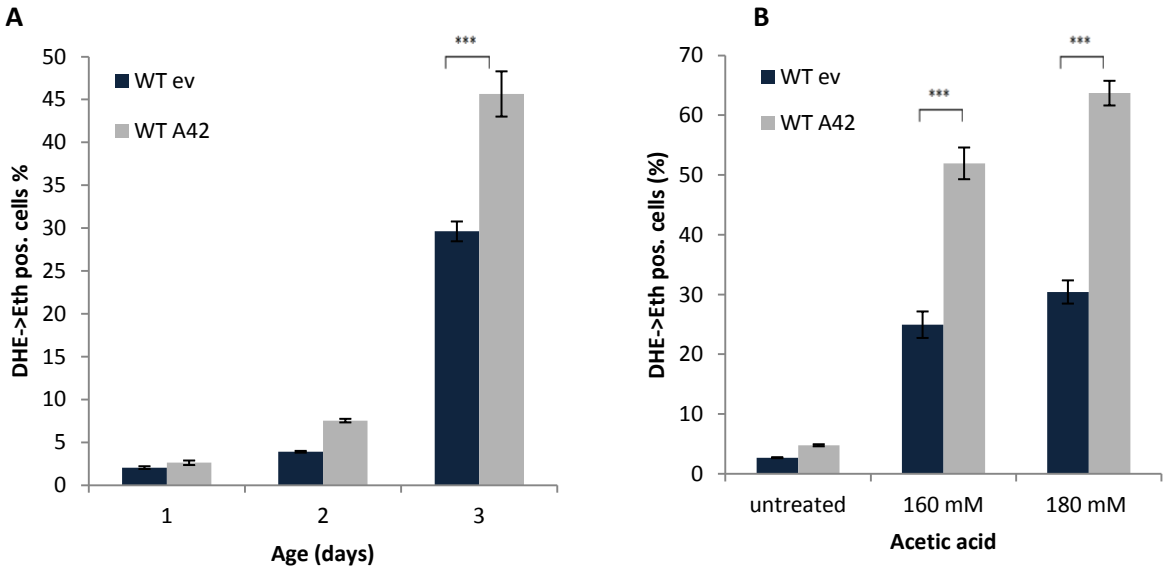

Figure 4.1. Heterologous expression of human A42 leads to decreased viability and increased ROS levels in yeast BY4741 during chronological aging and acetic acid treatment. A BY4741 yeast cells were chronologically aged 3 days. **B** Yeast cultures were treated with acetic acid 16h after EGFP-A42 expression and 4h after were treated with

acetic acid treatment. ROS levels were quantified by DHE-staining. DHE converse to Ethidium due to reaction with ROS, which can be measured by FACS analysis. 30 000 cells were evaluated in each experiment. Data show one representative experiment, mean of 6 tested clones and the error bars, the standard error ($p < 0.001$ = ***, $p < 0.01$ = **, $p < 0.05$ = *).

As expected human A42 expression in yeast showed cytotoxicity, increase in ROS levels during the chronological aging in both, 96 deep well plates and 100 ml flasks (Figure 4.1 and Figure 4.2).

In this work, it was validated that A42-mediated cytotoxicity in yeast cells is accelerated by supplementation of acetic acid compared to the corresponding vector control.

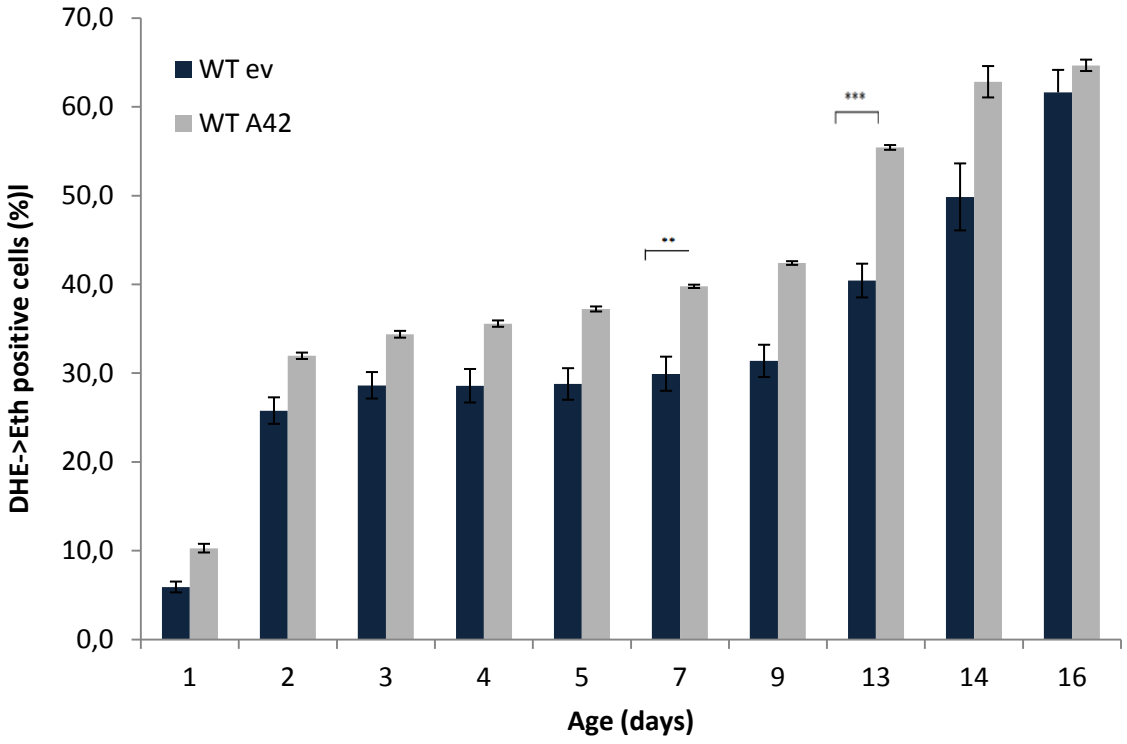

Figure 4.2 **The heterologous expression of human A42 in yeast BY4741 leads to increase of ROS accumulations in chronologically aged cells in flasks.** BY4741 yeast cells were chronologically aged 16 days. ROS levels were quantified by DHE-staining. DHE converse to Ethidium due to reaction with ROS, which can be measured by FACS analysis. 30 000 cells were evaluated in each experiment. Data show one representative experiment, mean of 6 tested clones and the error bars, the standard error ($p < 0.001$ = ***, $p < 0.01$ = **, $p < 0.05$ = *).

The cytotoxicity effect of A42 was more prominent in aging experiments performed in 96 deep well plates. Therefore flasks were not used for aging or stress stimuli in this work.

4.1.2 Disrupting the two hydrophobic domains of A42 totally abolish its cytotoxic phenotype during chronological aging in wild type yeast

It has been hypothesized that the A42 cytotoxicity is mediated by generation of low-n oligomers, in comparison to fibrillar nontoxic forms. This oligomerization is mainly stimulated due to the hydrophobic nature of the A42 peptide. A42 variants with 2 (A42m1) or 3 (A42m2) mutations, disrupting one or both hydrophobic domains of the peptide, showed a decreased amount of toxic oligomers [Bagriantsev and Liebman, 2006]. We used A42m1 (F19T and F20T) and A42m2 (F19T, F20T and I31P), as controls compared to A42, to modulate oligomerization and investigate if there is a decrease in toxicity.

To investigate if substitutions of hydrophobic nature of A42 can abolish its cytotoxicity A42m1 and A42m2 (a kind gift of Susan Liebman) were cloned into pESC-his vector fused to EGFP, in the same manner as A42. To determine the effects of A42m1 and A42m2 on aging yeast cells compared to A42 and its vector control, chronological aging experiments were performed and ROS accumulation in aged cells was quantified (Figure 4.3).

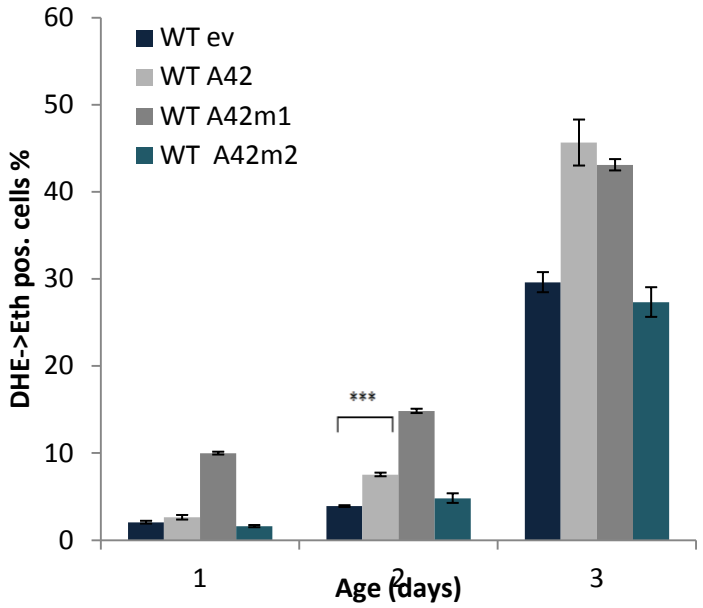

Figure 4.3. Total disruption of hydrophobicity of A42 abolishes cytotoxicity during chronological aging in wild type yeast BY4741. BY4741 yeast cells were chronologically aged 3 days and ROS levels were quantified. ROS was determined by conversion of DHE Ethidium and measured by FACS analysis. 30 000 cells were evaluated in each measurement. Data show one representative experiment, mean of 6 tested clones and the error bars, the standard error ($p < 0.001$ = ***, $p < 0.01$ = **, $p < 0.05$ = *).

The A42m2 mutant, which contains three mutations disrupting 2 regions responsible for the aggregation of A42, does not mediate cytotoxicity during the chronological aging of yeast cultures compared to the corresponding vector control (ev) expressing EGFP only. Cells expressing A42 showed impaired viability and increased ROS levels compared to A42m2 and its vector control. Cells expressing A42m1, which contains two mutations disrupting only one hydrophobic region, showed high ROS levels. Compared to A42, A42m1 shows acceleration in ROS production, as on day 1 there is already an increase of ROS compared to all others, however on day 3 A42 and A42m1 show same amount of ROS.

4.1.3 Mutation of the two hydrophobic regions in A42 prevents its aggregation and translocation to mitochondria

To compare the intracellular localization and aggregation of EGFP linked to A42, A42m1 and A42m2 and its corresponding vector control, wild type yeast cells were fluorescence microscoped under FITC filter for the green fluorescence of the EGFP protein. The chronologically aged yeast cells were analyzed by fluorescence microscopy after ~20h of expression (Figure 4.4).

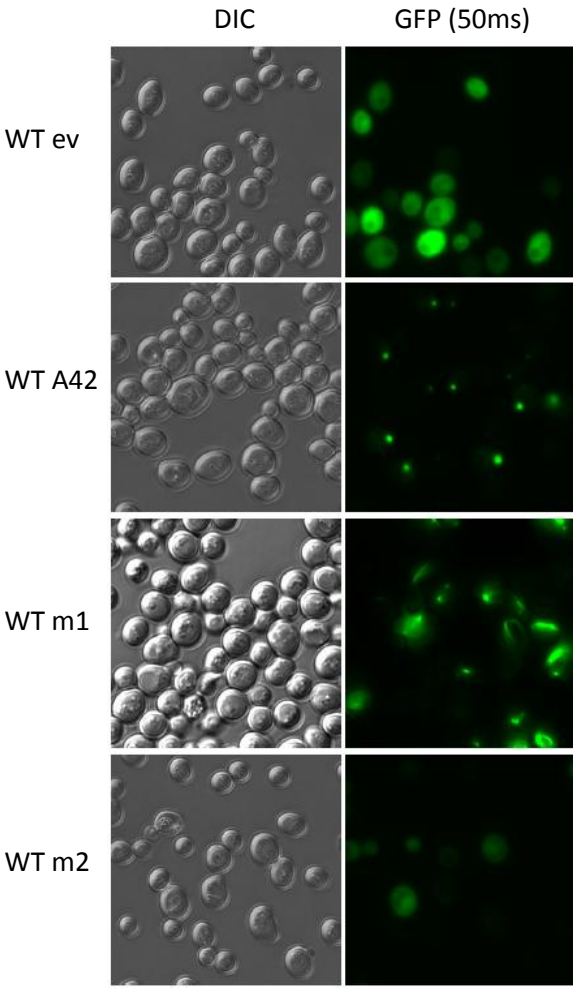

Figure 4.4. Fluorescence microscopy demonstrates that A42m2 mutant does not reveal puncative structures as A42. Wild type yeast cells with N-terminal EGFP-tagged human A42, A42m1 and A42m2 and corresponding vector control with EGFP only, were fluorescence microscoped after ~20h of expression. For the microscopy an aliquot of the yeast cultures was harvested and 2µl were taken from the cell pellet. FITC filter was used for the green fluorescence of EGFP-constructs. Representative micrographs are shown.

Fluorescence microscopy revealed aggregate-like structures in cells expressing A42. Wild type cells expressing EGFP-A42m2 displayed cytosolically distributed localization such as wild type cells expressing only EGFP. Wild type cells expressing EGFP-A42m1 displayed rather linear than puncative structures.

To further investigate the localization of the EGFP-A42 variants, a cellular fractionation was performed by Dirk Mossmann, Chris Meisinger group in Freiburg. 70OD cells were harvested after 16h of constructs expression and cellular fractionation was performed. The fractions include total fraction, so called post nuclear supernatant (PNS), mitochondria fraction (P13), ER and microsomes fraction (P100)

and cytosolic fraction. To investigate if the fractions are contaminated with other fractions, a control gel was run. Mitochondria fraction was examined with the Tom22 antibody, due to the fact that Tom22 protein localize only to the mitochondria. Similarly, ER/microsome (P100) fraction was examined with antibodies which can bind to Kar2 and Sss1 and the cytosolic fraction (S100) was tested with Pgk1 antibody, which binds to cytosolic protein. The EGFP-Aβ variants were detected using an Aβ antibody (Figure 4.5).

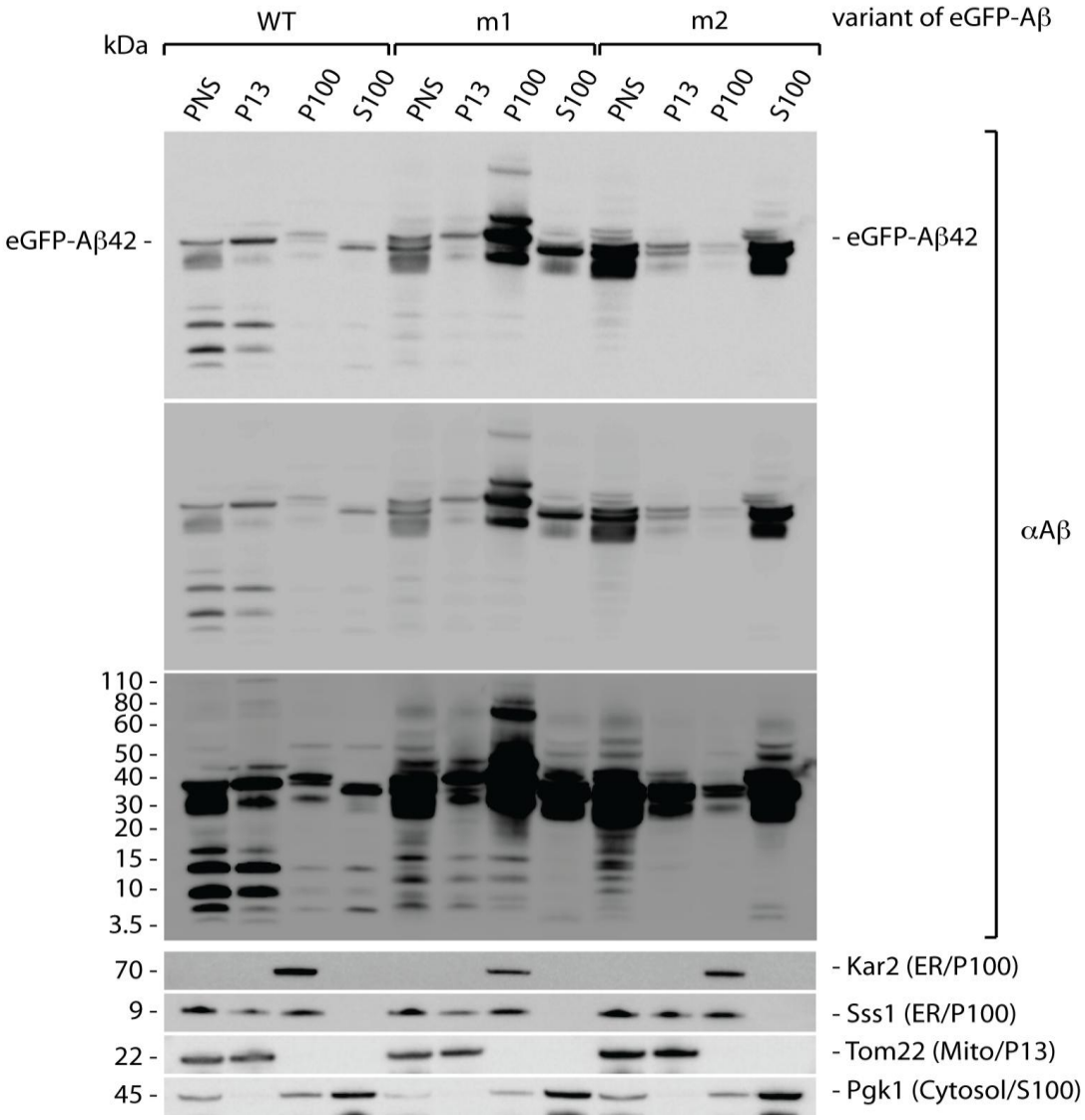

Figure 4.5. A42 localizes mainly to the mitochondria fraction whereas A4m2 localizes mainly to cytosolic fraction and A42m1 to microsome fraction (Dirk Mossmann, AG Chris Meisinger, Freiburg, Germany). The cellular fractionation was performed 16h after the constructs expression in BY4741 yeast cells. The obtained fractions were loaded to the 4%-12% Bis-Tris NuPage gel after which polyacrylamide gel electrophoresis was performed.

The proteins from the gel were transferred to the membrane using semi dry transfer blotting method, after which the membranes were ready for blocking and immunodecoration. Representative blot is shown. Aβ antibody was used for the recognition of Aβ-variants. Post nuclear supernatant (PNS); mitochondria fraction (P13) – Tom22 antibody; ER/microsome fraction (P100) – Kar2 and Sss1 antibodies; cytosolic fraction (S100) – Pgk1 antibody.

The full length of EGFP-Aβ variants is ~34kDa. According to the performed cellular fractionation A42-construct localizes mainly to the mitochondria fraction, whereas A42m2-contruct localizes in the cytosolic fraction. On the other hand the A42m1-construct localizes to the ER/microsome fraction. In addition, other bands, which differ in length, are also visible. The smallest band is around 3.5kDa indicating to A42 monomer or EGFP-A42 fragment which is still detectible with the Aβ-antibody. Cells expressing EGFP-A42 also distributed bands size ~7kDa, ~10kDa, ~15kDa, 18kDa and some higher than the full length construct. In contrary, cells expressing EGFP-A42m2 do not distribute the smaller size bands. However, bands at the size ~3.5kDa and ~7kDa are slightly visible. The band muster of the EGFP-A42m1 differ from the other two Aβ variants and reveals fewer amount of smaller bands than the EGFP-A42.

4.2 Impact of human A42 in wild type yeast BY4741 compared to the controls: ev, A40, A42m2 and C57

Due to the fact that the deletion of hydrophobic regions (A42m2) abolishes A42 mediated cytotoxicity during chronological aging and A42m2 mainly localizes to the cytosol and not to the mitochondria, it was decided to use strain expressing EGFP-A42m2 as a control strain to the EGFP-A42. A40 is less toxic than A42 in AD pathology, since A42 is more prone to aggregate. In this work strains expressing EGFP-A40 were also used as a less toxic control to the strains expressing EGFP-A42. Furthermore, C57 fragment was used as a nontoxic control. C57 is an intermediate of the last step of APP processing, C-terminal fragment of C99, whereas A42 is N-terminal. Additionally, vector control expressing only EGFP, was used as control for all of the EGFP constructs.

4.2.1 Human A42 is cytotoxic in wild type yeast compared to the peptide controls (A40, C57 and A42m2)

To validate the A42 cytotoxicity in yeast cells, wild type cells expressing EGFP-A42 were compared to the wild type cells expressing EGFP- A40, -A42m2, -C57 and EGFP alone as a vector control in chronologically aging (Figure 4.6).

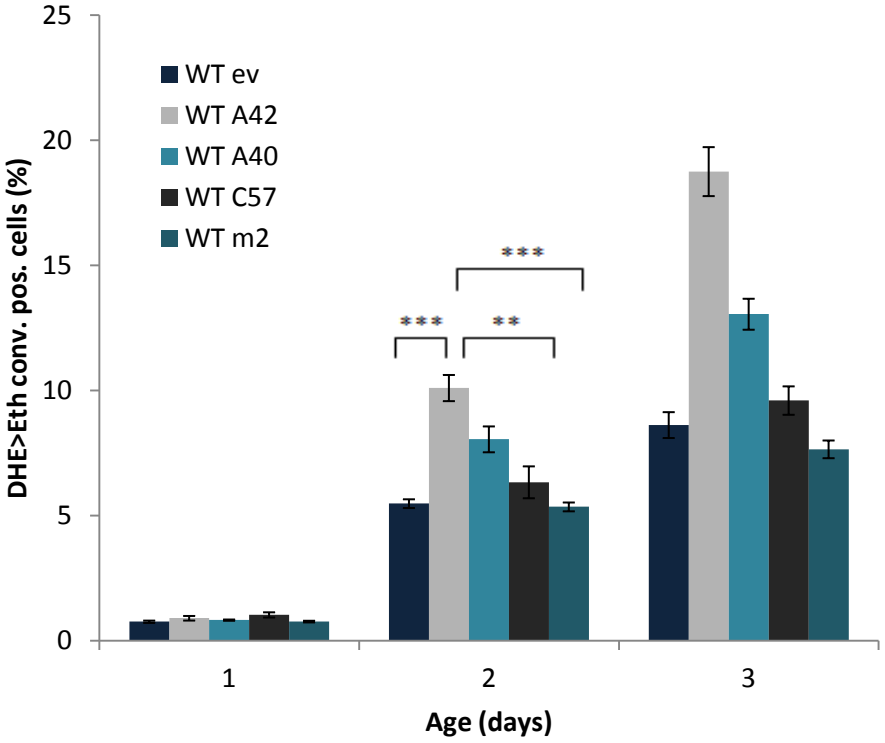

Figure 4.6. Human A42 is cytotoxic in wild type yeast compared to the peptide controls used in this work. BY4741 yeast cells were chronologically aged for 3 days. ROS levels were quantified by DHE-staining. DHE converse to Ethidium due to reaction with ROS, which can be measured by FACS analysis. 30 000 cells were evaluated in each experiment. Data show one representative experiment, mean of 6 tested clones and the error bars, the standard error ($p < 0.001$ = ***, $p < 0.01$ = **, $p < 0.05$ = *).

Heterologous expression of human A42 in BY4741 decreases cell viability compared to ev, A40, A42m2 and C57 during the chronological aging. Wild type expressing EGFP-A42 shows more ROS accumulations than the other controls. The statistical significant testing demonstrates that A42 is significantly more toxic compared to its controls.

For intracellular localization studies of EGFP linked to A42, A40, C57 and A42m2 and its corresponding vector control, yeast cells were fluorescence microscoped under FITC filter for the green fluorescence of the EGFP protein. The chronologically aged yeast cells were analyzed by fluorescence microscopy after ~20h of expression (Figure 4.7).

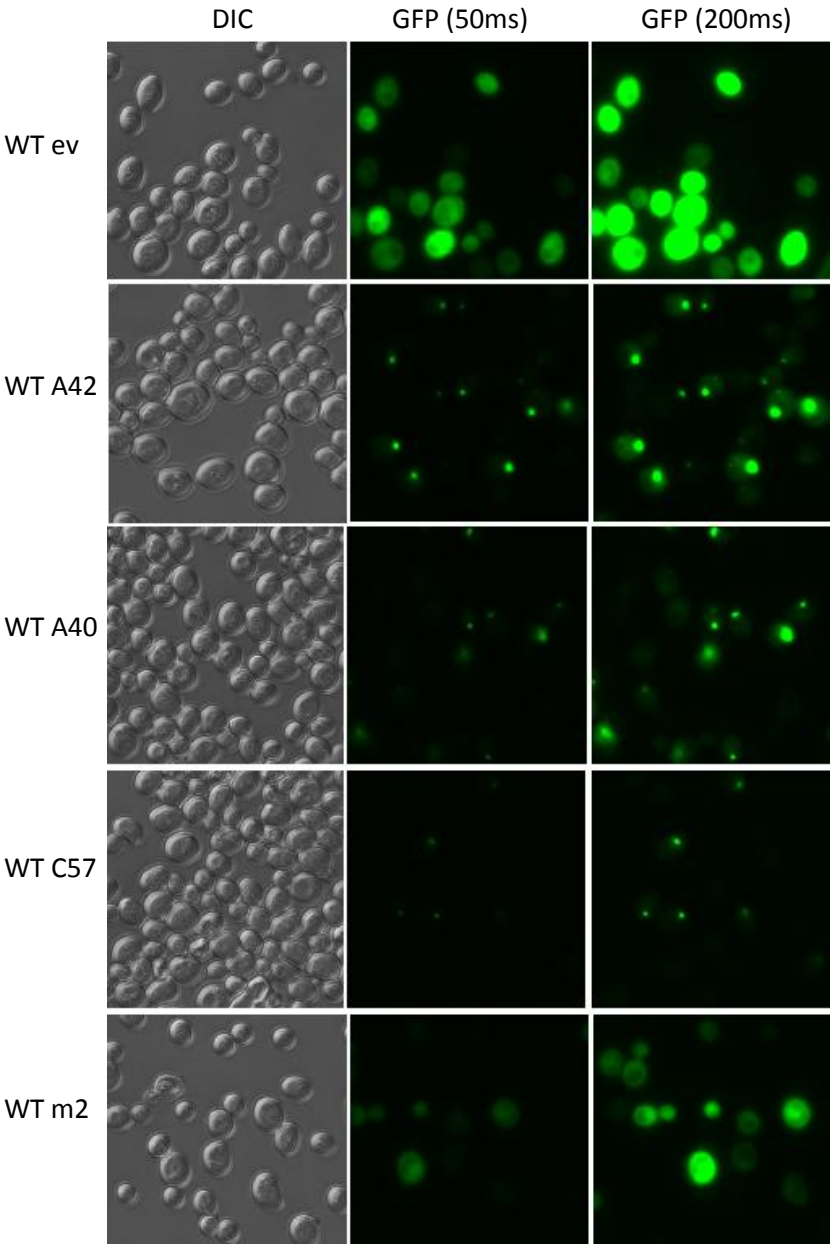

Figure 4.7. Fluorescence microscopy on BY4741 expressing A42, A40 and C57 reveals aggregate-like structures, whereas yeast vector control and A42m2 displays cytosolically distributed localization. Wild type yeast cells with N-terminal EGFP-tagged human A42, A40, C57 and A42m2 and corresponding vector control with EGFP only, were

fluorescence microscoped after ~20h of expression. For the microscopy an aliquot of the yeast cultures was harvested and 2µl were taken from the cell pellet. FITC filter was used for the green fluorescence of EGFP-constructs. Representative micrographs are shown.

Fluorescence microscopy revealed aggregate-like structures in the cells expressing A42, A40 and C57. Wild type cells expressing EGFP-A42 displayed more puncative formation than wild type expressing less toxic 40 and nontoxic C57. On the other hand, both of the remaining controls, namely cells expressing A42m2 and its vector control displayed cytosolically distributed localization.

4.2.2 A42 forms potential oligomer species mainly localizing to mitochondria

Whole yeast cell extracts of wild type cells expressing EGFP- A42, -A40 and -A42m2 and corresponding vector control were compared in polyacrylamide gel electrophoresis. After 16h of constructs expression, 10OD of the cells was harvested and disrupted. The membrane was decorated with Aβ antibody (Figure 4.8).

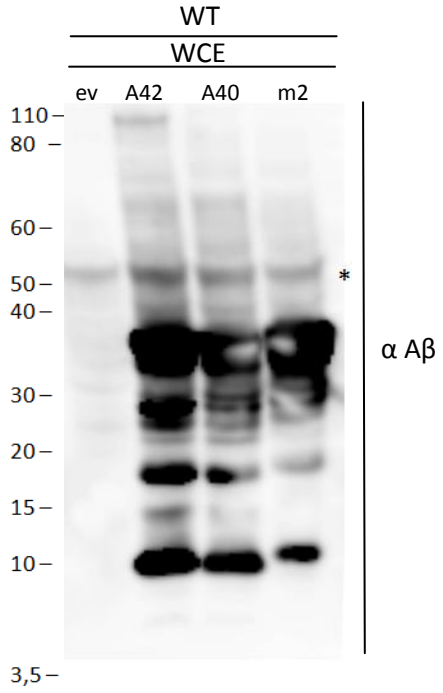

Figure 4.8. A42 forms potential oligomer species. BY4741 yeast lysis was performed 16h after the constructs expression. The obtained whole yeast extracts were loaded to the 4%-12% Bis-Tris NuPage gel and a polyacrylamide

gel electrophoresis was performed. The proteins from the gel were transferred to the membrane using semi dry transfer blotting method, after which the membranes were ready for blocking and immunodecoration. Aβ antibody was used for the recognition of Aβ-variants. Representative blot is shown. * - is an unspecific band. This experiment was performed at the "Institute of biochemistry and molecular biology" in Freiburg.

The full length of EGFP-Aβ variants is ~34kDa, as already mentioned above. In addition to the full length band, other bands, which differ in length, are also visible. The smallest band is around 3.5kDa indicating to A42 monomer or EGFP-A42 fragment which is still detectible with the Aβ-antibody. Cells expressing EGFP-A42 also distributed bands size ~7kDa, ~10kDa, ~15kDa, 18kDa and some higher than the full length construct. Additionally, A40 has less higher bands than A42 and A42m2 has nearly no higher bands. The most prominent higher band is the band at ~110 kDa size. Cells expressing EGFP-A40 and EGFP-A42m2 do not distribute the ~110 band. Furthermore cells expressing EGFP-A42m2 do not distribute the smaller size bands. However, bands at the size ~10kDa and ~20kDa are slightly visible. In addition band muster of A42m2 differs than A42 or A40. As expected no specific bands were detected in vector control. The visible smaller bands could be potential oligomeres, due to the fact that potential monomer at 3.5kDa is visible, however, it is possible that the smaller detectible bands correspond to degraded products of the full-length construct.

To determine localization of EGFP-A42, EGFP-A40, EGFP-C57, EGFP-A42m2, especially to investigate if different oligomer/fragments localize to different compartments in the cell, a cellular fractionation was performed. Cellular fractionation of cells expressing EGFP-C57 was separately performed. 70OD cells were harvested after 16h of expression and cellular fractionation was performed. The fractions include post nuclear supernatant (PNS), mitochondria fraction (P13), ER and microsomes fraction (P100) and cytosolic fraction. To investigate if the fractions are contaminated with other fractions, a control gel was run. Mitochondrial fraction was examined with the Tom22 antibody. ER/Microsome (P100) fraction was examined with antibodies which can bind to Sec61 and Sss1 and cytosolic fraction (S100) was tested with Ssa1 antibody. The EGFP-Aβ variants were detected using an Aβ antibody and EGFP-C57 was detected with GFP-antibody.

Additionally, fibrillization of synthetic A42 and A40 was done by incubating the peptides in 1xPBS for 24 hours and 37°C, after which Laemmli without β-mercaptoethanol was added (Figure 4.9).

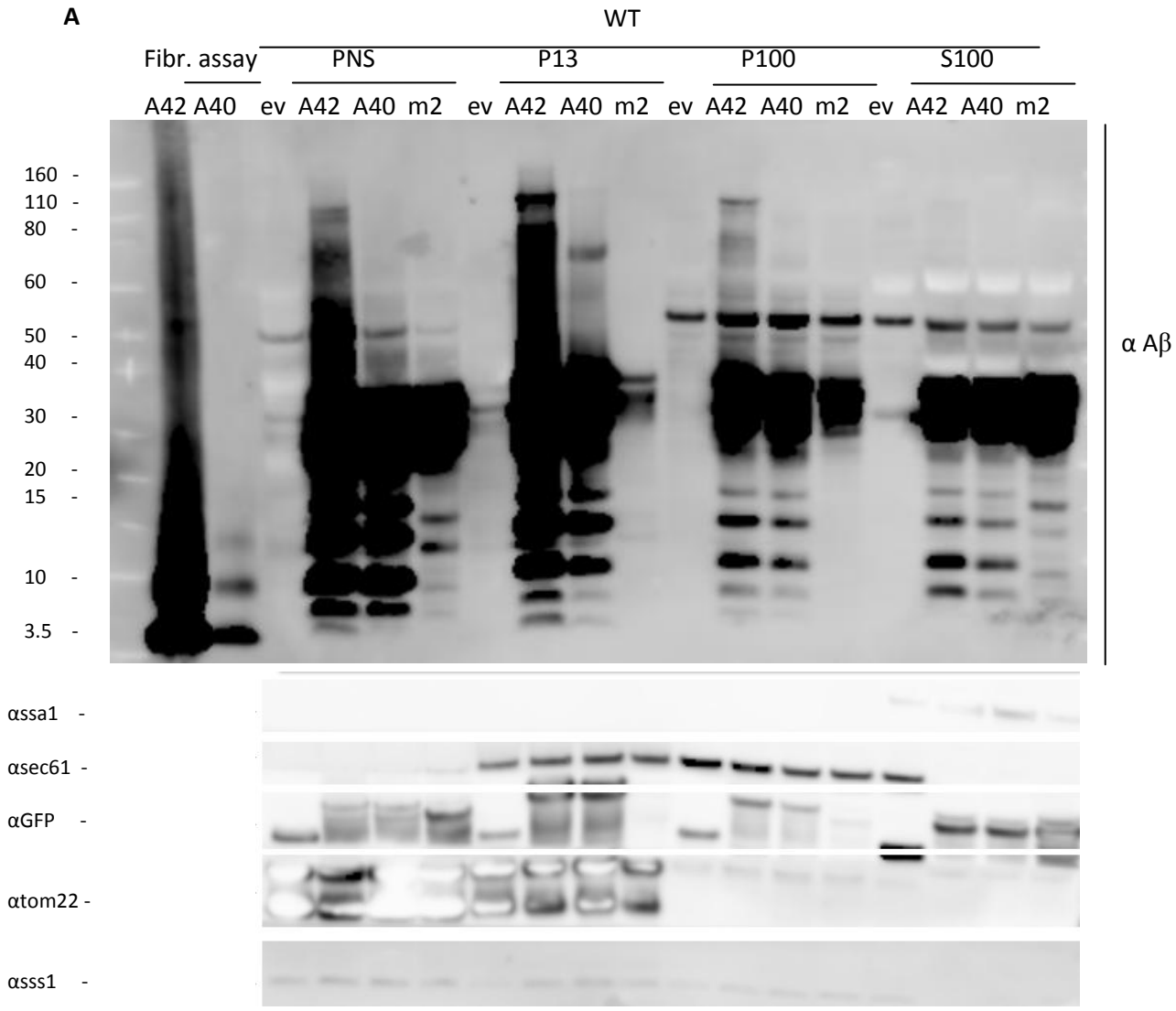
A
WT
Fibr. assay
PNS
P13
P100
S100
A42 A40 ev A42 A40 m2 ev A42 A40 m2 ev A42 A40 m2 ev A42 A40 m2
160 -
110 -
80 -
60 -
50 -
40 -
30 -
20 -
15 -
10 -
3.5 -
α Aβ
αssa1 -
αsec61 -
αGFP -
αtom22 -
αsss1 -

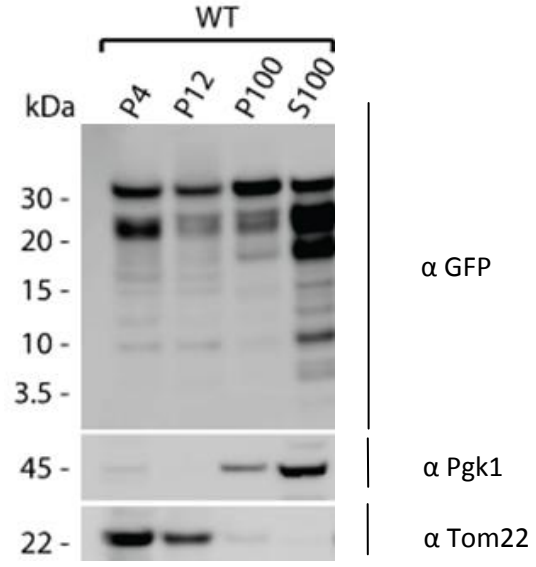
B
WT
kDa
P4
P12
P100
S100
30 -
20 -
15 -
10 -
3.5 -
45 -
22 -
α GFP
α Pgk1
α Tom22

Figure 4.9. Potential A42 oligomer localizes to mitochondria fraction The cellular fractionation of the yeast cells expressing 16h after the constructs expression in BY4741 yeast cells and fibrillization assay of synthetic A42 and A40 were performed. The obtained fractions and fibrillized synthetic A42 and A40 were loaded to the 4%-12% Bis-Tris NuPage gel after which polyacrylamide gel electrophoresis was performed. The proteins from the gel were transferred to the membrane using semi dry transfer blotting method, after which the membranes were ready for blocking and immunodecoration. Representative blot is shown**. A** Fibrillization assay and cellular fractionation of yeast cells expressing EGFP-A42, -A40, A42m2 and its vector control. **B** cellular fractionation of yeast cells expressing EGFP-C57. Aβ antibody was used for the recognition of Aβ-variants and GFP-antibody for recognition of EGFP-C57. Post nuclear supernatant (PNS); mitochondria fraction (P13) – Tom22 antibody; ER/microsome fraction (P100) – Sec61 and Sss1 antibodies; cytosolic fraction (S100) – Ssa1 antibody. Vector control cytosolic fraction was contaminated with ER/microsome fraction. This experiment was performed at the "Institute of biochemistry and molecular biology" in Freiburg.

Fibrillization assay displays typical amyloid fibrillization pattern, visible monomer band, low-n- and higher-oligomer bands. The monomer band is visible at ~3.5, dimer band at ~8kDa, trimer at ~12kDa and tetramer at ~17kDa as well as 12-mer at ~56kDa. Fibrilization assay revealed that A42 is more prone to aggregate than A40. This band pattern highly remind of the bands observed in cellular fractionation of wild type cells expressing EGFP linked to A42 and A40.

As observed in whole yeast extract and as already described above, A42 and A40 display lower and higher bands. The smaller bands correlate to the synthetic low-n-oligomers, indicating that the detectible fragments could be potential low-n oligomers formed by A42 without EGFP, instead of degraded products of the whole construct. A42m2 as already described above do not show fibrillization pattern at all. In addition, the higher band ~110 (potential EGFP-A42 oligomer) is observed in A42 fractions. A40 and A42m2 do not display ~110 band.

A42 predominantly localizes to the mitochondrial fraction. Similar to A42, A40 also localizes mainly to the same fraction, whereas A42m2 mainly localizes to the cytosolic fraction compared to the A40 and A42. Cellular fractionation of the wild type expressing EGFP-C57 revealed that the C57 mainly localizes to the cytosolic fraction. Smaller bands are also visible, indicating to the degraded fragments of the EGFP-C57 construct or oligomeric structures of C57 only.

To further elucidate if our potential higher oligomers have known oligomeric features (SDS-stable and heat instability) we performed and "SDS-assay" with and without heatshock. It has been shown that the amyloid oligomers are SDS stable and can be disaggregated by boiling [Bagriantsev and Liebman, 2006]. 10OD of the cells were harvested after 16h of the construct expression. After Laemmli was added to the cells, cells were incubated in two different conditions, at room temperature (RT) and 95°, after which the samples were ready for the gel loading. A42 was compared to A40, A42m2 and corresponding vector control. The EGFP-Aβ variants were detected using an Aβ and GFP antibody (Figure 4.10).

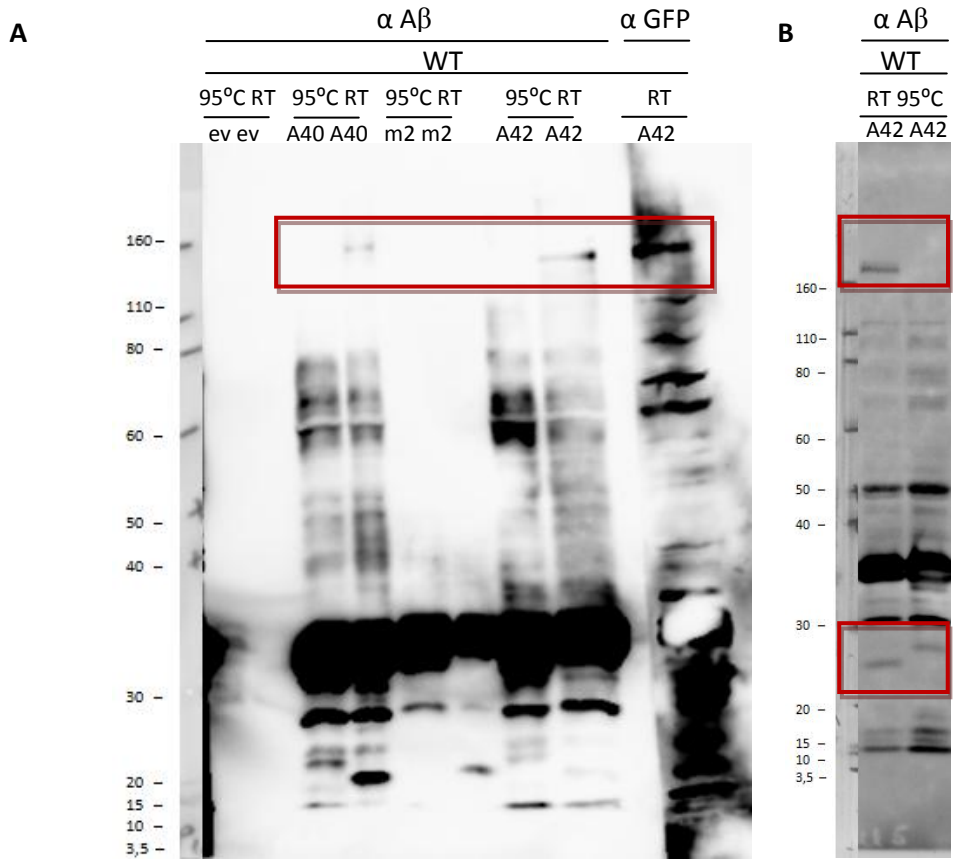

Figure 4.10. EGFP-A42 forms SDS stable oligomer. BY4741 yeast lysis SDS assay was performed 16h after the constructs expression at two different conditions, RT and 95°C. The obtained whole yeast extracts were loaded to the 10% SDS gels and a polyacrylamide gel electrophoresis was performed. The proteins from the gel were transferred to the membrane using semi dry transfer blotting method, after which the membranes were ready for blocking and immunodecoration. Aβ- and GFP- antibody were used for the recognition of Aβ-variants and the EGFP-constructs. **A** and **B** are representative blots from two different experiments. This experiment was performed at the "Institute of biochemistry and molecular biology" in Freiburg.

SDS assay revealed potential EGFP-A42 oligomer, at ~110kDa which disappears after boiling, indicating to SDS-stable but heat instable oligomer. This oligomer is detected with Aβ and GFP antibody. Whole yeast cell extract of A40 and A42m2 did not reveal this higher band. However, there is a slightly bigger band in A40 yeast extract, which is probably unspecific band. This band was observed in A42, A40 and A42m2 yeast extracts in additional performed experiments. In addition, A42 displays smaller band at ~20kDa which also disappears after boiling and one new band slightly higher than ~20kDa band which is generated after the boiling step.

4.2.3 EGFP-A42 oligomer is formed in time dependent manner

To investigate formation of the EGFP-A42 oligomer, 10OD of the BY4741 wild type yeast cells expressing EGFP linked to A42, A40 and A42m2 and EGFP only were harvested at specific time points. One of the time points was shortly after the constructs expression, 4h. The second time point was after 17h of the EGFP-constructs expression, at the time when the constructs expression is the highest, according to some earlier experiments. Two further time points were after 25h and 40h after start of expression. The EGFP-Aβ variants were detected using an Aβ (Figure 4.11).

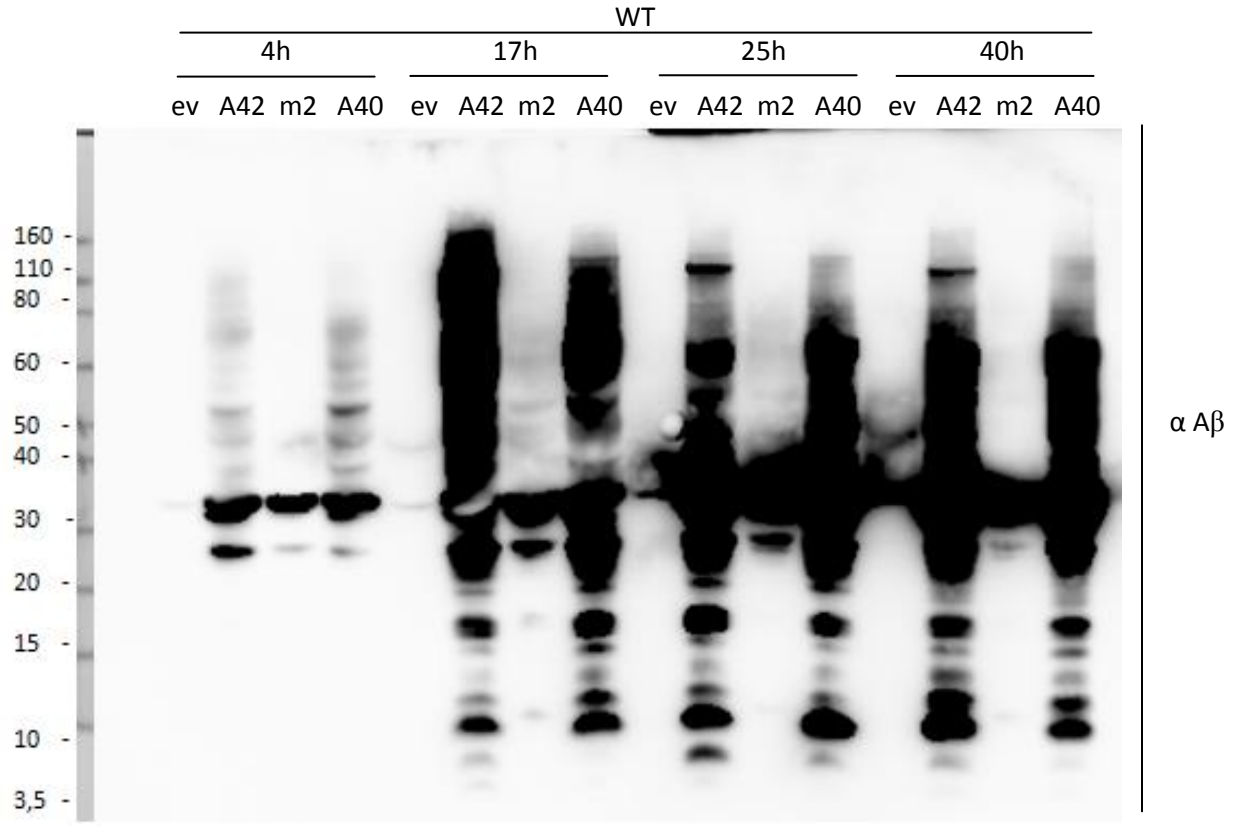

Figure 4.11. EGFP-A42 forms SDS stable oligomer in time dependent manner. BY4741 yeast lysis was performed at four time points, 4h, 17h, 25h and 40h, after the constructs expression. The obtained whole yeast extracts were loaded to the 4%-12% Bis-Tris NuPage gel and a polyacrylamide gel electrophoresis was performed. The proteins from the gel were transferred to the membrane using semi dry transfer blotting method, after which the membranes were ready for blocking and immunodecoration. Aβ antibody was used for the recognition of Aβ-variants. Representative blot was shown. This experiment was performed at the "Institute of biochemistry and molecular biology" in Freiburg.

Time course experiment revealed that the EGFP-A42 ~110kDa band appears after some time of the expression and is slowly degraded after. Similarly, the smaller bands appear after some time of the expression. The longer the incubation of the cells, the higher is amount of the most of the smaller bands detected with Aβ antibody. As expected A42m2 did not reveal fibrillization pattern, which are typical for hydrophobic A42. The fibrillization pattern of the higher band of A40 is also visible, but not as intense as in case of A42, and the 110 kDa oligomer is missing.

4.3 Investigation of key players in wild type yeast BY4741

As already mentioned in 1.3.3 screen of 157 deletion strains was performed which revealed few potential “hits” which could modulate A42-mediated toxicity. In this work a part of these “hits” were investigated. These include two chaperones Ssa1p and Ydj1p, one protein involved in mitochondrial import, Tom70p and two respiratory deficient strains, rho^0 and *OXA1* deletion strain.

4.3.1 Deletion of *SSA1* and *YDJ1* prevents A42mediated ROS accumulation and cell death in yeast during chronologically aging

Ssa1p belongs to class of cytosolic heat shock protein 70 (Hsp70). There are four genes encoding proteins of the Ssa family, namely *SSA1*, *SSA2*, *SSA3* and *SSA4*. Ssa1p is involved in protein folding and translocation and can be induced upon stress. Ydj1p induces the Ssa1p ATPase activity, while accelerating a conformational change for ATP hydrolysis. It was demonstrated that Hsp70 protein family modulates transport to the mitochondria and the ER. Additionally, it was shown that Ydj1 is required for this transport [Verghese *et al*., 2012; Caplan *et al*., 1992].

To confirm the result of the screen, chronological experiments of Dssa1 and Dydj1 expressing EGFP-A42 and corresponding vector control, compared to wild type, were performed. During the chronological aging, generation of ROS levels was investigated by DHE staining. Yeast cells were 3 days chronologically aged and analyzed (Figure 4.12).

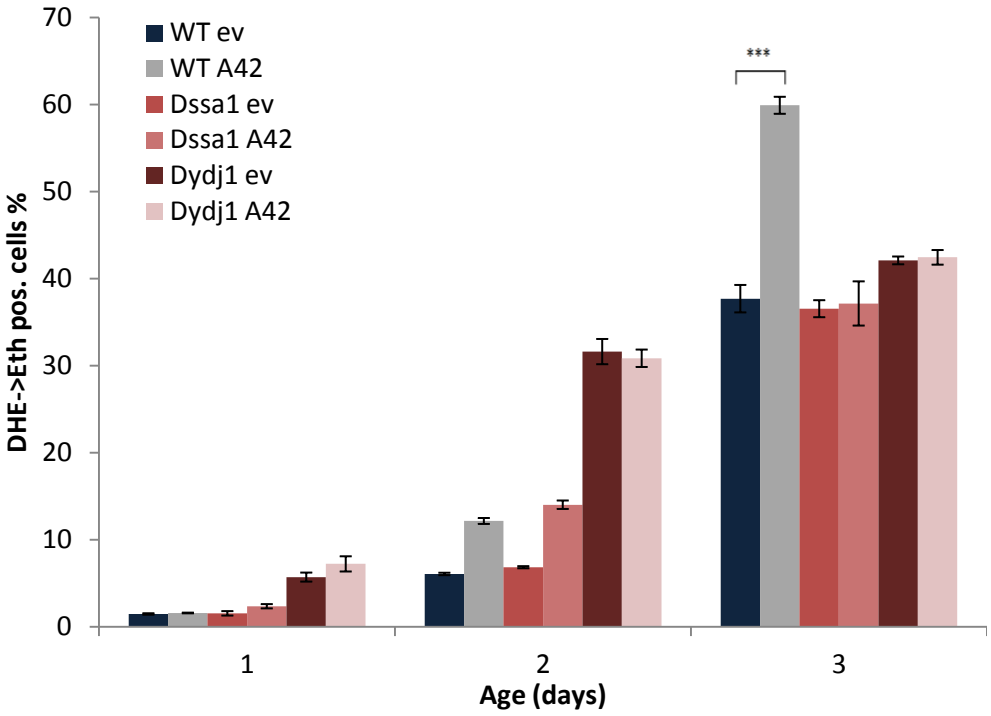

Figure 4.12. Deletion of *SSA1* and *YDJ1* rescues A42-toxicity-mediated ROS accumulation in yeast during chronologically aging. Yeast cells were chronologically aged for 3 days. ROS levels were quantified by DHE-staining. DHE converse to Ethidium due to reaction with ROS, which can be measured by FACS analysis. 30 000 cells were evaluated in each experiment. Data show one representative experiment, mean of 6 tested clones and the error bars, the standard error ($p < 0.001$ = ***, $p < 0.01$ = **, $p < 0.05$ = *).

The DHE staining of Dssa1 and Dydj1 compared to wild type cells confirmed the screen result, especially on day 3 of chronological aging. Deletion of *YDJ1* prevents A42 mediated ROS accumulation constantly during the chronological aging, whereas deletion of *SSA1* reduced the ROS accumulations only on day 3 in yeast cells.

During performed chronological aging of Dssa1 and Dydj1 compared to the wild type, determination of the cell dead fraction by PI staining was investigated. Yeast cells were 3 days chronologically aged and analyzed (Figure 4.13).

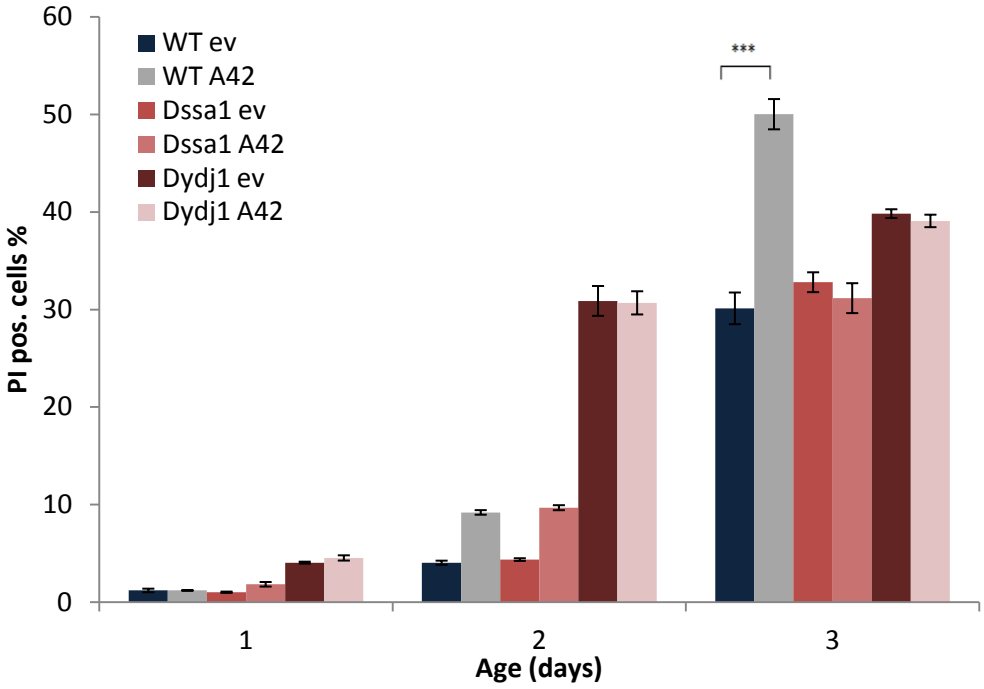

Figure 4.13. Deletion of *SSA1* and *YDJ1* rescues A42 induced cell death in yeast during chronological aging. BY4741 yeast cells were chronologically aged for 3 days. Cell death fraction was characterized by PI staining. PI stains the cells which lost their membrane integrity as a necrotic marker. 30 000 cells were evaluated in each experiment. Data show one representative experiment, mean of 6 tested clones and the error bars, the standard error ($p < 0.001$ = ***, $p < 0.01$ = **, $p < 0.05$ = *).

Similar to ROS accumulation quantification of *YDJ1* and *SSA1* deletion strains expressing EGFP-A42 and only EGFP it could be shown that deletion of *YDJ1* and *SSA1* rescue A42-mediated cell death quantified by PI staining compared to the wild type cells.

4.3.2 Deletion of *SSA1*, *SSA2*, *SSA3* and *SSA4* rescues A42-toxicity-mediated ROS accumulation during chronologically aging

In addition, in this work, deletion strains of all of the four yeast Ssa members, expressing EGFP-A42 and only EGFP were investigated and compared to the wild type cells. During the 3 day chronologically aging, generation of ROS levels was investigated by DHE staining (Figure 4.14).

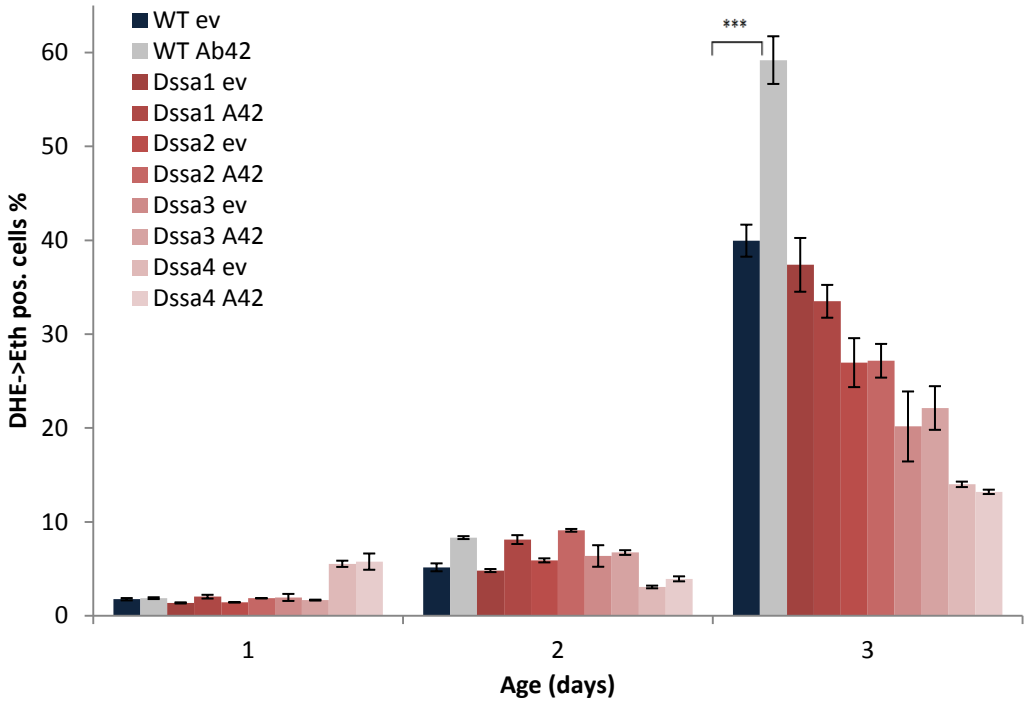

4.14 Deletion of *SSA1*, *SSA2*, *SSA3* and *SSA4* rescues A42-toxicity-mediated ROS accumulation during chronologically aging. Yeast cells were chronologically aged for 3 days. ROS levels were quantified by DHE-staining. DHE converse to Ethidium due to reaction with ROS, which can be measured by FACS analysis. 30 000 cells were evaluated in each experiment. Data show one representative experiment, mean of 6 tested clones and the error bars, the standard error ($p < 0.001$ = ***, $p < 0.01$ = **, $p < 0.05$ = *).

Deletion of *SSA1* and *SSA2* rescued A42-mediated toxicity on day 3 of chronological aging, whereas deletion of *SSA3* and *SSA4* rescued constantly during the aging. It should be mentioned that Dssa4 showed impaired growth compared to other strains and less expression of EGFP-A42 compared to the other strains.

4.3.3 Deletion of *YDJ1* rescues A42-toxicity-mediated ROS accumulation after acetic acid treatment

To investigate if deletion of *YDJ1* also can prevent the acetic acid A42 mediated cell death in yeast cultures, yeast cells were treated with acetic acid after 16h of the construct expression. Cells were incubated with acetic acid for 4h after which they were DHE stained for the ROS accumulations quantification (Figure 4.15).

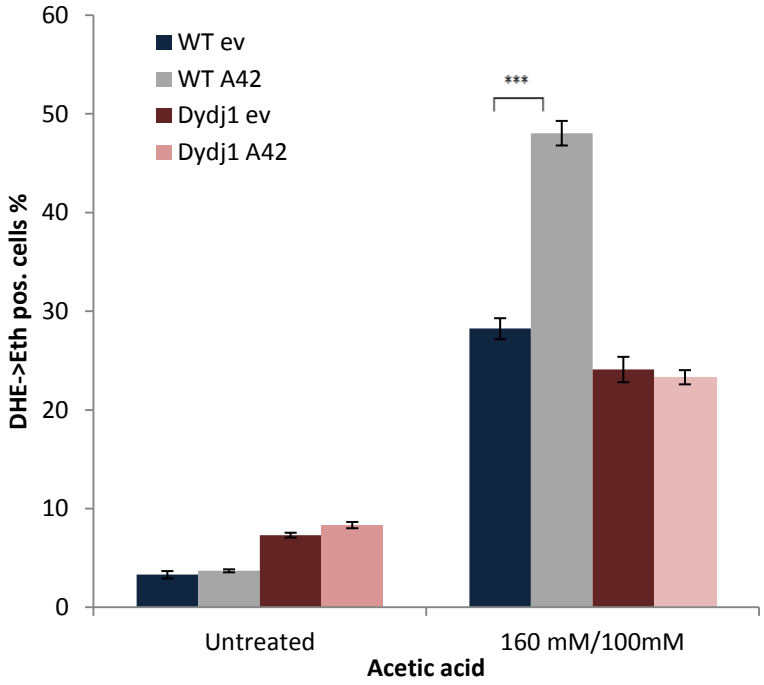

Figure 4.15. Deletion of YDJ1 rescues A42-toxicity-mediated ROS accumulation after acetic acid treatment. Yeast cells were treated with acetic acid 16h after A42-constructs expression and 4h after acetic acid treatment, ROS levels were quantified by DHE-staining. DHE converse to Ethidium due to reaction with ROS, which can be measured by FACS analysis. 30 000 cells were evaluated in each experiment. Data show one representative experiment, mean of 6 tested clones and the error bars, the standard error ($p < 0.001$ = ***, $p < 0.01$ = **, $p < 0.05$ = *).

Cell viability of *YDJ1* deletion strain expressing EGFP-A42 after stress stimuli with acetic acid was not impaired. Deletion of *YDJ1* rescued the A42-mediated ROS accumulation induced by acetic acid. Wild type cells expressing EGFP linked to A42 compared yeast cells expressing only EGFP showed impaired cell viability and accumulation of ROS after acetic acid treatment.

4.3.4 Fluorescence microscopy of Dssa1 and Dydj1 indicates a modification in A42 aggregation

Since Ssa1p and Ydj1p build a complex and are involved in protein aggregation and disassembling of protein aggregates of misfolded proteins, yeast cells were analyzed under fluorescence microscope. To investigate if the deletion of *SSA1* and *YDJ1* influence A42 aggregation, cells were harvested after ~20

hours of construct expression. FITC filter was used for the green fluorescence of the EGFP protein (Figure 4.16 and 4.17).

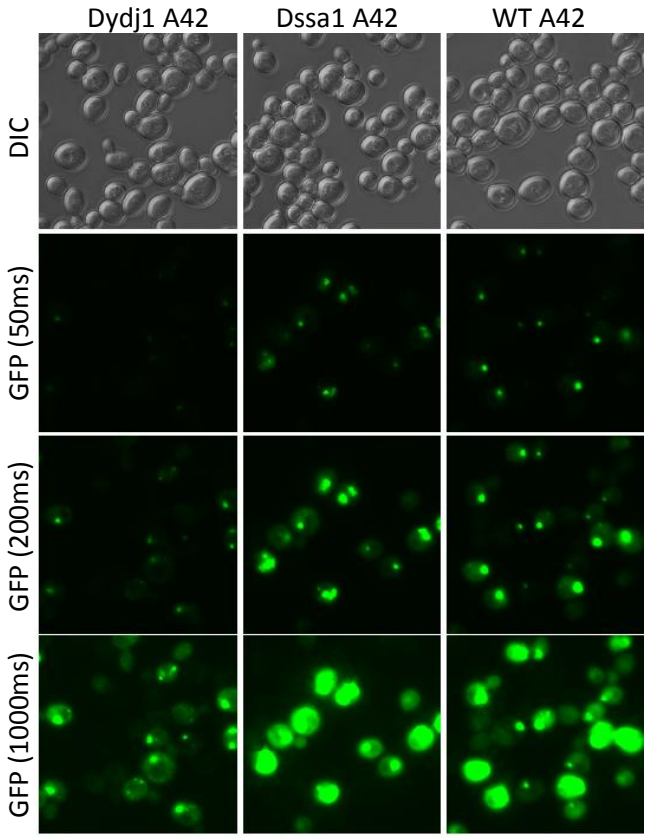

Figure 4.19. Deletion of *SSA1* and *YDJ1* influence the A42 aggregation. Yeast cells, Dydj1, Dssa1 and wild type expressing N-terminal EGFP-tagged human A42 and corresponding vector control, were fluorescence microscoped after ~20h of expression. For the microscopy an aliquot of the yeast cultures were harvested and 2µl was taken from the cell pellet. FITC filter was used for the green fluorescence of EGFP-constructs. Representative micrographs are shown.

Fluorescence microscopy revealed puncative structures in all of the three strains. However form and sizes of the aggregate-like structures differ in Dydj1 and Dssa1 compared to the wild type. The EGFP-A42 aggregate structures in Dssa1 are concentrated in bigger structures compared to the wild type. On the other hand the aggregate structures in Dydj1 are rather smaller and distributed within cells, compared to the WT. Deletion of *YDJ1* indicates to decrease of EGFP-A42 aggregation. Enlarged micrographs showing different aggregates structures can be seen in 4.20.

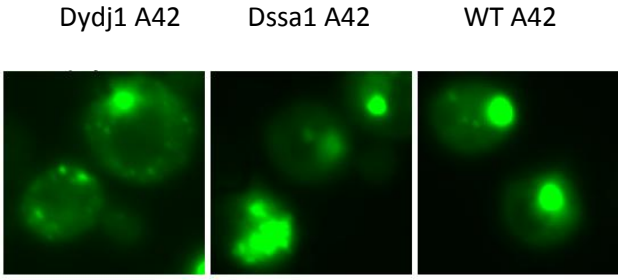

Figure 4.17. Deletion of *SSA1* and *YDJ1* influence the A42 aggregation in different manner. Yeast cells, Dydj1, Dssa1 and WT expressing N-terminal EGFP-tagged human A42 and corresponding vector control, were fluorescence microscoped after ~20h of expression. For the microscopy an aliquot of the yeast cultures were harvested and 2µl were taken from the cell pellet. FITC filter was used for the green fluorescence of EGFP-constructs. Representative micrographs are shown.

4.3.5 Protein levels of chaperones indicate an induction of the Ydj1p and Ssa1p expression in BY4741 Alzheimer's model

Furthermore, in this work the protein levels of corresponding chaperons in BY4741 yeast cells expressing EGFP-A42 were compared, such as Ydj1p, Ssa1p and Ssc1p. To investigate the protein levels, whole yeast extract of wild type cells expressing EGFP linked to A42, A40, A42m2 and C57 and corresponding vector control were compared. After 16h of constructs expression, 2.5 OD of the cells was harvested and disrupted. The membrane was decorated with corresponding antibodies (Figure 4.18). Pgk1 was used as a loading control.

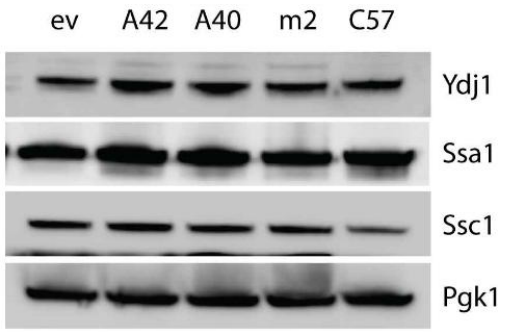

4.18. Protein levels of chaperones indicate an induction of the Ydj1p and Ssa1p expression in BY4741 wild type expressing EGFP-A42. BY4741 yeast lysis was performed 16h after the constructs expression. The obtained whole yeast extracts were loaded to the 4%-12% Bis-Tris NuPage gel after which polyacrylamide gel electrophoresis was performed. The proteins from the gel were transferred to the membrane using semi dry transfer blotting method,

after which the membranes were ready for blocking. To detect chaperones, antibodies binding to the corresponding chaperones were used. This experiment was performed at the "Institute of biochemistry and molecular biology" in Freiburg.

Revealed protein levels indicate to higher levels of Ydj1p and Ssa1p in wild type expressing EGFP linked to A42 compared to its nontoxic controls, namely wild type cells expressing EGFP linked to A42m2 and C57 and EGFP only. The chaperone levels of Ydj1p and Ssa1p are slightly higher in wild type expressing EGFP-A42 than in wild type expressing less toxic EGFP-A40.

4.3.6 Whole yeast extracts of Dssa1 and Dydj1 indicate to modification in A42 fibrillization pattern

Whole yeast extracts of wild type, Dssa1 and Dydj1 cells expressing EGFP-A42 and its vector control were compared. The yeast cell extracts were twice loaded to the gel and cut in the middle due to decoration with two different antibodies, namely Aβ and GFP antibody. After 16h of constructs expression, 10OD of the cells was harvested and disrupted (Figure 4.19).

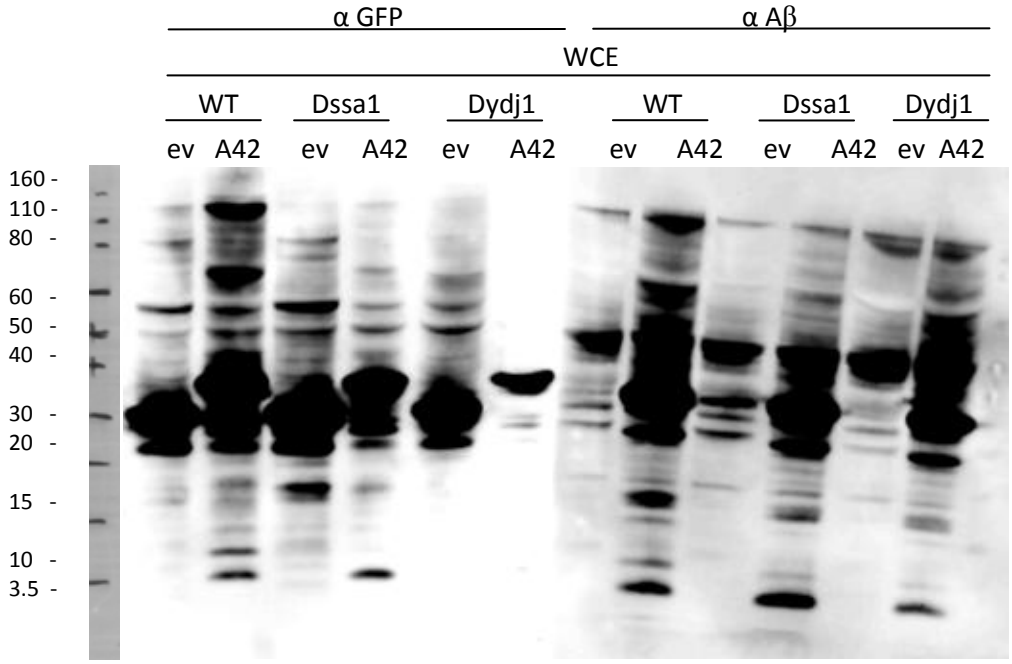

Figure 4.19. Deletion of *SSA1* and *YDJ1* slightly influence the A42 fibrillization pattern. Yeast lysis was performed 16h after the constructs expression. The obtained whole yeast extracts were loaded to the 4%-12% Bis-Tris NuPage gel after which polyacrylamide gel electrophoresis was performed. The proteins from the gel were transferred to the membrane using semi dry transfer blotting method, after which the membranes were ready for blocking and

immunodecoration. Aβ and GFP antibody were used for decoration of the membranes. Representative blot is shown. This experiment was performed at the "Institute of biochemistry and molecular biology" in Freiburg.

Whole yeast extracts of Dssa1 and Dydj1 were compared to the wild type. The higher ~110kDa band is detected in wild type A42 yeast extract with the GFP and Aβ-antibody, whereas Dssa1 and Dydj1 yeast extracts did not reveal this band. In addition, smaller bands differ in intensity between the strains. The EGFP-A42 level in Dydj1 yeast extract is lower compared to the Dssa1 and wild type cells. The measured OD_{600} of Dydj1 before cell lysis was twice as smaller compared to Dssa1 and WT strains.

4.3.7 Deletion of *SSA1* did not significantly influence the A42 localization

To investigate the localization of EGFP-A42 in Dssa1 strain, a cellular fractionation was performed and compared to the wild type fractions. 70OD cells were harvested after 16h of constructs expression and cellular fractionation was performed as described above. The EGFP-Aβ variants were detected using an Aβ antibody. The measured OD_{600} before the cell harvesting was similar between WT and Dssa1 strain (Figure 4.20).

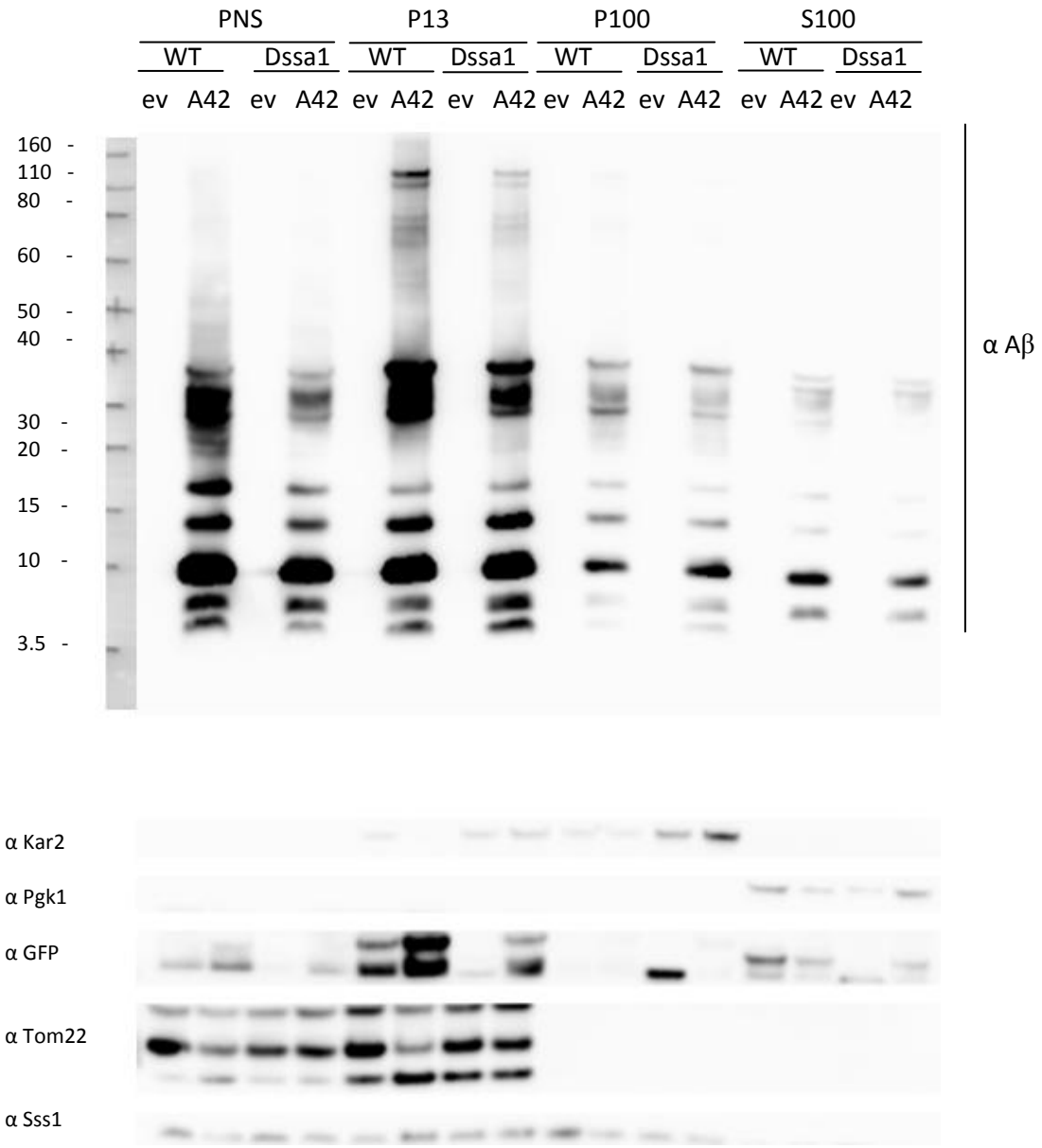

Figure 4.20. Deletion of *SSA1* did not significantly influence the A42 localization. The cellular fractionation was performed 16h after the constructs expression in yeast cells. The obtained fractions were loaded to the 4%-12% Bis-Tris NuPage gel after which polyacrylamide gel electrophoresis was performed. The proteins from the gel were transferred to the membrane using semi dry transfer blotting method, after which the membranes were ready for blocking and immunodecoration. Representative blot is shown. Aβ antibody was used for the membrane decoration. Post nuclear supernatant (PNS); mitochondria fraction (P13) – Tom22 antibody; ER/microsome fraction (P100) – Kar2 and Sss1 antibodies; cytosolic fraction (S100) – Pgk1 antibody. This experiment was performed at the "Institute of biochemistry and molecular biology" in Freiburg.

The cellular fractionation of Dssa1 compared to the wild type revealed no significant changes in A42 localization between the strains. However, the intensity of visible smaller bands is higher in mitochondria and ER fraction of the Dssa1 strain compared to the wild type, whereas the intensity of the EGFP-A42 construct of the wild type is higher in all fractions compared to Dssa1. The higher ~110kDa band is in both mitochondria fractions of wild type and Dssa1 strain. However, the intensity of the ~110kDa band is lower in Dssa1 mitochondria fraction, even though the measured OD_{600} of Dssa1 was similar to the wild type.

4.3.8 Cellular fractionation of Dydj1 indicates to different A42 localization and A42 level in cells

To investigate the localization of EGFP-A42 in Dydj1 strain, a cellular fractionation was performed as described above and compared to the wild type fractions. The measured OD_{600} of Dydj1 before the cell harvesting was twice lower than the WT (Figure 4.21).

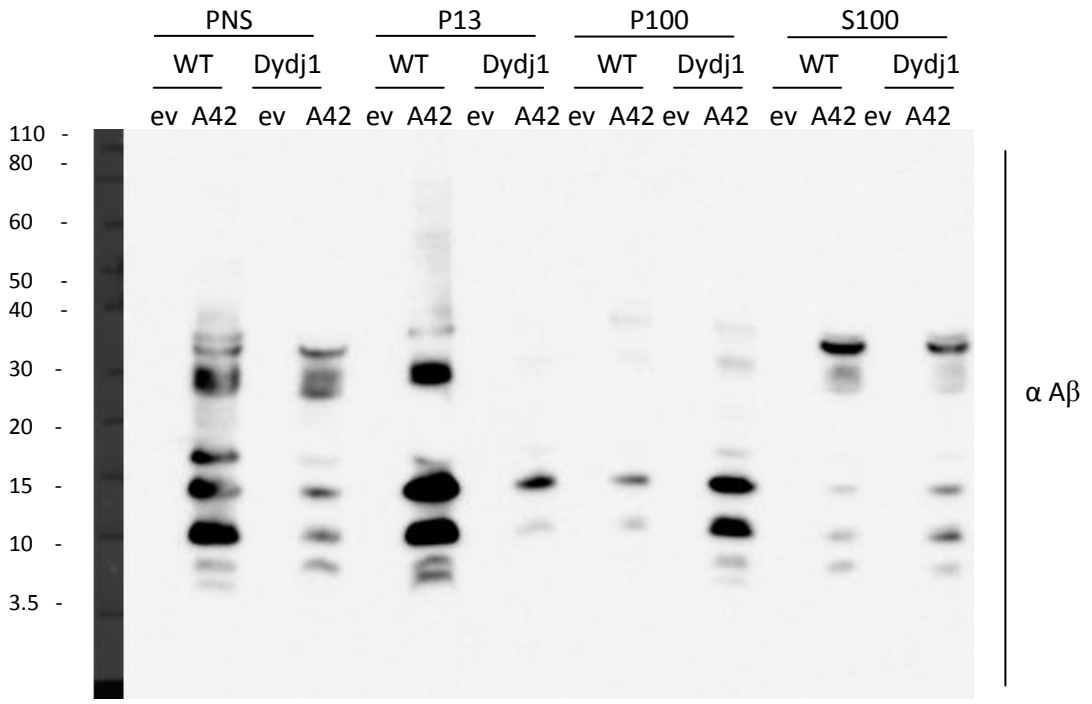

Figure 4.21. Deletion of *YDJ1* influenced the A42 localization. The cellular fractionation was performed 18h after the constructs expression in yeast cells. The obtained fractions were loaded to the 4%-12% Bis-Tris NuPage gel after which polyacrylamide gel electrophoresis was performed. The proteins from the gel were transferred to the membrane using semi dry transfer blotting method, after which the membranes were ready for blocking and immunodecoration. Representative blot is shown. Aβ antibody was used for the membrane decoration. Post nuclear supernatant (PNS); mitochondria fraction (P13); ER/microsome fraction (P100); cytosolic fraction (S100) – Pgk1 antibody. This experiment was performed at the "Institute of biochemistry and molecular biology" in Freiburg.

The cellular fractionation of Dydj1 revealed changes in A42 localization compared to the wild type. While A42 mainly localizes to the mitochondria fraction in the wild type, in Dydj1 strain A42 is mainly detected in the ER and microsomal fraction. The levels of EGFP-A42 and its "fragments" in Dydj1 fractions are lower than in the wild type. Control gel was also run, but on two different gels.

4.3.9 Overexpression of YDJ1 in wild type expressing A42 leads to increase of ROS accumulation during chronological aging and acetic acid treatment

Due to the fact that the deletion of *YDJ1* revealed promising results, overexpression of YDJ1 in BY4741 expressing EGFP-A42 was performed. Deletion of *YDJ1* rescued the A42-mediated toxicity, modified the A42 aggregation, and influenced the A42 localization and its fibrillization, for that reason overexpression of Ydj1p should be investigated. BY4741 yeast cells expressing A42 and YDJ1 were compared to Dydj1 as a control. Yeast cells were 3 days chronologically aged and generation of ROS levels was investigated by DHE staining (Figure 4.22).

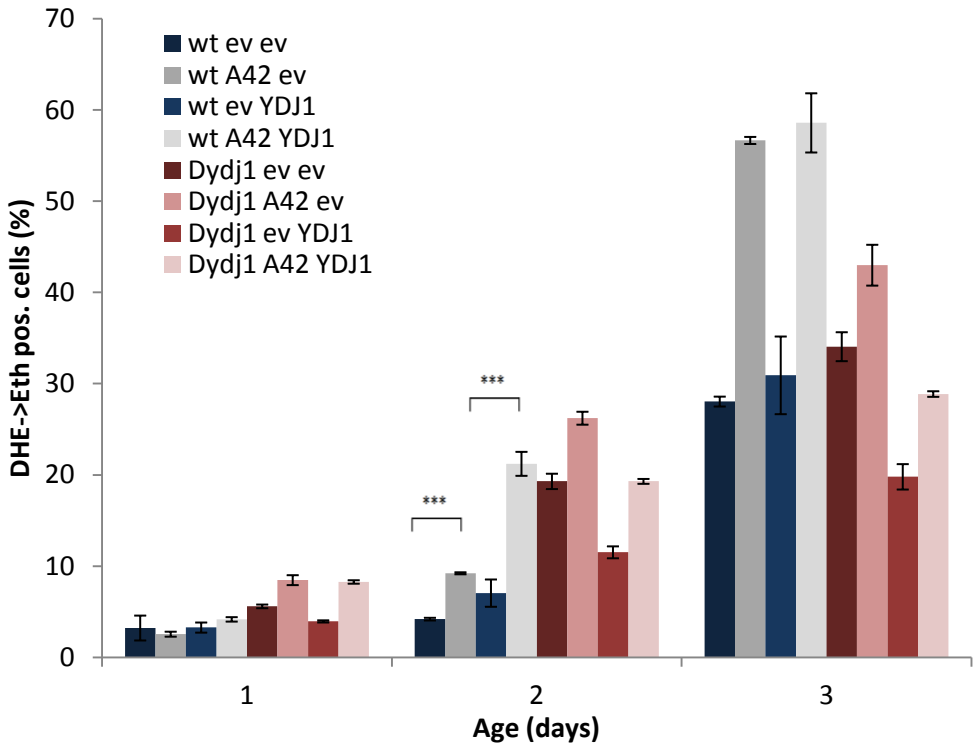

Figure 4.22. Overexpression of YDJ1 in wild type expressing A42 leads to increase of ROS accumulation during chronological aging. Yeast cells were chronologically aged for 3 days. ROS levels were quantified by DHE-staining. DHE converse to Ethidium due to reaction with ROS, which can be measured by FACS analysis. 30 000 cells were evaluated in each experiment. Data show one representative experiment, mean of 6 tested clones and the error bars, the standard error ($p < 0.001$ = ***, $p < 0.01$ = **, $p < 0.05$ = *).

Overexpression of YDJ1 leads to increase of ROS accumulation during chronological aging in BY4741 yeast expressing EGFP-A42 compared to its vector control, on day two. Yeast cells overexpressing YDJ1 were compared to the wild type cells expressing EGFP-A42 and only EGFP. On day 3 no significant differences were observed between wild type A42 and wild type A42 with the YDJ1 overexpression.

To investigate if overexpression of YDJ1 also can influence the acetic acid A42 mediated cell death in yeast cultures, yeast cells were treated with acetic acid after 16h of the construct expression. Cells were incubated with acetic acid for 4h after which they were DHE stained for the ROS accumulations quantification (Figure 4.23).

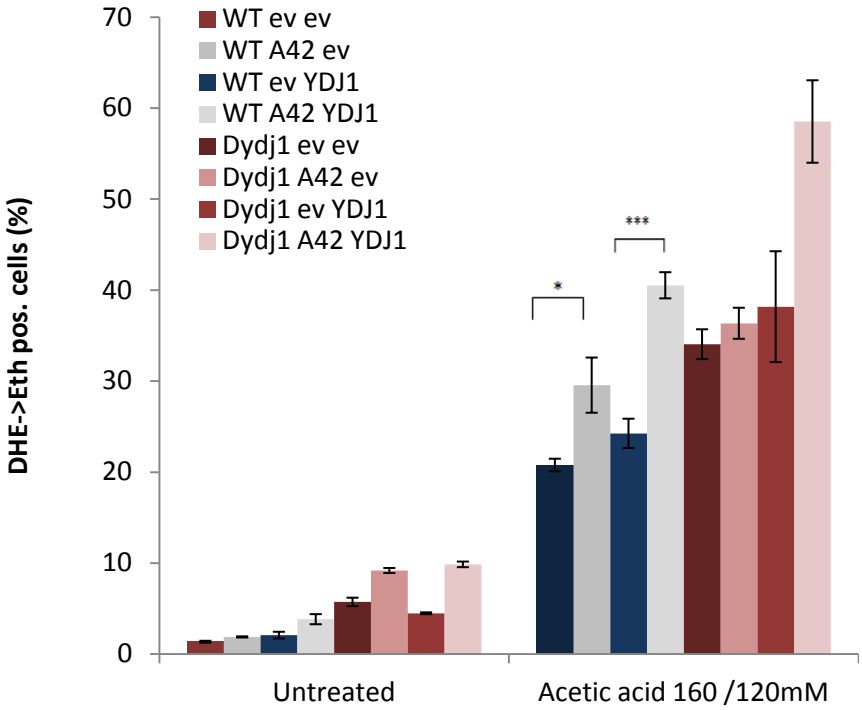

Figure 4.23. Overexpression of YDJ1 in wild type expressing A42 leads to increase of ROS accumulation after acetic acid treatment. Yeast cells were treated with acetic acid 16h after A42-constructs expression and 4h after acetic acid treatment, ROS levels were quantified by DHE-staining. DHE converse to Ethidium due to reaction with ROS, which can be measured by FACS analysis. 30 000 cells were evaluated in each experiment. Data show one representative experiment, mean of 6 tested clones and the error bars, the standard error ($p < 0.001$ = ***, $p < 0.01$ = **, $p < 0.05$ = *).

The overexpression of YDJ1 in BY4741 yeast expressing EGFP-A42 induced ROS accumulation after acetic acid treatment compared to the wild type expressing EGFP-A42. Dydj1 rescued as expected the A42-mediated ROS accumulation after acetic acid treatment. In addition, overexpression of YDJ1 in Dydj1 restored the A42 mediated cytotoxicity.

4.3.10 Overexpression of YDJ1 in influence species A42 aggregate formation and translocation

Due to the fact that *YDJ1* deletion influenced the A42 aggregation, BY4741 yeast cells expressing EGFP-A42 and YDJ1 were analyzed under fluorescence microscope. To investigate if the overexpression of YDJ1 influences A42 aggregation and in which manner, cells were harvested after ~20 hours of construct expression. Wild type expressing EGFP-A42 and the vector control was compared to the wild type expressing EGFP-A42 and YDJ1. FITC filter was used for the green fluorescence of the EGFP protein (Figure 4.24).

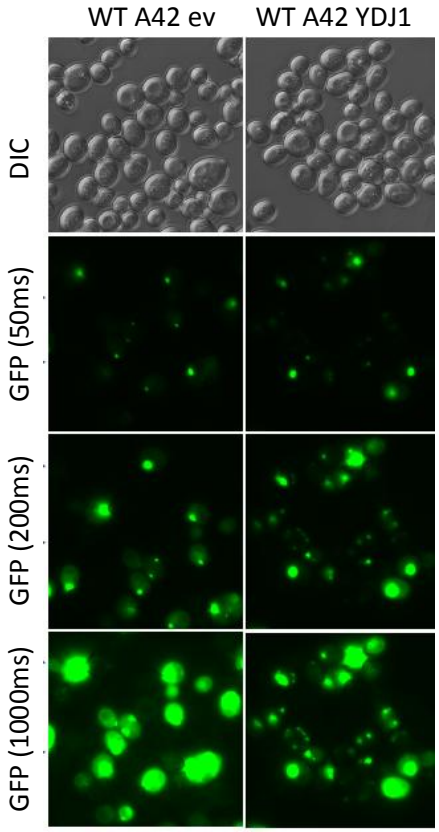

Figure 4.24. Overexpression of YDJ1 in BY4741 Alzheimer's model influences the A42 aggregation. Yeast wild type cells, expressing N-terminal EGFP-tagged human A42 and corresponding YDJ1 vector control and wild type yeast cells expressing EGFP-A42 and YDJ2, were fluorescence microscoped after ~20h of expression. For the microscopy an aliquot of the yeast cultures was harvested and 2µl were taken from the cell pellet. FITC filter was used for the green fluorescence of EGFP-constructs. Representative micrographs are shown.

Fluorescence microscopy revealed puncative structures in the wild type expressing EGFP-A42 and wild type expressing EGFP-A42 and YDJ1. However form and sizes of the aggregate-like structures are different between the strains. The aggregate structures in wild type expressing EGFP-A42 and YDJ1 are rather smaller and distributed within cells, compared to the wild type expressing only EGFP-A42, similar

to the Dydj1 strain expressing A42. However, wild type expressing EGFP-A42 and YDJ1 did not reveal decrease in EGFP-A42 aggregation, due to additional bigger aggregates which were not observed in *YDJ1* deletion strain.

Due to the fact that deletion of *YDJ1* influenced the A42 localization, additional cellular fractionation was performed. Wild type cells expressing EGFP-A42 and its vector control were compared to the wild type expressing only YDJ1 and wild type expressing EGFP-A42 and YDJ1. 70OD cells were harvested after 16h of constructs expression and cellular fractionation was performed as described above (Figure 4.25).

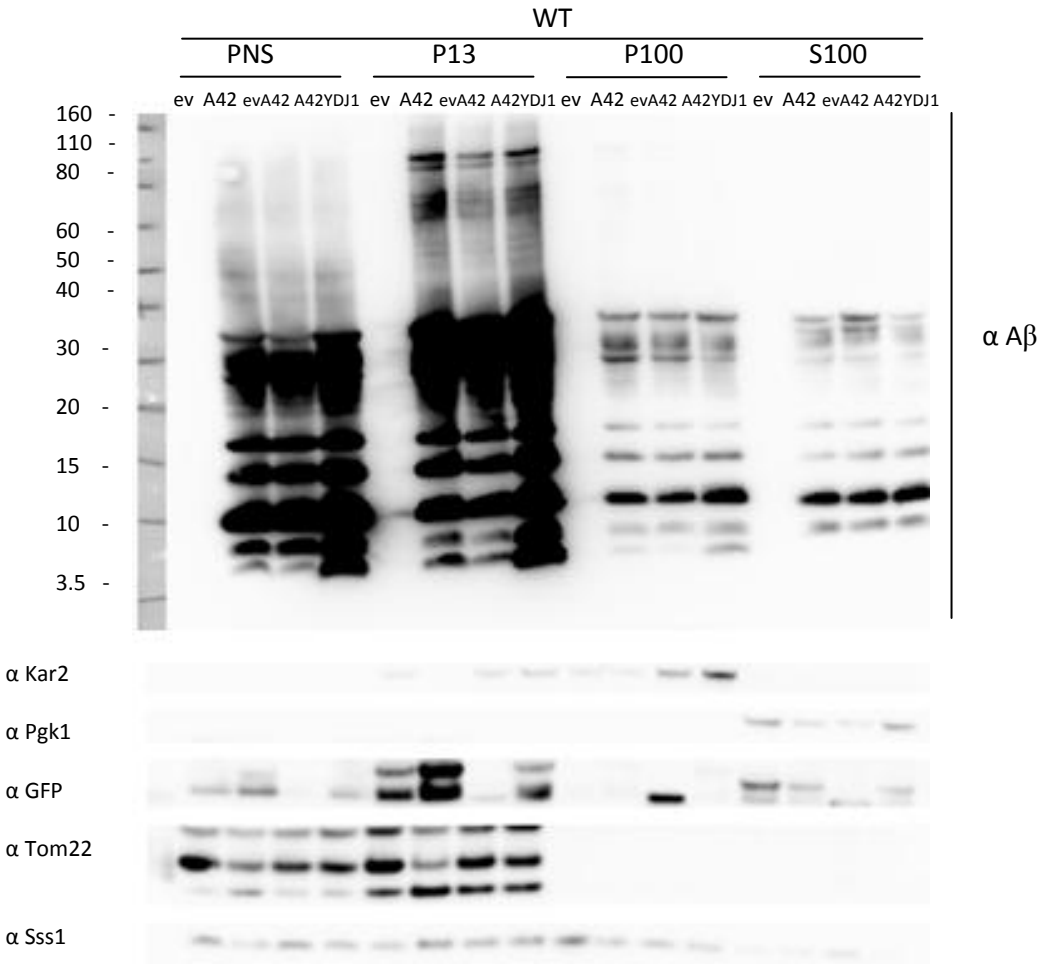

Figure 4.25. Cellular fractionation of BY4741 Alzheimer's model overexpressing YDJ1 indicates to different A42 localization The cellular fractionation was performed 16h after the constructs expression in yeast cells. The obtained fractions were loaded to the 4%-12% Bis-Tris NuPage gel after which polyacrylamide gel electrophoresis was performed. The proteins from the gel were transferred to the membrane using semi dry transfer blotting method, after which the membranes were ready for blocking and immunodecoration. Representative blot is shown. Aβ antibody was used for the membrane decoration. Post nuclear supernatant (PNS); mitochondria

fraction (P13) – Tom22 antibody; ER/microsome fraction (P100) – Kar2 and Sss1 antibodies; cytosolic fraction (S100) – Pgk1 antibody. This experiment was performed at the "Institute of biochemistry and molecular biology" in Freiburg.

Cellular fractionation revealed that YDJ1 overexpression influences the A42 localization within cell. A42 colocalized mainly to the mitochondria in the wild type expressing EGFP-A42 and YDJ1, as in wild type expressing only EGFP-A42. In addition, more A42 was detected in ER fraction in strain expressing YDJ1 and EGFP-A42 compared to the wild type expressing only EGFP-A42. Also, the intensity of the A42 in all fractions is higher in wild type expressing EGFP-A42 and EGFP, which indicates that YDJ1 could protect the EGFP-A42. A42 in deletion strain Dydj1 was mainly concentrated to the ER fraction, what indicates that the YDJ1 protein is involved in translocation of the A42 to the specific organelles.

4.3.11 Tom70 displays a crucial role in A42 mediated toxicity, however does not influence its aggregation or localization

Tom70 is one of the potential key players which were elucidated by the screen of 157 deletion strains. This protein is part of the translocase of outer membrane (TOM) and is able to recognize and import the proteins directed into mitochondria [Dekker *et al.,* 1998]. Cytosolic domains can interact with hydrophobic precursor proteins and cytosolic Hsp70 family chaperones of Ssa subfamily [Wu and Sha, 2006]. Due to previous results, which indicate a mitochondria involvement in A42 mediated cell death pathways, in this work, Tom70p was investigated more in detail to shed light on its role in A42 mediated toxicity.

To investigate the role of Tom70 in A42 mediated toxicity, ROS levels of corresponding strains were determined upon aging and stress conditions. In this work, it was examined if TOM70 influences the A42-mediated cytotoxicity. For this reason a deletion strain Dtom70 was chronologically aged for 3 days, during which ROS accumulations were measured by DHE staining (Figure 4.26).

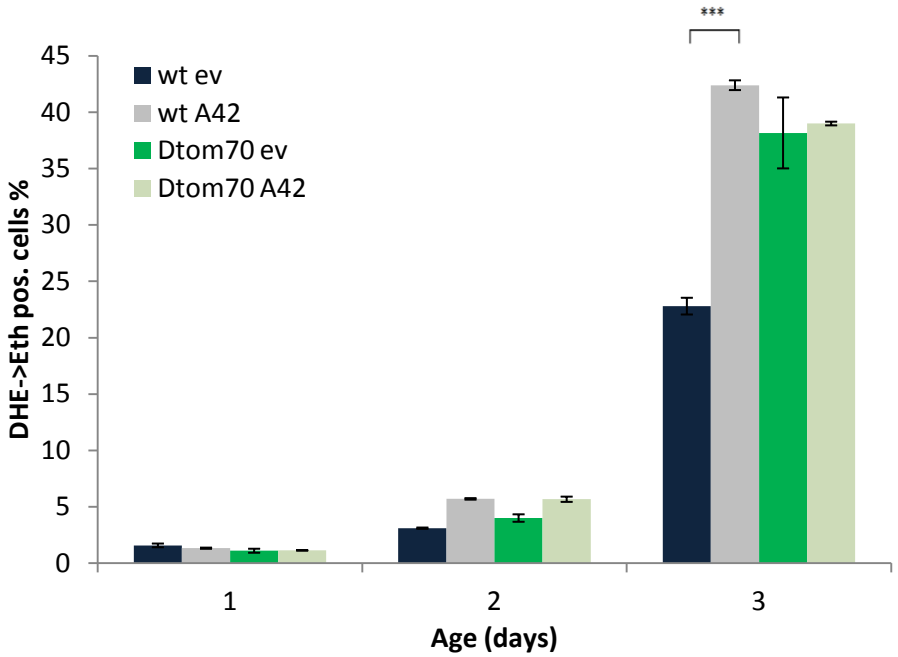

Figure 4.26. Deletion of TOM70 rescues A42-toxicity-mediated ROS accumulation during chronologically aging. Yeast cells were chronologically aged for 3 days. ROS levels were quantified by DHE-staining. DHE converse to Ethidium due to reaction with ROS, which can be measured by FACS analysis. 30 000 cells were evaluated in each experiment. Data show one representative experiment, mean of 6 tested clones and the error bars, the standard error ($p < 0.001$ = ***, $p < 0.01$ = **, $p < 0.05$ = *).

The DHE staining of Dtom70 strain compared to the wild type confirmed the screen result especially on day 3 of chronological aging. Dtom70 rescued A42-mediated ROS accumulation during the chronological aging, whereas wild type expressing EGFP-A42 compared to its vector control showed impaired cell viability and accumulation of ROS within cell.

In addition to chronological aging, cells were also treated with acetic acid to investigate if Dtom70 can rescue A42-mediated ROS accumulation after stress stimuli. Yeast cells were treated with acetic acid after 16h of the construct expression. Cells were incubated with acetic acid for 4h after which they were DHE stained for the ROS accumulations quantification (Figure 4.27).

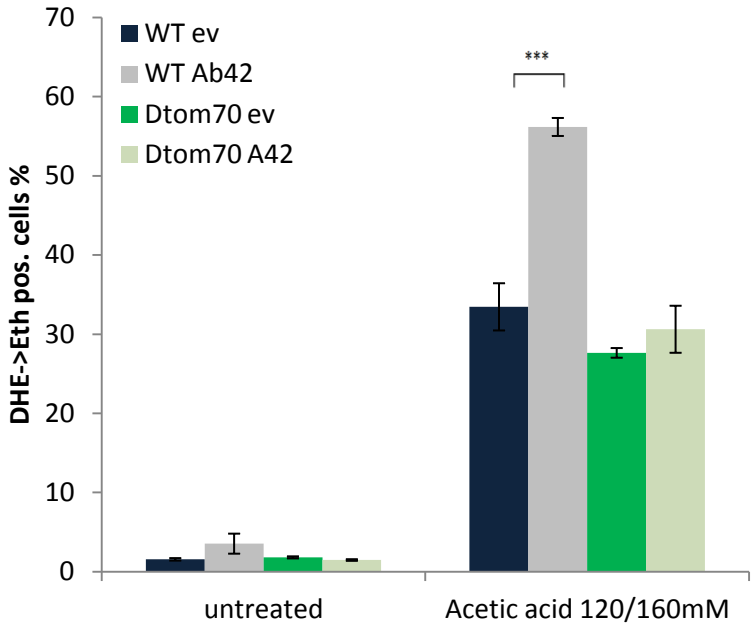

Figure 4.27. **Deletion of TOM70 rescues A42-mediated ROS accumulation after acetic acid treatment.** Yeast cells were treated with acetic acid 16h after A42-constructs expression and 4h after acetic acid treatment, ROS levels were quantified by DHE-staining. DHE converse to Ethidium due to reaction with ROS, which can be measured by FACS analysis. 30 000 cells were evaluated in each experiment. Data show one representative experiment, mean of 6 tested clones and the error bars, the standard error ($p < 0.001$ = ***, $p < 0.01$ = **, $p < 0.05$ = *).

Cell viability, after acetic acid treatment of the cells Dtom70 expressing EGFP-A42 was not impaired. Deletion of *TOM70* rescued the A42-mediated ROS accumulation induced by acetic acid. Wild type expressing EGFP-A42 compared to its vector control, showed impaired cell viability and accumulation of ROS.

Do to the fact that deletion of *TOM70* rescued A42-mediated ROS accumulations during chronological aging and after stress stimuli, the influence of *TOM70* deletion on EGFP-A42 aggregation was investigated by fluorescence microscopy. Yeast cells were harvested after ~20 hours of construct expression. Wild type and Dtom70 expressing EGFP-A42 were compared. FITC filter was used for the green fluorescence of the EGFP protein (Figure 4.28).

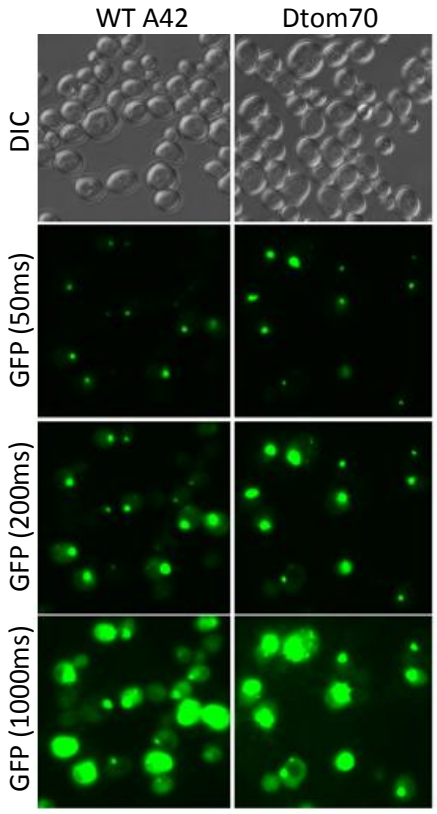

Figure 4.28. Deletion of *TOM70* has no influence on A42 aggregation. Yeast wild type and Dtom70 cells, expressing N-terminal EGFP-tagged human were fluorescence microscoped after ~20h of expression. For the microscopy an aliquot of the yeast cultures were harvested and 2µl were taken from the cell pellet. FITC filter was used for the green fluorescence of EGFP-constructs. Representative micrographs are shown.

Fluorescence microscopy revealed puncative structures of EGFP-A42 in both of the strains, wild type and Dtom70, which indicates that Tom70p as a protein involved in mitochondrial import machinery does not have any influence on aggregation or disaggregation of EGFP-A42.

Cellular fractionation was performed as described above and used to determine if deletion of tom70 has influence of A42's localization to mitochondria. In general we can say that results of cell fraction are similar to those observed in WT. Unfortunately we do not have a direct comparision to WT in this experiment, to investigate if certain bands show different intensities or distribution within cell fractionations. For more detailed investigations this experiment has to be repeated simultaneously with WT expressing EGFP-A42. Of note, the double band at 110kDa is nicely visible here (Figure 4.29).

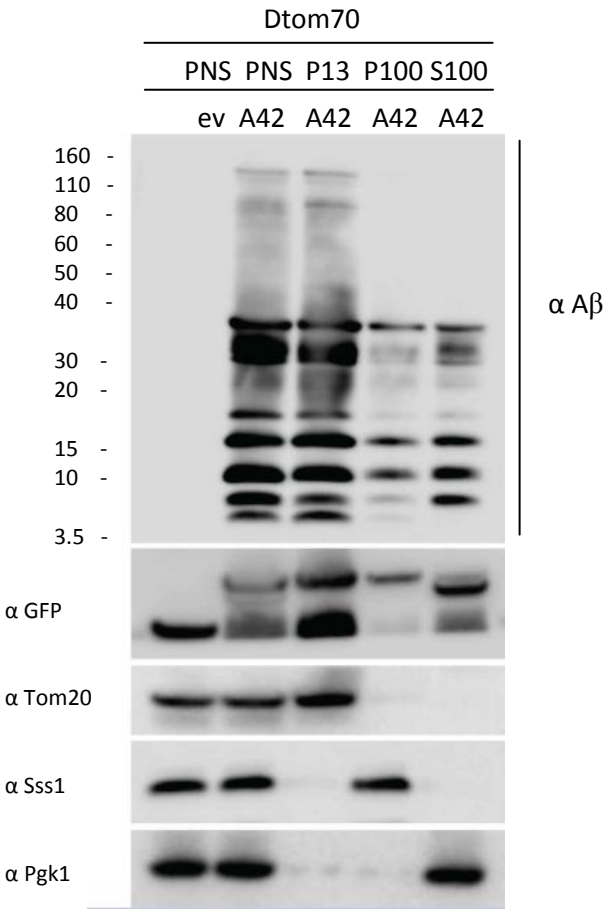

Figure 4.29. Dtom70 has no influence on A42 fibrillization pattern or A42 localization (Dirk Mossmann, AG Chris Meisinger, Freiburg, Germany). The cellular fractionation was performed 16h after the constructs expression in yeast cells. The obtained fractions were loaded to the 4%-12% Bis-Tris NuPage gel after which polyacrylamide gel electrophoresis was performed. The proteins from the gel were transferred to the membrane using semi dry transfer blotting method, after which the membranes were ready for blocking and immunodecoration. Representative blot is shown. Aβ antibody was used for the membrane decoration. Post nuclear supernatant (PNS); mitochondria fraction (P13) – Tom20 antibody; ER/microsome fraction (P100) – Sss1 antibody; cytosolic fraction (S100) – Pgk1 antibody.

4.3.12 Involvement of mitochondrial respiratory in yeast Alzheimer's disease model

Due to mitochondria involvement in Alzheimer's disease and due to the fact that most of the elucidated "hits" from deletion strains screen were mitochondrial proteins, two respiratory deficient strains were additionally analyzed in this work. Production of ROS is a regular process during mitochondrial

respiratory chain activity. The overproduction of ROS could be involved in the pathogenesis of the Alzheimer's disease. Rho0 is a respiratory deficient strain due to lacking mitochondrial DNA and is incapable of oxidative phosphorylation. Oxa1p is a mitochondrial inner membrane insertase and can mediate the insertion of the proteins from matrix into the inner mitochondrial membrane. Deletion of *OXA1* in yeast leads to respiratory deficiency as a result of impaired function of cytochrome oxidase. These two strains were already analyzed separately from the screen by Dr. Julia Ring and Mag. Sandra Seba. It could be shown that deletion of *OXA1* and lack of the mitochondrial DNA can rescue A42-mediated ROS accumulation and decrease in viability of the cells during chronological aging and after stress stimuli. Due to galactose promoter which is used for the induction of EGFP-A42 expression, cells had to be shifted to the galactose media. However, cells showed impaired growth and protein expression. Therefore new scheme for respiratory deficient strain inoculation was developed which was used in this work (Figure 3.2).

4.3.13 New inoculation scheme influenced expression of EGFP-A42 in the wild type and Doxa1 strain

To investigate if new inoculation scheme changes the expression levels of EGFP-A42 in wild type and Doxa1 and influences A42 localization, cellular fractionation of these two strains expressing EGFP-A42 using both schemes was performed as described above. Cells were inoculated as already described in 3.10, using both schemes, after which 70OD of cells were harvested (Figure 4.30 and 4.31).

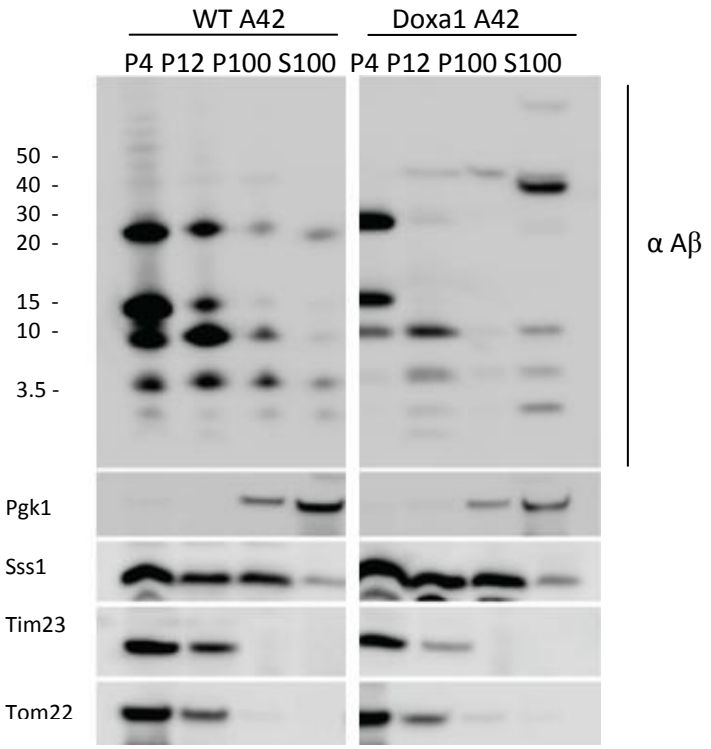

Figure 4.30.Using inoculation scheme 1, expression of EGFP-A42 in Doxa1 is weak compared to the EGFP-A42 in wild type. (Dirk Mossmann, AG Chris Meisinger, Freiburg, Germany). The cellular fractionation was performed 16h after the constructs expression in yeast cells induced by 2% galactose minimal media. The obtained fractions were loaded to the 4%-12% Bis-Tris NuPage gel after which polyacrylamide gel electrophoresis was performed. The proteins from the gel were transferred to the membrane using semi dry transfer blotting method, after which the membranes were ready for blocking and immunodecoration. Representative blot is shown. Aβ antibody was used for the membrane decoration. Post nuclear supernatant (P4); Mitochondria fraction (P13) – Tom20 and Tim23 antibody; ER/microsome fraction (P100) – Sss1; Cytosolic fraction (S100) – Pgk1 antibody.

Inoculation scheme 1 showed poor expression of EGFP-A42 in Doxa1 compared to the wild type. A42 mainly localizes to the mitochondria fraction in the wild type, whereas A42 mainly localizes to cytosolic fraction in Doxa1. However, using inoculation scheme 1, wild type and Doxa1 should not be compared due to differences in expression levels of the EGFP-A42.

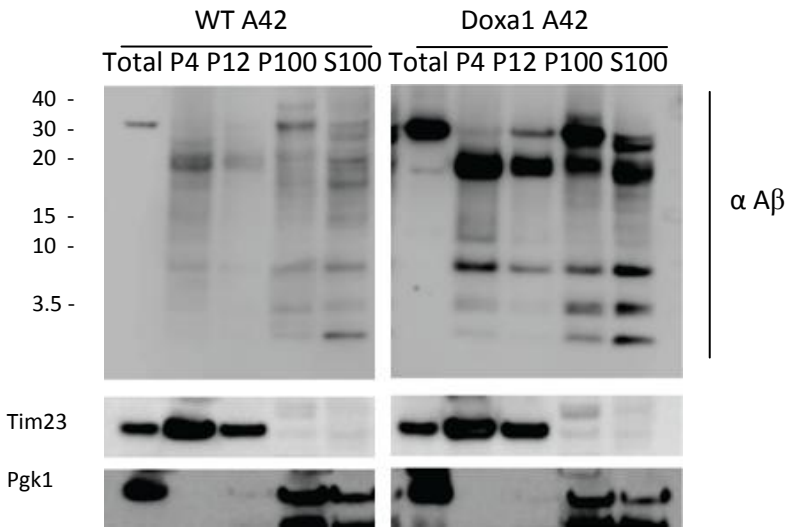

Figure 4.31.Using inoculation scheme 2, expression of EGFP-A42 in Doxa1 is stronger compared to the EGFP-A42 in wild type. (Dirk Mossmann, AG Chris Meisinger, Freiburg, Germany). The cellular fractionation was performed 16h after second inoculation to 1.8% galactose/0.2% glucose minimal media. Second inoculation was performed 24h after induction of galactose promoter with 2% of galactose. The obtained fractions were loaded to the 4%-12% Bis-Tris NuPage gel and a polyacrylamide gel electrophoresis was performed. The proteins from the gel were transferred to the membrane using semi dry transfer blotting method, after which the membranes were ready for blocking and immunodecoration. Representative blot is shown. Aβ antibody was used for the membrane decoration. Total – whole yeast extract; Post nuclear supernatant (P4); Mitochondria fraction (P13) – Tim23 antibody; ER/microsome fraction (P100); Cytosolic fraction (S100) – Pgk1 antibody.

Inoculation scheme 2 showed poor expression of EGFP-A42 in wild type compared to *OXA1* deletion strain. On the other hand expression of EGFP-A42 in Doxa1 was improved by the new scheme. A42 localize in all fractions of Doxa1, mainly in ER and cytosol fraction, whereas A42 in wild type is presented as degradation products. No significant changes in fibrillization pattern of A42 in Doxa1 were observed. Since membrane was cut, no higher ~110kDa bad can be seen, for that reason this experiment should be repeated. Nevertheless, inoculation of these two strains is still not improved due to differences in EGFP-A42 expression in wild type and Doxa1.

4.3.14 New inoculation scheme influenced A42 cytotoxicity during chronological aging in Doxa1 and wild type cells expressing EGFP-A42

To investigate if new inoculation can influence A42 cytotocixity in Doxa1 and wild type expressing EGFP-A42 compared to its vector control, yeast cells were 4 days chronologically aged and analyzed. Due to

the fact that Doxa1 cells show accelerated cell death, cells were twice a day analyzed by ROS accumulation quantification (Figure 4.32).

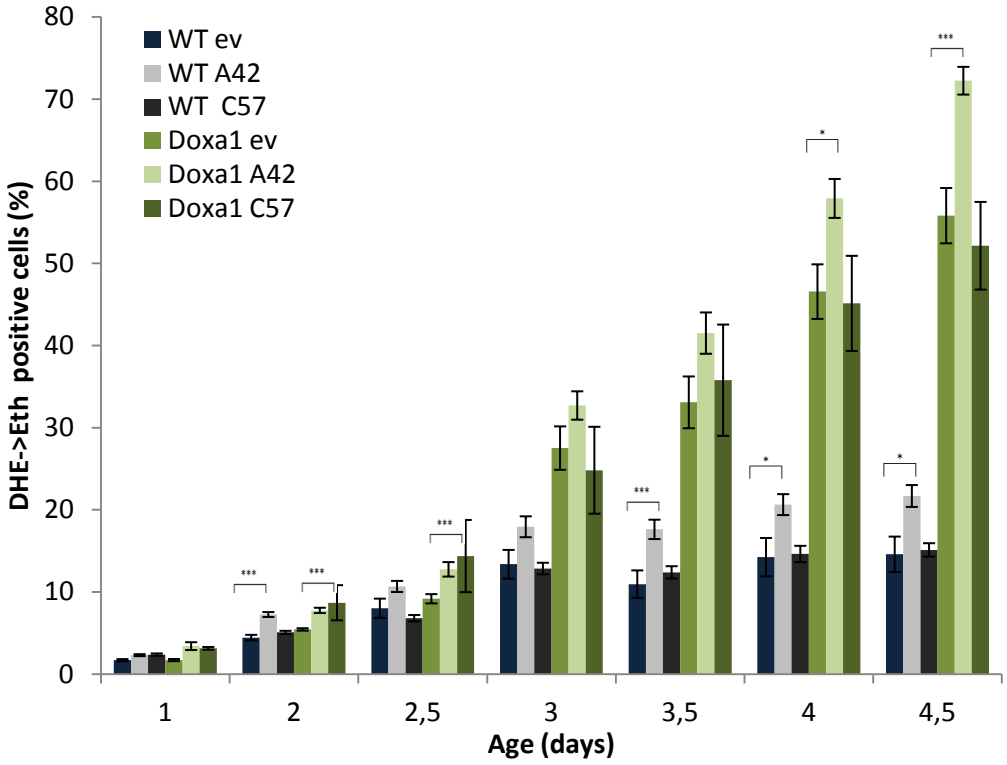

Figure 4.32. New inoculation scheme influenced A42 cytotoxicity in Doxa1 and wild type expressing EGFP-A42. Yeast cells were chronologically aged for 4 days. Second inoculation with 1.8% galactose/0.2 glucose medium was performed 24h after induction of galactose promoter with 2% of galactose. ROS levels were quantified by DHE-staining. DHE converse to Ethidium due to reaction with ROS, which can be measured by FACS analysis. 30 000 cells were evaluated in each experiment. Data show one representative experiment, mean of 6 tested clones and the error bars, the standard error ($p < 0.001$ = ***, $p < 0.01$ = **, $p < 0.05$ = *).

ROS measurements of chronologically aged yeast cells which were inoculated using new scheme revealed changes in A42 cytotoxicity. A42 mediated ROS accumulations in wild type were decreased using new scheme for inoculation. Differences in ROS accumulations between wild type cells expressing EGFP-A42 and its vector control were not constantly significant during chronological aging. On the other hand deletion on *OXA1* did not completely rescued A42-mediated ROS accumulations during chronological aging.

4.3.15 New inoculation scheme influenced A42 cytotoxicity after stress stimuli in wild type cells expressing EGFP-A42

To investigate if new inoculation can influence A42 cytotocixity during stress stimuli in Doxa1 and wild type expressing EGFP-A42 compared to its vector control, yeast cells were treated with acetic acid and 4h later analyzed. In addition, one parallel experiment was performed in which yeast cells were inoculated using scheme 1. These cells were also treated with acetic acid and after 4h DHE stained for ROS accumulation measurements (Figure 4.33).

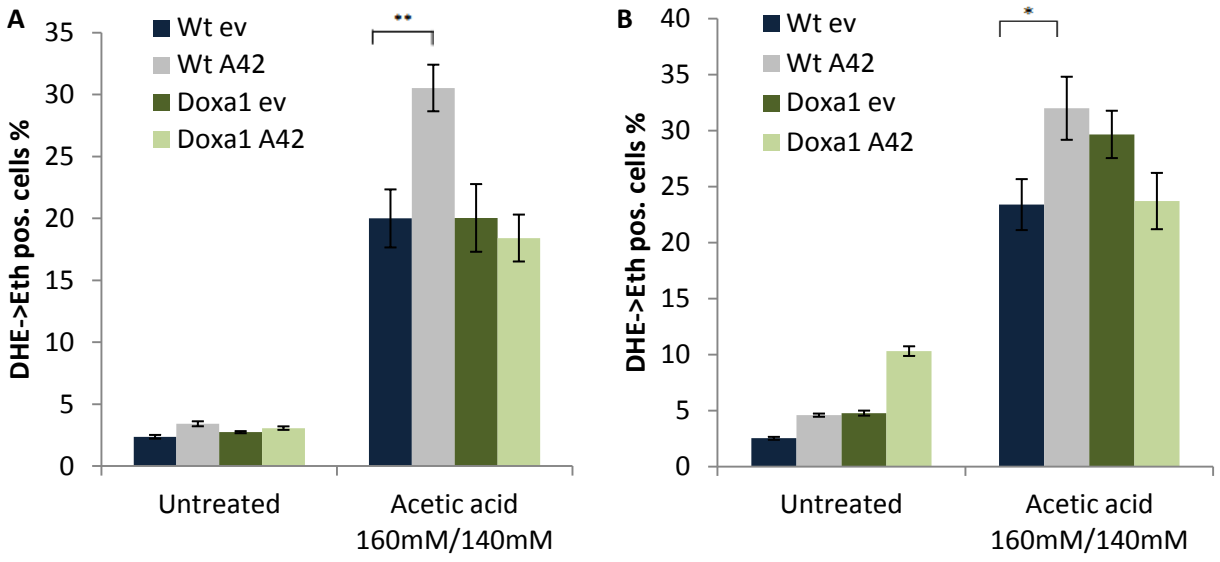

Figure 4.33. New inoculation scheme influenced A42 cytotoxicity after stress stimuli in wild type cells expressing EGFP-A42. Yeast cells were treated with acetic acid and 4h after treatment, ROS levels were quantified by DHE-staining. **A** acetic acid added after 16h of construct expression induced by 2% galactose, scheme 1. **B** Acetic acid added 16h after second inoculation in 1.8%galactose/0.2%glucose medium, scheme 2. DHE converse to Ethidium due to reaction with ROS, which can be measured by FACS analysis. 30 000 cells were evaluated in each experiment. Data show one representative experiment, mean of 6 tested clones and the error bars, the standard error ($p < 0.001$ = ***, $p < 0.01$ = **, $p < 0.05$ = *)

New inoculation scheme influenced A42 mediated ROS accumulation after stress stimuli with acetic acid in wild type. Expression of EGFP-A42 significantly induced ROS accumulations in wild type cells inoculated using scheme 1 compared to its vector control. On the other hand expression of EGFP-A42 only slightly induced ROS accumulation in wild type cells inoculated using scheme 2, whereas no

significant changes in A42-mediated cytotoxicity were observed in Doxa1 cells inoculated with both schemes. Deletion of *OXA1* rescued A42 mediated ROS accumulations in cells inoculated using both schemes.

4.3.16 New inoculation scheme influenced aggregation of EGFP-A42 in wild type and Doxa1

In addition to cellular fractionation and aging experiments, yeast wild type and Doxa1 inoculated with both schemes were analyzed under fluorescence microscope. Yeast cells were harvested after ~20 hours of construct expression with 2% galactose in scheme 1 and ~20 hours after second inoculation to the 1.8% galactose/0.2% glucose medium in scheme 2. FITC filter was used for the green fluorescence of the EGFP protein (Figure 4.34 and 4.35).

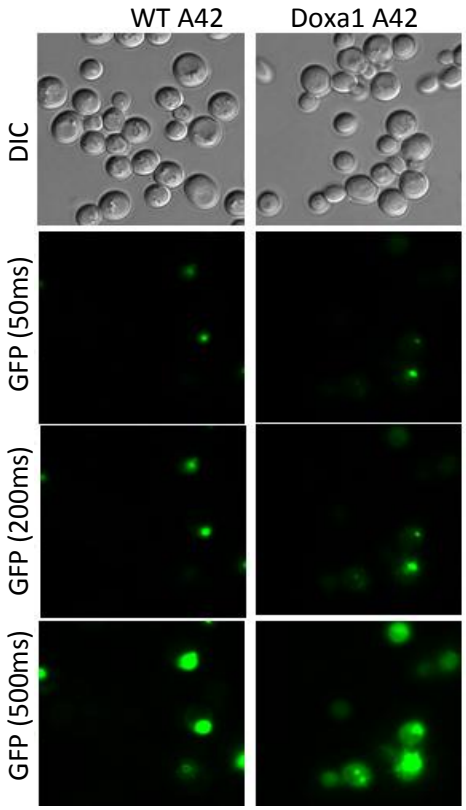

Figure 4.34. Deletion *OXA1* has influence on A42 aggregation in scheme 1. Yeast wild type and Doxa1 cells expressing N-terminal EGFP-tagged human A42 were fluorescence microscoped after ~20h of expression. For the microscopy an aliquot of the yeast cultures were harvested and 2µl were taken from the cell pellet. FITC filter was

used for the green fluorescence of EGFP-constructs. Representative micrographs are shown.

Fluorescence microcopy confirmed cellular fractionation of yeast cells inoculated using scheme 1. EGFP-A42 in *OXA1* deletion strain revealed puncative structures, as well as cytosolic localization within cell, compared to the wild type cells revealing EGFP-A42 aggregate like structures.

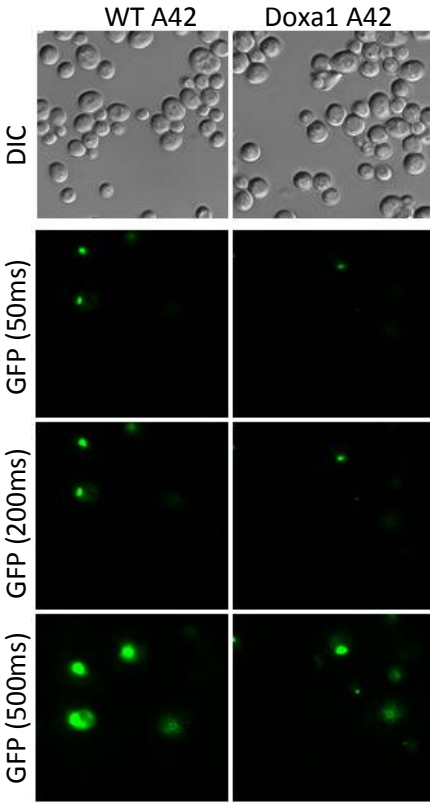

Figure 4.35. Deletion *OXA1* has influence on A42 aggregation in scheme 2. Yeast wild type and Doxa1 cells expressing N-terminal EGFP-tagged human A42 were fluorescence microscoped ~20h after second inoculation to the 1.8% galactose/0.2% glucose medium. For the microscopy an aliquot of the yeast cultures were harvested and 2µl were taken from the cell pellet. FITC filter was used for the green fluorescence of EGFP-constructs. Representative micrographs are shown.

New inoculation scheme influenced aggregation of EGFP-A42 in *OXA1* deletion strain and wild type cells. Wild type cells expressing EGFP-A42 inoculated with scheme 2 revealed less puncative structures and more EGFP-A42 within cytosol, than wild type cells inoculated with scheme 1. On the other hand, *OXA1* deletion strain revealed aggregation like structures. However, due to differences in EGFP-A42 expression which were observed in western blotting experiments, wild type cells and *OXA1* deletion strain expressing this construct should not be compared.

4.3.17 New inoculation scheme influenced expression of EGFP-A42 in the wild type and Rho0 strain

To investigate if new inoculation scheme induced expression levels of A42 in Rho0 strain as in Doxa1, cellular fractionation of wild type and Rho0 strain expressing EGFP-A42 using both schemes was performed as described above. Cells were inoculated as already described in 3.10, using both schemes, after which 70OD of cells were harvested (Figure 4.36 and 4.37).

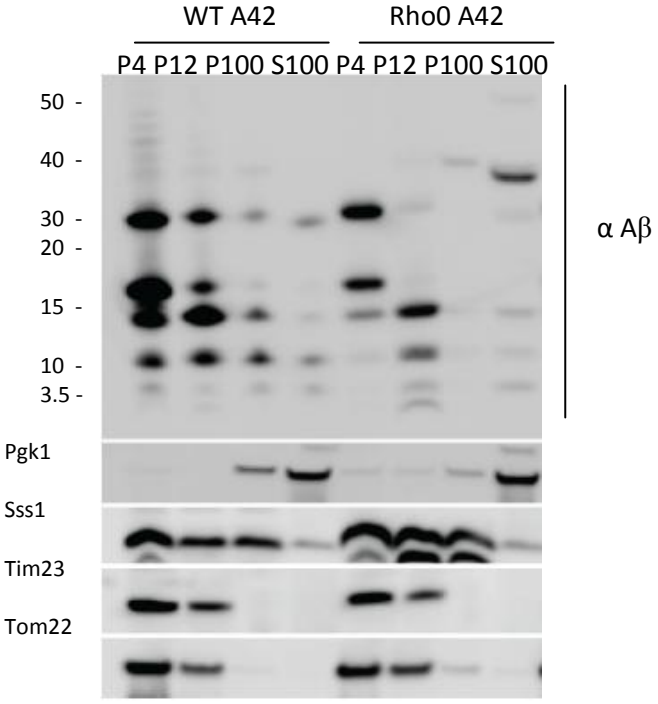

Figure 4.36. Using inoculation scheme 1, expression of EGFP-A42 in Rho0 is weak compared to the EGFP-A42 in wild type. (Dirk Mossmann, AG Chris Meisinger, Freiburg, Germany). The cellular fractionation was performed 16h after the constructs expression in yeast cells induced by 2% galactose minimal media. The obtained fractions were loaded to the 4%-12% Bis-Tris NuPage gel after which polyacrylamide gel electrophoresis was performed. The proteins from the gel were transferred to the membrane using semi dry transfer blotting method, after which the membranes were ready for blocking and immunodecoration. Representative blot is shown. Aβ antibody was used for the membrane decoration. Post nuclear supernatant (P4); mitochondria fraction (P13) – Tom20- and Tim23- antibody; ER/microsome fraction (P100) – Sss1; cytosolic fraction (S100) – Pgk1 antibody.

Inoculation scheme 1 showed poor expression of EGFP-A42 in Rho0 strain compared to the wild type. A42 mainly localizes to the mitochondria fraction in the wild type, as expected. The full construct EGFP-

A42 localizes mainly to cytosol fraction, whereas small “fragments” localize to mitochondria fraction in rho0 strain. However, using inoculation scheme 1, wild type and Rho0 should not be compared due to differences in expression levels of the EGFP-A42.

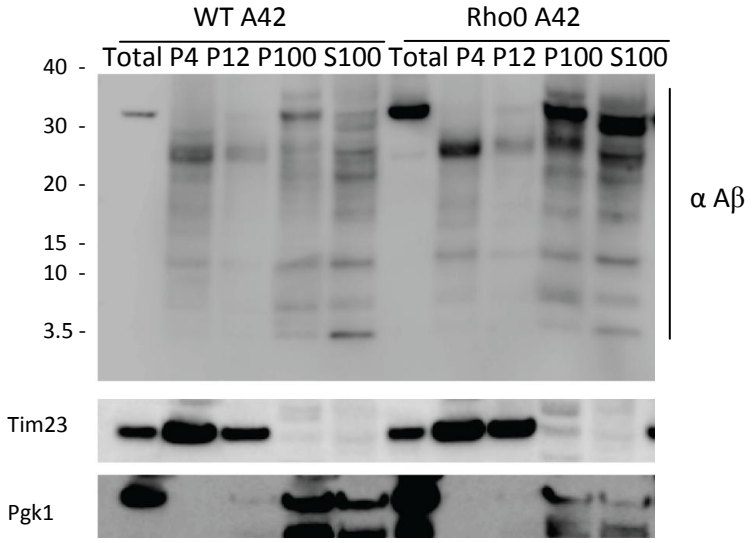

Figure 4.37. Using inoculation scheme 2, expression of EGFP-A42 in Rho0 is stronger compared to the EGFP-A42 in wild type. (Dirk Mossmann, AG Chris Meisinger, Freiburg, Germany). The cellular fractionation was performed 16h after second inoculation to 1.8% galactose/0.2% glucose minimal media. Second inoculation was performed 24h after induction of galactose promoter with 2% of galactose. The obtained fractions were loaded to the 4%-12% Bis-Tris NuPage gel after which polyacrylamide gel electrophoresis was performed. The proteins from the gel were transferred to the membrane using semi dry transfer blotting method, after which the membranes were ready for blocking and immunodecoration. Representative blot is shown. Aβ antibody was used for the membrane decoration. Total – whole yeast extract; post nuclear supernatant (P4); mitochondria fraction (P13) – Tim23 antibody; ER/microsome fraction (P100); cytosolic fraction (S100) – Pgk1 antibody.

Inoculation scheme 2 showed poor expression of EGFP-A42 in wild type compared to Rho0 strain. On the other hand expression of EGFP-A42 in Rho0 was improved by the new scheme. A42 localizes mainly in ER and cytosol fraction in Rho0 fractions, whereas A42 in wild type is presented as degradation products. However, A42 in Rho0 inoculated with scheme 2 revealed no A42 in mitochondria fraction as in Rho0 inoculated with scheme 1. No significant changes in fibrilization pattern of A42 in Rho0 were observed. Since membrane was cut, no higher ~110kDa bad can be seen, for that reason this experiment should be repeated. Nevertheless, inoculation of these two strains is still not improved due to differences in EGFP-A42 expression in wild type and Rho0. Rho0 cellular fractionation revealed similar results as the same experiment in *OXA1* deletion strain, which is also respiratory deficient strain.

4.3.18 Respiratory deficient strain Rho0 inoculated with new scheme 2 rescues A42-mediated cytotoxicity during chronological aging

To investigate if new inoculation scheme influences A42 cytotocixity in Rho0 expressing EGFP-A42 compared to its vector control, yeast cells were 4 days chronologically aged and analyzed compared to the wild type. It should be mentioned that the growth rates vary among different clones of Rho0. Yeast cells were DHE strained to quantify ROS accumulations during aging (Figure 4.38).

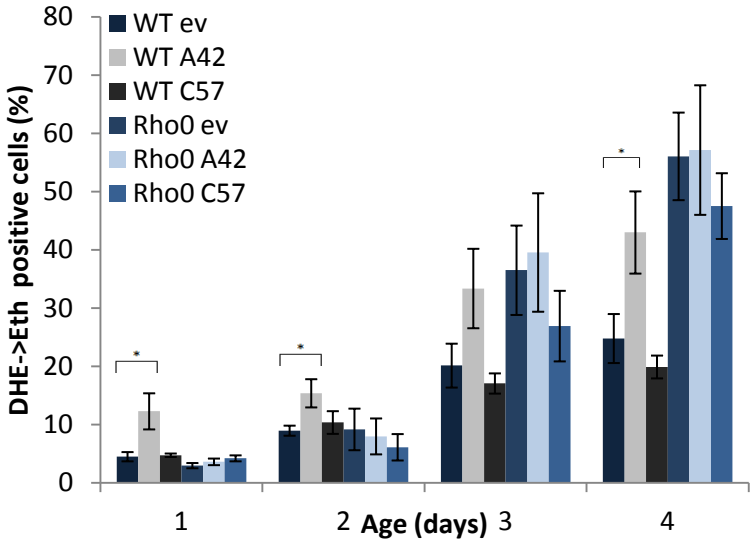

Figure 4.38. Respiratory deficient strain Rho0 inoculated with new scheme 2 rescues A42-mediated cytotoxicity during chronological aging. Yeast cells were chronologically aged for 4 days. Second inoculation was performed 24h after induction of galactose promoter with 2% of galactose. ROS levels were quantified by DHE-staining. DHE converse to Ethidium due to reaction with ROS, which can be measured by FACS analysis. 30 000 cells were evaluated in each experiment. Data show one representative experiment, mean of 6 tested clones and the error bars, the standard error ($p < 0.001$ = ***, $p < 0.01$ = **, $p < 0.05$ = *).

ROS measurements of chronologically aged yeast cells which were inoculated using new scheme revealed changes in A42 cytotoxicity in wild type cells expressing EGFP-A42. Differences in ROS accumulations between wild type cells expressing EGFP-A42 and its vector control were not constantly significant during chronological aging. However, Rho0 inoculated with new scheme rescued A42

mediated ROS during chronological aging. Nevertheless, due to high variations between Rho0 clones, error bars were too high to discuss the results.

4.3.19 Respiratory deficiency strain Rho0 inoculated with new scheme 2 rescues A42-mediated cytotoxicity after stress stimuli with acetic acid

To investigate if new inoculation can influence A42 cytotocixity during stress stimuli in Rho0 expressing EGFP-A42 compared to its vector control, yeast cells were treated with acetic acid and 4h later DHE stained for ROS measurements. Rho0 cells were compared to the wild type cells (Figure 4.39).

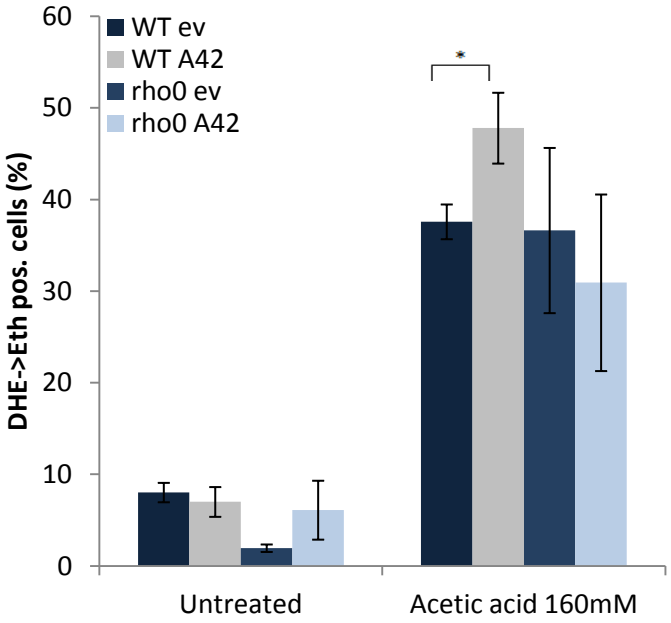

Figure 4.39. Respiratory deficient strain Rho0 inoculated with new scheme 2 rescues A42-mediated cytotoxicity after stress stimuli with acetic acid. Yeast cells were treated with acetic acid and 4h after treatment, ROS levels were quantified by DHE-staining. Acetic acid added 16h after second inoculation in 1.8%galactose/0.2%glucose, scheme 2. DHE converse to Ethidium due to reaction with ROS, which can be measured by FACS analysis. 30 000 cells were evaluated in each experiment. Data show one representative experiment, mean of 6 tested clones and the error bars, the standard error ($p < 0.001$ = ***, $p < 0.01$ = **, $p < 0.05$ = *)

New inoculation scheme influenced A42 mediated ROS accumulation after stress stimuli with acetic acid in wild type. Expression of EGFP-A42 slightly induced ROS accumulation in wild type cells inoculated using scheme 2, whereas no significant changes in A42-mediated cytotoxicity were observed in Rho0 cells. Respiratory deficient strain, lacking mitochondrial DNA rescued A42 mediated ROS accumulations

in yeast cells after stress stimuli with acetic acid. However, high variations between Rho0 clones showed high error bars.

4.3.20 New inoculation scheme influenced aggregation of EGFP-A42 in Rho0 and wild type strain

In addition to cellular fractionation-, chronological aging- and stress stimuli- experiments, Rho0 strain expressing EGFP-A42 was analyzed under fluorescence microscope and its influence on EGFP-A42 aggregation was investigated. Yeast cells were harvested after ~20 hours of construct expression, scheme 1 and ~20 hours after second inoculation inoculation to the 1.8% galactose/0.2% glucose medium in scheme 2. WT expressing EGFP-A42 was compared to the Rho0 expressing EGFP-A42. FITC filter was used for the green fluorescence of the EGFP protein (Figure 4.40 and 4.41).

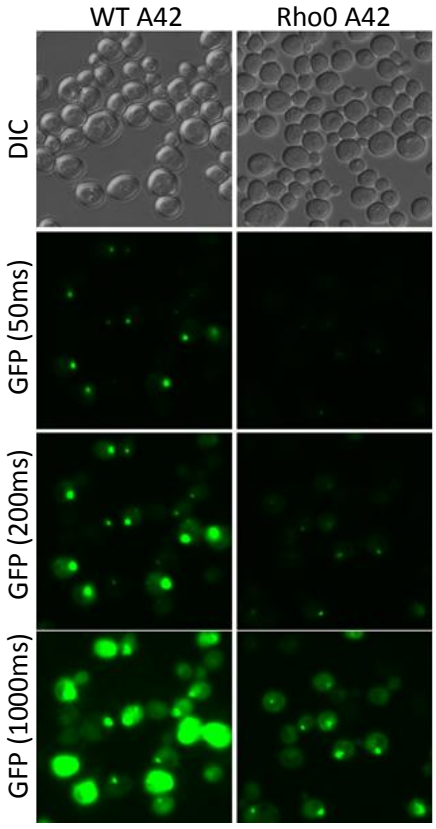

Figure 4.40. Respiratory deficient strain, Rho0 inoculated with scheme 1 revealed less aggregation-like structures compared to the wild type cells. Yeast wild type cells and Rho0 strain, expressing N-terminal EGFP-tagged human A42 were fluorescence microscoped after ~20h of expression. For the microscopy an aliquot of the

yeast cultures were harvested and 2µl was taken from the cell pellet. FITC filter was used for the green fluorescence of EGFP-constructs. Representative micrographs are shown.

Fluorescence microscopy of respiratory deficient strain Rho0 expressing EGFP-A42 revealed decrease in EFP-A42 aggregation, compared to the wild type expressing the same construct. Wild type cells expressing EGFP-A42 displayed puncative aggregate-like structures, whereas Rho0 cells showed smaller puncative structures and mainly cytosolic localization of EGFP-A42.

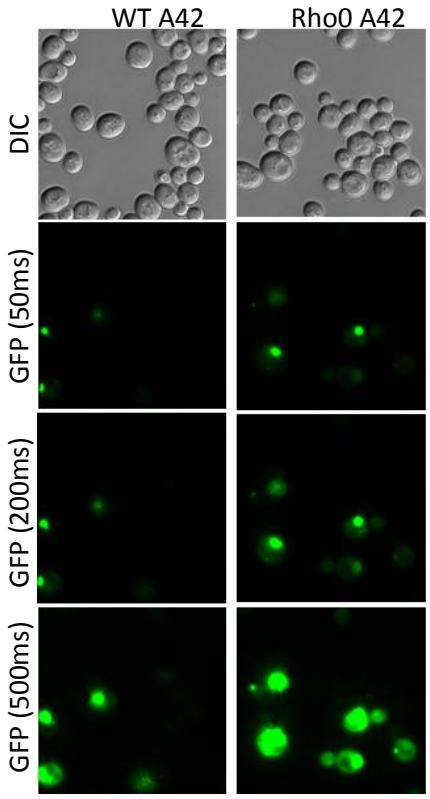

Figure 4.41. Respiratory deficient strain, Rho0 inoculated with scheme 2 revealed aggregation-like structures. Yeast wild type and Rho0 cells expressing N-terminal EGFP-tagged human A42 were fluorescence microscoped ~20h after second inoculation to the 1.8% galacotse/0.2% glucose medium. For the microscopy an aliquot of the yeast cultures was harvested and 2µl were taken from the cell pellet. FITC filter was used for the green fluorescence of EGFP-constructs. Representative micrographs are shown.

In contrast to scheme 1, Rho0 cells expressing EGFP-A42 inoculated with scheme 2 revealed aggregate like structures as wild type cells inoculated with scheme 1. On the contrary, wild type cells inoculated with scheme 2 showed less aggregate-like structures compared to scheme 1. Therefore these two strains should not be compared using both schemes.

5. DISCUSSION

5.1 Heterologous expression of A42 shows a cytotoxic effect in yeast BY4741

AD is most common age-related neurodegenerative disease and one of the biggest social burdens in the world. Much effort is invested in preventing and curing AD. However, there is still no cure for AD, and research society is still searching for new treatments which could alter the course of the disease, or at least improve the quality of life for affected people. Till now, most of the studies were carried out using cell cultures or transgenic mouse models or higher eukaryotes, while recently a new AD research field is opened involving yeast as a model for AD. Yeast is a useful toolbox for investigation of cellular mechanism involved in AD, due to well characterized biology and its simplicity. During this project a yeast model to investigate toxicity of intracellular A42 was established. This model was used to investigate the impact of A42 on yeast BY4741, as well as for the elucidation of the key players, which could potentially be involved in cellular pathways of AD mediated pathology. This project followed the hypothesis, that intracellular A42 species are responsible for elevated ROS and neurodegeneration during AD [Pimentel *at al,.* 2012]. Therefore, yeast cells expressing human A42 were chronologically aged and put under stress stimuli, after which ROS accumulation in cells was quantified. To ensure stability of A42 within the cell it was N-terminally fused to EGFP. Additional a linker was inserted between A42 and EGFP to ensure proper folding of EGFP, as well as of A42 [Caine *at al,.* 2007]. One of the first goals of this study was to investigate the A42 cytotoxicity. It could be shown that the heterologous expression of A42 in BY4741 yeast can elevate ROS levels during chronological aging (Figure 4.1 and 4.2). In addition, A42 expression decreased cell viability of BY4741 yeast cells after stress stimuli (Figure 4.1). Furthermore, A42-mediated cytotoxicity is linked to necrotic cell death (Figure 1.5).

A strong correlation between synaptic loss and soluble Aβ oligomers levels in AD brains was reported, in contrast, senile plaques only poorly correlate with local neuronal death or cognitive impairment. It could be shown that Aβ oligomer are more cytotoxic than fibrillar Aβ aggregates [Sakono and Zak,. 2009]. The next step in this work was to investigate if this cytotoxicity is linked to the soluble Aβ oligomers hypothesis. For that reason, A42 mutants which are not able to aggregate or oligomerize are linked to EGFP in the same manner as A42 and transformed to BY4247 yeast cells. A42m1 contains two mutations disrupting only one hydrophobic region responsible for A42 oligomerization, whereas A42m2 contains three mutations disrupting both hydrophobic regions essential for its oligomerization.

We could show that cell viability of cells expressing A42m2 was not impaired during chronological aging (Figure 4.3). In addition, yeast cells expressing A42m2 did not show aggregate-like structures as A42 under fluorescence microscope or mitochondrial localization as seen with normal A42 (Figure 4.4, and 4.5). These results implicated the involvement of A42 oligomers in A42-mediated cytotoxicity. This finding was confirmed by detection of different A42 species and aggregation states by localization studies, SDS assay, as well as time curse of A42 detection. The most constant and striking band was shown to be ~110kDa higher band, detected with Aβ- and GFP-antibody, which disappears after boiling the samples during SDS assay. This result leads to conclusion that this band correspond to SDS stable heat sensitive n-low oligomer of EGFP-A42 construct (due to detection with both antibodies) (Figure 4.10). In addition this band appears after some time of construct expression, is mainly localized to the mitochondrial fraction and not detected in wild type expressing A42m2 fractions (Figure 4.8 and 4.9). Similar results were published by Bagriantsev and Liebman, who introduced mutations in A42 to disrupt the regions responsible for the oligomerization. They also observed that their A42-construct can form SDS stable oligomers in yeast, which disappeared after boiling and were not detected in yeast cells expressing A42 mutants [Bagriantsev and Liebman, 2006]. Besides higher ~110kDa band, smaller size bands were detected with Aβ-antibody. Even though slightly shifted upwards, these smaller bands remind and correlated in size to the A42 oligomers seen in fibrillization assay with synthetic A42 (Figure 4.9). Most importantly, these bands also mainly localize to the mitochondria fraction and were not detected in wild type expressing A42m2 fractions. However, only one band ~25 kDa was not detected after boiling the samples during SDS assay. This finding could implicate that these smaller bands correspond to degraded fragments of EGFP-A42 construct. Nevertheless, these smaller bands are detected with Aβ antibody and the smallest band is the same kDa size as A42 monomer (~3,5 kDa). This could indicate that smaller “fragments” could aggregate, due to fibrillization nature of A42. Furthermore, fibrillization pattern of synthetic A42 is very similar to A42 in mitochondrial fraction of wild type and A40 which is less toxic and less prone to aggregate shows less fibrillization than A42, whereas A42m2 does not show fibrillization patter at all (Figure 4.9).

It is very likely that the small bands we see on western blots are a mixture of EGFP-A42 fragments as well as A42 oligomers. As we see A42 monomers and it is known that A42 has a high tendency to aggregate/form oligomers with other A42 monomers, it is very likely that free A42 monomers form either oligomers or are degraded.

Next interesting finding is that C57 which is used in this work as a control for A42-mediated cytotoxicity revealed also aggregate-like structures under fluorescence microscope (Figure 4.7). Even though, C57 aggregated similar to A42, it localizes mainly to cytosol fraction and does not influence yeast cell viability (Figure 4.6 and 4.9). This finding implicates that the A42's translocation to mitochondria and mediated cytotoxicity is not simple due to its aggregation, but a specific physiological phenotype. Of note, A42m1 induced ROS accumulations in yeast cells during the aging, ER localization and revealed linear structures under fluorescence microscope. It appears that the mutations changed the nature of A42 and generated artificial A42 system (Figure 4.3, 4.4 and 4.5).

5.2 Ssa1p and Ydj1p influence A42 aggregation and localization in BY4741 yeast cells

Data are accumulating demonstrating high relevance of chaperones in Alzheimer's disease, due to protein aggregates which are involved in AD pathology. It could be shown that specific chaperones are up-regulated in the AD brains and can bind to A42, such as Hsp70. A previously performed screen revealed two chaperones as potential key players of AD pathology, namely Ssa1p and Ydj1p. It could be shown that deletions of *SSA1* and *YDJ1* can rescue A42-mediated toxicity, such as ROS accumulation during chronological aging or after stress stimuli (Figure 4.12, 4.13 and 4.15).

Additionally, in this work, it was demonstrated that levels of Ydj1p and Ssa1p are elevated in yeast cells expressing A42 (Figure 4.18). These findings correlate to published data which demonstrated up-regulation of some chaperones in AD brains [Wilhelmus *et al*., 2007; Perez *et al*., 1991]. These proteins work orchestrated and can dissolve aggregates of misfolded proteins within the cells and translocate them to ER and mitochondria. Additionally, they can bind to freshly synthesized proteins and prevent their aggregation. This correlates also to our results. Fluorescence microcopy revealed that Ssa1p and Ydj1p can influence the A42 aggregation (Figure 4.19 and 4.20) and localization studies showed that Ssa1p and Ydj1p can influence A42 translocation in the cell (Figure 4.21, 4.20 and 4.25). This is a very dynamic process and there is high probability of involvement of other proteins in this process. Deletion of *SSA1* revealed big aggregates. One possibility is that Ssa1p prevents aggregation of A42. It has been published that Hsp70 in combination with Hsp40 partially prevent A42 aggregation and assembly *in vitro* generating roughly circular structures. Hsp40 alone is not able to prevent the aggregation, whereas Hsp70 can block the A42 aggregation alone, even though it is less efficient than in combination with

Hsp40 [Evans *et al*., 2011]. The second possibility is that Ssa1p disaggregates big aggregates together with Ydj1p. On the other hand deletion of *YDJ1* revealed almost no A42 aggregation which indicates that Ssa1p requires Ydj1p for preventing A42 aggregation due to ATPase activity. Another hypothesis would be that Ydj1p somehow stabilizes A42 and protects it against degradation an aggregation, as Ydj1p A42 co-expressing cells show high amount of small A42 species, (Figure 4.25). It has been already published that Hsp40 somehow protects A42 and elevate A42 levels when overexpressed in specific neurons [Carnini *et al*., 2012]. It has been also hypothesized that some chaperones could act as "sick chaperones" during aging and neurodegenerative diseases. In this case, chaperones can be sequestered onto amyloid aggregates and be re-directed from their normal tasks [Satyal *et al*., 2000]. However, many researchers see chaperones as promising therapeutic opportunities for AD, due to the fact that some chaperones can prevent aggregation of misfolded proteins and suppress Alzheimer's disease-related phenotypes by over-expression of Hsp70 [Hoshino *et al*., 2011]. This approach should be evaluated carefully, as the overexpression of some chaperones may result in the instability of cell-stress mechanism or re-direct chaperone activity which could induce cell system to collapse. In addition, results revealed in this work found a link between chaperones and mitochondria as well as ROS accumulation within cells, which could be responsible for yeast cell death similar as in neurons in brains of AD patients. There are few possibilities how chaperones can influence A42 in yeast cells, possible pathways, can be seen in Figure 5.1.

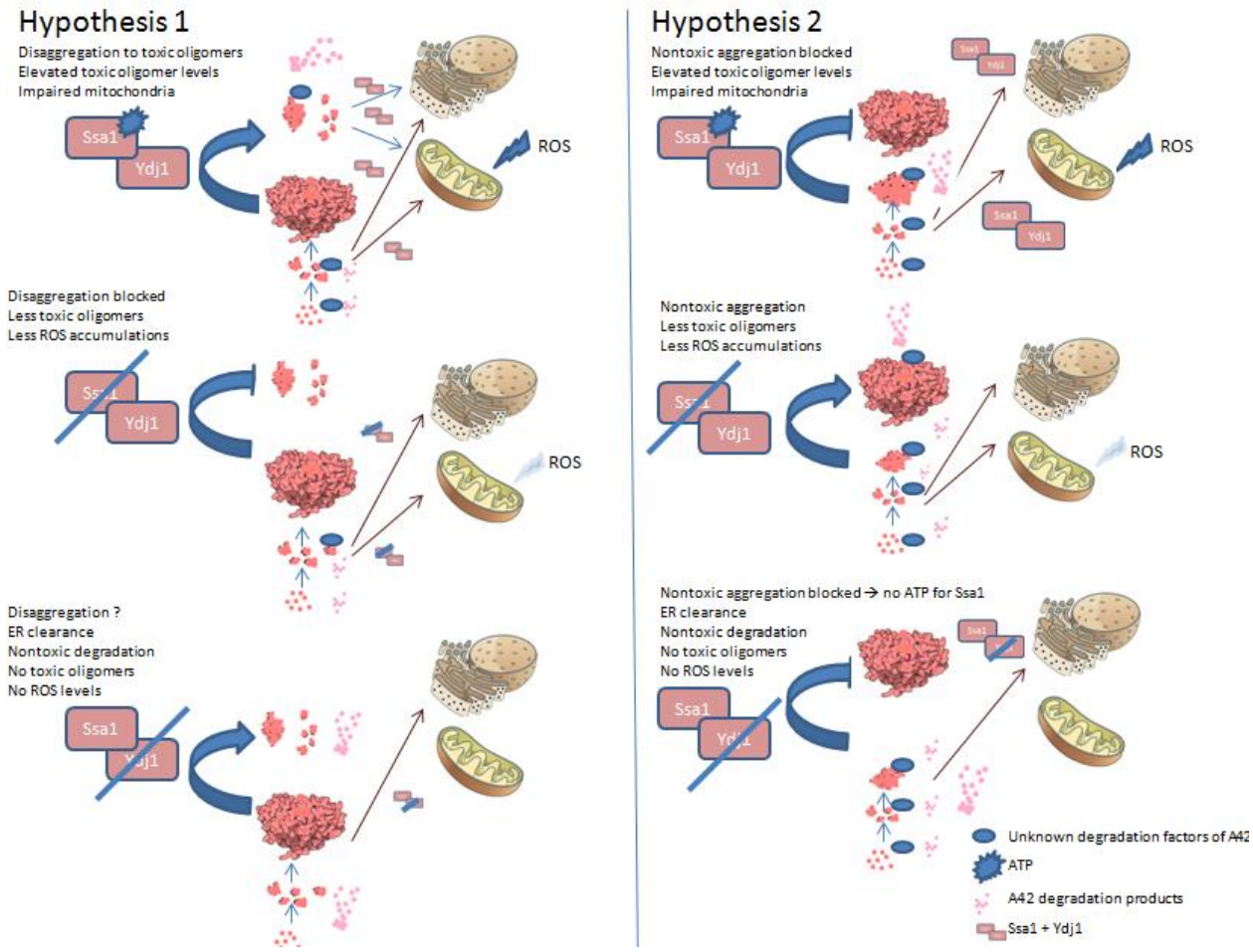

Figure 5.1. Chaperones influence A42 aggregation and induce accumulations of ROS levels in yeast cells expressing A42. Chaperones may give a rise to toxic oligomers and other aggregation assemblies in yeast cells expressing A42. In the first hypothesis Ssa1p and Ydj1p are orchestrated to disaggregate A42 aggregates to toxic oligomers after which they translocate them to ER or mitochondria. In the second hypothesis these two chaperones are preventing assembly of A42 to bigger protective aggregates and translocate generated toxic oligomers to the ER and mitochondria.

5.3 Tom70p may bind to A42 to the outer mitochondrial membrane hence providing A42 toxicity

Tom70p was also revealed as potential key player from previously performed screen. In this work, it could be confirmed that deletion of *TOM70* can rescue A42 mediated cytotoxicity (Figure 4.26 and 4.27). Most of the proteins targeted to the mitochondria are transported by translocase of the outer membrane (TOM) complex. Tom70p is an essential surface receptor for mitochondrial precursors. It has

been suggested that TOM import machinery imports amyloid beta peptides into mitochondria [Petersen *et al*., 2008]. Localization studies in this work revealed A42 localization to the mitochondria. However, even though deletion of *TOM70* did not significantly influence the A42 translocation (Figure 4.29) it does prevent A42 mediated toxcicity. It has been hypothesized that A42 can bind to Tom70p via hydrophobic interactions and most importantly, the insertion of A42 to the mitochondria is dependent on length, hydrophobicity and helix potential. In this work, A42 is linked to EGFP which could influence insertion into the mitochondria. However, there is a possibility that smaller fragments detected with Aβ antibody could be inserted into mitochondria and impair its function.

5.4 Involvement of mitochondria in AD pathology

A majority of the elucidated potential key players of performed screen were mitochondrial proteins. Two deficient respiratory strains were additionally analyzed in this work, namely Rho0 and *OXA1* deletion strain. Due to galactose promoter which is used for induction of the A42 expression in this work, inoculation of these strains was inconvenient for the optimal growth and protein expression. New inoculation scheme which should improve A42 expression and growth of respiratory deficient strains was developed. Indeed, A42 expression was improved, however, A42 expression in wild type cells was negatively influenced (Figure 4.30, 4.31, 4.36 and 4.37). A42-mediated cytotoxicity in wild type cells was decreased by new inoculation scheme (Figure 4.32 and 4.38). Therefore, comparison between respiratory deficient strains and wild type was complicated. A42-mediated ROS accumulation induced by stress stimuli was rescued by deletion of *OXA1* and Rho0 strain, despite increased A42 levels in yeast cells (Figure 4.33 and 4.39). Deletion of *OXA1* did not completely rescued A42 mediated ROS accumulation during chronological aging (Figure 4.32). On the other hand A42 expressed in Rho0 strain did not display cytotoxicity during chronological aging compared to the wild type (4.38). However, Rho0 clones were variable in growth and A42 expression. Nevertheless, altogether revealed results indicate involvement of mitochondria and/or respiration in AD pathology. This goes along with a study were it has been shown that some cells in AD patient's brain are resistant to A42 mediated toxicity and cell death, due to the fact that they switched their metabolism to aerobic glycolysis (Warburg effect) by which they avoided respiration [Newington *et al*., 2011].

References

Ahmed, Mahiuddin; Davis, Judianne; Aucoin, Darryl; Sato, Takeshi; Ahuja, Shivani; Aimoto, Saburo et al. (2010): Structural conversion of neurotoxic amyloid-beta(1-42) oligomers to fibrils. In: *Nat. Struct. Mol. Biol* 17 (5), S. 561–567.

Ahn, Sung-Hee; Henderson, Kiersten A.; Keeney, Scott; Allis, C. David (2005): H2B (Ser10) phosphorylation is induced during apoptosis and meiosis in S. cerevisiae. In: *Cell Cycle* 4 (6), S. 780–783.

Alzheimer, A.; Stelzmann, R. A.; Schnitzlein, H. N.; Murtagh, F. R. (1995): An English translation of Alzheimer's 1907 paper, „Uber eine eigenartige Erkankung der Hirnrinde". In: *Clin Anat* 8 (6), S. 429–431.

Baehrecke, Eric H. (2002): How death shapes life during development. In: *Nat. Rev. Mol. Cell Biol* 3 (10), S. 779–787.

Bayer (2010): Intracellular accumulation of amyloid-beta – a predictor for synaptic dysfunction and neuron loss in Alzheimer's disease. In: *Fronti.Ag.Neurosci*.

Bharadwaj, Prashant; Martins, Ralph; Macreadie, Ian (2010): Yeast as a model for studying Alzheimer's disease. In: *FEMS Yeast Research* 10 (8), S. 961–969.

Bharadwaj, Prashant; Waddington, Lynne; Varghese, Jose; Macreadie, Ian G. (2008): A new method to measure cellular toxicity of non-fibrillar and fibrillar Alzheimer's Abeta using yeast. In: *J. Alzheimers Dis* 13 (2), S. 147–150.

Bitan, Gal; Kirkitadze, Marina D.; Lomakin, Aleksey; Vollers, Sabrina S.; Benedek, George B.; Teplow, David B. (2003): Amyloid beta –protein (Abeta) assembly: Abeta 40 and Abeta 42 oligomerize through distinct pathways. In: *Proc. Natl. Acad. Sci. U.S.A* 100 (1), S. 330–335.

Brenner, S. (1974): The genetics of Caenorhabditis elegans. In: *Genetics* 77 (1), S. 71–94.

Büttner, Sabrina; Eisenberg, Tobias; Herker, Eva; Carmona-Gutierrez, Didac; Kroemer, Guido; Madeo, Frank (2006): Why yeast cells can undergo apoptosis: death in times of peace, love, and war. In: *J. Cell Biol* 175 (4), S. 521–525.

Büttner, Sabrina; Ruli, Doris; Vögtle, F-Nora; Galluzzi, Lorenzo; Moitzi, Barbara; Eisenberg, Tobias et al. (2011): A yeast BH3-only protein mediates the mitochondrial pathway of apoptosis. In: *The EMBO Journal* 30 (14), S. 2779–2792.

Caine, Jo; Sankovich, Sonia; Antony, Helma; Waddington, Lynne; Macreadie, Peter; Varghese, Jose; Macreadie, Ian (2007): Alzheimer's AÎ² fused to green fluorescent protein induces growth stress and a heat shock response. In: *FEMS Yeast Research* 7 (8), S. 1230–1236.

Caine, Joanne M.; Bharadwaj, Prashant R.; Sankovich, Sonia E.; Ciccotosto, Giuseppe D.; Streltsov, Victor A.; Varghese, Jose (2011): Oligomerization and toxicity of Aβ fusion proteins. In: *Biochem. Biophys. Res. Commun* 409 (3), S. 477–482.

Caplan, Avrom J.; Cyr, Douglas M.; Douglas, Michael G. (1992): YDJ1p facilitates polypeptide translocation across different intracellular membranes by a conserved mechanism. In: *Cell* 71 (7), S. 1143–1155.

Carmona-Gutierrez, D.; Fröhlich, K-U; Kroemer, G.; Madeo, F. (2010): Metacaspases are caspases. Doubt no more. In: *Cell Death Differ* 17 (3), S. 377–378.

Carnini, Anna; Scott, Lucas O. M.; Ahrendt, Eva; Proft, Juliane; Winkfein, Robert J.; Kim, Sung-Woo et al. (2012): Cell Line Specific Modulation of Extracellular Aβ42 by Hsp40. In: *PloS ONE* 7 (5), S. e37755.

Chen, Sheng; Brown, Ian R. (2007): Neuronal expression of constitutive heat shock proteins: implications for neurodegenerative diseases. In: *Cell Stress Chaper* 12 (1), S. 51.

Clifford, Peter M.; Zarrabi, Shabnam; Siu, Gilbert; Kinsler, Kristin J.; Kosciuk, Mary C.; Venkataraman, Venkateswar et al. (2007): Abeta peptides can enter the brain through a defective blood-brain barrier and bind selectively to neurons. In: *Brain Res* 1142, S. 223–236.

Cohen, E.; Bieschke, J.; Perciavalle, R. M.; Kelly, J. W.; Dillin, A. (2006): Opposing Activities Protect Against Age-Onset Proteotoxicity. In: *Science* 313 (5793), S. 1604–1610.

D'Angelo, Fabien; Vignaud, Hélène; Di Martino, Julie; Salin, Bénédicte; Devin, Anne; Cullin, Christophe; Marchal, Christelle (2013): A yeast model for amyloid-β aggregation exemplifies the role of membrane trafficking and PICALM in cytotoxicity. In: *Dis Model Mech* 6 (1), S. 206–216.

Dekker, P. J.; Ryan, M. T.; Brix, J.; Müller, H.; Hönlinger, A.; Pfanner, N. (1998): Preprotein translocase of the outer mitochondrial membrane: molecular dissection and assembly of the general import pore complex. In: *Mol. Cell. Biol* 18 (11), S. 6515–6524.

Eisenberg, Tobias; Carmona-Gutierrez, Didac; Büttner, Sabrina; Tavernarakis, Nektarios; Madeo, Frank (2010): Necrosis in yeast. In: *Apoptosis* 15 (3), S. 257–268.

Ellis, H. M.; Horvitz, H. R. (1986): Genetic control of programmed cell death in the nematode C. elegans. In: *Cell* 44 (6), S. 817–829.

Evans, Christopher G.; Wisén, Susanne; Gestwicki, Jason E. (2006): Heat shock proteins 70 and 90 inhibit early stages of amyloid beta-(1-42) aggregation in vitro. In: *J. Biol. Chem* 281 (44), S. 33182–33191.

Fabrizio, Paola; Battistella, Luisa; Vardavas, Raffaello; Gattazzo, Cristina; Liou, Lee-Loung; Diaspro, Alberto et al. (2004): Superoxide is a mediator of an altruistic aging program in Saccharomyces cerevisiae. In: *J. Cell Biol* 166 (7), S. 1055–1067.

Fahrenkrog, Birthe; Sauder, Ursula; Aebi, Ueli (2004): The S. cerevisiae HtrA-like protein Nma111p is a nuclear serine protease that mediates yeast apoptosis. In: *J. Cell. Sci* 117 (Pt 1), S. 115–126.

Falsone, S. F.; Kungl, A. J.; Rek, A.; Cappai, R.; Zangger, K. (2009): The Molecular Chaperone Hsp90 Modulates Intermediate Steps of Amyloid Assembly of the Parkinson-related Protein -Synuclein. In: *Journal of Biological Chemistry* 284 (45), S. 31190–31199.

Fonte, Virginia; Kapulkin, Wadim Jan; Kapulkin, Vadim; Taft, Andrew; Fluet, Amy; Friedman, David; Link, Christopher D. (2002): Interaction of intracellular beta amyloid peptide with chaperone proteins. In: *Proc. Natl. Acad. Sci. U.S.A* 99 (14), S. 9439–9444.

Galluzzi, L.; Vitale, I.; Abrams, J. M.; Alnemri, E. S.; Baehrecke, E. H.; Blagosklonny, M. V. et al. (2011): Molecular definitions of cell death subroutines: recommendations of the Nomenclature Committee on Cell Death 2012. In: *Cell Death Differ* 19 (1), S. 107–120.

Galluzzi, Lorenzo; Vanden Berghe, Tom; Vanlangenakker, Nele; Buettner, Sabrina; Eisenberg, Tobias; Vandenabeele, Peter et al. (2011): Programmed necrosis from molecules to health and disease. In: *Int Rev Cell Mol Biol* 289, S. 1–35.

Giuffrida, M. L.; Caraci, F.; Pignataro, B.; Cataldo, S.; Bona, P. de; Bruno, V. et al. (2009): -Amyloid Monomers Are Neuroprotective. In: *Journal of Neuroscience* 29 (34), S. 10582–10587.

GLÜCKSMANN, A. (1951): CELL DEATHS IN NORMAL VERTEBRATE ONTOGENY. In: *Biological Reviews* 26 (1), S. 59–86.

Haass, Christian; Selkoe, Dennis J. (2007): Soluble protein oligomers in neurodegeneration: lessons from the Alzheimer's amyloid beta-peptide. In: *Nat. Rev. Mol. Cell Biol* 8 (2), S. 101–112.

Hansson Petersen, Camilla A.; Alikhani, Nyosha; Behbahani, Homira; Wiehager, Birgitta; Pavlov, Pavel F.; Alafuzoff, Irina et al. (2008): The amyloid beta-peptide is imported into mitochondria via the TOM import machinery and localized to mitochondrial cristae. In: *Proc. Natl. Acad. Sci. U.S.A* 105 (35), S. 13145–13150.

Hölttä, Mikko; Hansson, Oskar; Andreasson, Ulf; Hertze, Joakim; Minthon, Lennart; Nägga, Katarina et al. (2013): Evaluating Amyloid-β Oligomers in Cerebrospinal Fluid as a Biomarker for Alzheimer's Disease. In: *PloS ONE* 8 (6), S. e66381.

Hoshino, Tatsuya; Murao, Naoya; Namba, Takushi; Takehara, Masaya; Adachi, Hiroaki; Katsuno, Masahisa et al. (2011): Suppression of Alzheimer's disease-related phenotypes by expression of heat shock protein 70 in mice. In: *J. Neurosci* 31 (14), S. 5225–5234.

Hughes, S. R.; Goyal, S.; Sun, J. E.; Gonzalez-DeWhitt, P.; Fortes, M. A.; Riedel, N. G.; Sahasrabudhe, S. R. (1996): Two-hybrid system as a model to study the interaction of beta-amyloid peptide monomers. In: *Proc. Natl. Acad. Sci. U.S.A* 93 (5), S. 2065–2070.

Kerr, J. F.; Wyllie, A. H.; Currie, A. R. (1972): Apoptosis: a basic biological phenomenon with wide-ranging implications in tissue kinetics. In: *Br. J. Cancer* 26 (4), S. 239–257.

King, Michael; Nafar, Firoozeh; Clarke, Joseph; Mearow, Karen (2009): The small heat shock protein Hsp27 protects cortical neurons against the toxic effects of beta-amyloid peptide. In: *J. Neurosci. Res* 87 (14), S. 3161–3175.

Kirkitadze, Marina D.; Kowalska, Anna (2005): Molecular mechanisms initiating amyloid beta-fibril formation in Alzheimer's disease. In: *Acta Biochim. Pol* 52 (2), S. 417–423.

Kish, Stephen J.; Bergeron, Catherine; Rajput, Ali; Dozic, Slobodan; Mastrogiacomo, Frank; Chang, Li-Jan et al. (1992): Brain Cytochrome Oxidase in Alzheimer's Disease. In: *J Neurochem* 59 (2), S. 776–779.

Kroemer, G.; El-Deiry, W. S.; Golstein, P.; Peter, M. E.; Vaux, D.; Vandenabeele, P. Et al. (2005): Classification of cell death: recommendations of the Nomenclature Committee on Cell Death. In: *Cell Death Differ* 12, S. 1463–1467.

Kroemer, G.; Galluzzi, L.; Vandenabeele, P.; Abrams, J.; Alnemri, E. S.; Baehrecke, E. H. Et al. (2008): Classification of cell death: recommendations of the Nomenclature Committee on Cell Death 2009. In: *Cell Death Differ* 16 (1), S. 3–11.

Kumar, Sathish; Walter, Jochen (2011): Phosphorylation of amyloid beta (Aβ) peptides – a trigger for formation of toxic aggregates in Alzheimer's disease. In: *Aging (Albany NY)* 3 (8), S. 803–812.

LaFerla, Frank M.; Green, Kim N.; Oddo, Salvatore (2007): Intracellular amyloid-beta in Alzheimer's disease. In: *Nat. Rev. Neurosci* 8 (7), S. 499–509.

Lee, Il-Shin; Jung, Kwangsoo; Kim, Il-Sun; Park, Kook in (2013): Amyloid-β oligomers regulate the properties of human neural stem cells through GSK-3β signaling. In: *Exp Mol Med* 45 (11), S. e60.

Lewis, K. (2000): Programmed Death in Bacteria. In: *Microbiology and Molecular Biology Reviews* 64 (3), S. 503–514.

Lockshin, Richard A.; Zakeri, Zahra (2002): Caspase-independent cell deaths. In: *Current Opinion in Cell Biology* 14 (6), S. 727–733.

Longo, Valter D.; Shadel, Gerald S.; Kaeberlein, Matt; Kennedy, Brian (2012): Replicative and chronological aging in Saccharomyces cerevisiae. In: *Cell Metab* 16 (1), S. 18–31.

Ludovico, P.; Madeo, F.; Silva, Mt (2005): Yeast programmed cell death: an intricate puzzle. In: *IUBMB Life* 57 (3), S. 129–135.

Ludovico, P.; Sousa, M. J.; Silva, M. T.; Leão, C.; Côrte-Real, M. (2001): Saccharomyces cerevisiae commits to a programmed cell death process in response to acetic acid. In: *Microbiology (Reading, Engl.)* 147 (Pt 9), S. 2409–2415.

MacLean, M.; Harris, N.; Piper, P. W. (2001): Chronological lifespan of stationary phase yeast cells; a model for investigating the factors that might influence the ageing of postmitotic tissues in higher organisms. In: *Yeast* 18 (6), S. 499–509.

Madeo, F.; Fröhlich, E.; Fröhlich, K. U. (1997): A yeast mutant showing diagnostic markers of early and late apoptosis. In: *J. Cell Biol* 139 (3), S. 729–734.

Madeo, Frank; Engelhardt, Silvia; Herker, Eva; Lehmann, Nina; Maldener, Corinna; Proksch, Astrid et al. (2002): Apoptosis in yeast: a new model system with applications in cell biology and medicine. In: *Curr. Genet* 41 (4), S. 208–216.

Madeo, Frank; Herker, Eva; Maldener, Corinna; Wissing, Silke; Lächelt, Stephan; Herlan, Mark et al. (2002): A caspase-related protease regulates apoptosis in yeast. In: *Mol. Cell* 9 (4), S. 911–917.

Mager, Willem H.; Winderickx, Joris (2005): Yeast as a model for medical and medicinal research. In: *Trends in Pharmacological Sciences* 26 (5), S. 265–273.

Martin, S. J. (1995): Early redistribution of plasma membrane phosphatidylserine is a general feature of apoptosis regardless of the initiating stimulus: inhibition by overexpression of Bcl-2 and Abl. In: *Journal of Experimental Medicine* 182 (5), S. 1545–1556.

Masters, C. L.; Simms, G.; Weinman, N. A.; Multhaup, G.; McDonald, B. L.; Beyreuther, K. (1985): Amyloid plaque core protein in Alzheimer disease and Down syndrome. In: *Proc. Natl. Acad. Sci. U.S.A* 82 (12), S. 4245–4249.

Mehlen, P.; Bredesen, D. E. (2011): Dependence Receptors: From Basic Research to Drug Development. In: *Science Signaling* 4 (157), S. mr2.

Nardai, Gábor; Csermely, Péter; Söti, Csaba (2002): Chaperone function and chaperone overload in the aged. A preliminary analysis. In: *Exp. Gerontol* 37 (10-11), S. 1257–1262.

Newington, Jordan T.; Pitts, Andrea; Chien, Andrew; Arseneault, Robert; Schubert, David; Cumming, Robert C.; Okazawa, Hitoshi (2011): Amyloid Beta Resistance in Nerve Cell Lines Is Mediated by the Warburg Effect. In: *PloS ONE* 6 (4), S. e19191.

Oberhammer, F.; Wilson, J. W.; Dive, C.; Morris, I. D.; Hickman, J. A.; Wakeling, A. E. et al. (1993): Apoptotic death in epithelial cells: cleavage of DNA to 300 and/or 50 kb fragments prior to or in the absence of internucleosomal fragmentation. In: *EMBO J* 12 (9), S. 3679–3684.

Ojha, Juhi; Karmegam, Rajalakshmi V.; Masilamoni, J. Gunasingh; Terry, Alvin V.; Cashikar, Anil G.; Cotterill, Sue (2011): Behavioral Defects in Chaperone-Deficient Alzheimer's Disease Model Mice. In: *PloS ONE* 6 (2), S. e16550.

O'Nuallain, Brian; Freir, Darragh B.; Nicoll, Andrew J.; Risse, Emmanuel; Ferguson, Neil; Herron, Caroline E. et al. (2010): Amyloid beta-protein 116immers rapidly form stable synaptotoxic protofibrils. In: *J. Neurosci* 30 (43), S. 14411–14419.

Pagani, Lucia; Eckert, Anne (2011): Amyloid-Beta Interaction with Mitochondria. In: *International Journal of Alzheimer's Disease* 2011 (5), S. 1–12.

Parajuli, B.; Sonobe, Y.; Horiuchi, H.; Takeuchi, H.; Mizuno, T.; Suzumura, A. (2013): Oligomeric amyloid β induces IL-1β processing via production of ROS: implication in Alzheimer's disease. In: *Cell Death Dis* 4 (12), S. e975.

Park, Sei-Kyoung; Pegan, Scott D.; Mesecar, Andrew D.; Jungbauer, Lisa M.; LaDu, Mary Jo; Liebman, Susan W. (2011): Development and validation of a yeast high-throughput screen for inhibitors of $A\beta_{42}$ oligomerization. In: *Dis Model Mech* 4 (6), S. 822–831.

Pennell, R. I.; Lamb, C. (1997): Programmed Cell Death in Plants. In: *Plant Cell* 9 (7), S. 1157–1168.

Perez, N.; Sugar, J.; Charya, S.; Johnson, G.; Merril, C.; Bierer, L. et al. (1991): Increased synthesis and accumulation of heat shock 70 proteins in Alzheimer's disease. In: *Molecular Brain Research* 11 (3-4), S. 249–254.

Pimentel, Catarina; Batista-Nascimento, Liliana; Rodrigues-Pousada, Claudina; Menezes, Regina A. (2012): Oxidative Stress in Alzheimer's and Parkinson's Diseases: Insights from the Yeast Saccharomyces cerevisiae. In: *Oxidative Medicine and Cellular Longevity* 2012 (31), S. 1–9.

Piper, Peter W. (2006): Long-lived yeast as a model for ageing research. In: *Yeast* 23 (3), S. 215–226.

Porzoor, Afsaneh; Macreadie, Ian G. (2013): Application of yeast to study the tau and amyloid-β abnormalities of Alzheimer's disease. In: *J. Alzheimers Dis* 35 (2), S. 217–225.

Prasansuklab, Anchalee; Tencomnao, Tewin (2013): Amyloidosis in Alzheimer's Disease: The Toxicity of Amyloid Beta (A β), Mechanisms of Its Accumulation and Implications of Medicinal Plants for Therapy. In: *Evid Based Complement Alternat Med* 2013, S. 413808.

Reddy, P. Hemachandra (2009): Amyloid beta, mitochondrial structural and functional dynamics in Alzheimer's disease. In: *Exp. Neurol* 218 (2), S. 286–292.

Ridge, Perry G.; Ebbert, Mark T. W.; Kauwe, John S. K. (2013): Genetics of Alzheimer's disease. In: *Biomed Res Int* 2013, S. 254954.

Ring, Julia; Sommer, Cornelia; Carmona-Gutierrez, Didac; Ruckenstuhl, Christoph; Eisenberg, Tobias; Madeo, Frank (2012): The metabolism beyond programmed cell death in yeast. In: *Exp. Cell Res* 318 (11), S. 1193–1200.

Saido, Takaomi C. (2013): Metabolism of amyloid β peptide and pathogenesis of Alzheimer's disease. In: *Proc. Jpn. Acad., Ser. B, Phys. Biol. Sci* 89 (7), S. 321–339.

Sakono, Masafumi; Zako, Tamotsu (2010): Amyloid oligomers: formation and toxicity of Abeta oligomers. In: *FEBS J* 277 (6), S. 1348–1358.

Sakono, Masafumi; Zako, Tamotsu; Ueda, Hiroshi; Yohda, Masafumi; Maeda, Mizuo (2008): Formation of highly toxic soluble amyloid beta oligomers by the molecular chaperone prefoldin. In: *FEBS Journal* 275 (23), S. 5982–5993.

Satyal, S. H.; Schmidt, E.; Kitagawa, K.; Sondheimer, N.; Lindquist, S.; Kramer, J. M.; Morimoto, R. I. (2000): Polyglutamine aggregates alter protein folding homeostasis in Caenorhabditis elegans. In: *Proc. Natl. Acad. Sci. U.S.A* 97 (11), S. 5750–5755.

Scaffidi, Paola; Misteli, Tom; Bianchi, Marco E. (2002): Release of chromatin protein HMGB1 by necrotic cells triggers inflammation. In: *Nature* 418 (6894), S. 191–195.

Schweichel, J.-U; Merker, H.-J (1973): The morphology of various types of cell death in prenatal tissues. In: *Teratology* 7 (3), S. 253–266.

Severin, F. F.; Hyman, A. A. (2002): Pheromone induces programmed cell death in S. cerevisiae. In: *Curr. Biol* 12 (7), S. R233-5.

Shirwany, Najeeb A.; Payette, Daniel; Xie, Jun; Guo, Qing (2007): The amyloid beta ion channel hypothesis of Alzheimer's disease. In: *Neuropsychiatr Dis Treat* 3 (5), S. 597–612.

Sörgjerd, Karin Margareta; Zako, Tamotsu; Sakono, Masafumi; Stirling, Peter C.; Leroux, Michel R.; Saito, Takashi et al. (2013): Human Prefoldin Inhibits Amyloid-β (Aβ) Fibrillation and Contributes to Formation of Nontoxic Aβ Aggregates. In: *Biochemistry* 52 (20), S. 3532–3542.

Sulston, J.E; Horvitz, H.R (1977): Post-embryonic cell lineages of the nematode, Caenorhabditis elegans. In: *Developmental Biology* 56 (1), S. 110–156.

Syntichaki, Popi; Tavernarakis, Nektarios (2003): The biochemistry of neuronal necrosis: rogue biology? In: *Nat. Rev. Neurosci* 4 (8), S. 672–684.

Syntichaki, Popi; Xu, Keli; Driscoll, Monica; Tavernarakis, Nektarios (2002): Specific aspartyl and calpain proteases are required for neurodegeneration in C. elegans. In: *Nature* 419 (6910), S. 939–944.

Takata, Kazuyuki; Kitamura, Yoshihisa; Tsuchiya, Daiju; Kawasaki, Toshiyuki; Taniguchi, Takashi; Shimohama, Shun (2003): Heat shock protein-90-induced microglial clearance of exogenous amyloid-β1–42 in rat hippocampus in vivo. In: *Neuroscience Letters* 344 (2), S. 87–90.

Takashima, Akihiko; Honda, Toshiyuki; Yasutake, Kaori; Michel, Gilles; Murayama, Ohosi; Murayama, Miyuki et al. (1998): Activation of tau protein kinase I/glycogen synthase kinase-3β by amyloid β peptide (25–35) enhances phosphorylation of tau in hippocampal neurons. In: *Neuroscience Research* 31 (4), S. 317–323.

Treusch, S.; Hamamichi, S.; Goodman, J. L.; Matlack, K. E. S.; Chung, C. Y.; Baru, V. et al. (2011): Functional Links Between A Toxicity, Endocytic Trafficking, and Alzheimer's Disease Risk Factors in Yeast. In: *Science* 334 (6060), S. 1241–1245.

Uren, A. G.; O'Rourke, K.; Aravind, L. A.; Pisabarro, M. T.; Seshagiri, S.; Koonin, E. V.; Dixit, V. M. (2000): Identification of paracaspases and metacaspases: two ancient families of caspase-like proteins, one of which plays a key role in MALT lymphoma. In: *Mol. Cell* 6 (4), S. 961–967.

Verghese, Jacob; Abrams, Jennifer; Wang, Yanyu; Morano, Kevin A. (2012): Biology of the heat shock response and protein chaperones: budding yeast (Saccharomyces cerevisiae) as a model system. In: *Microbiol. Mol. Biol. Rev* 76 (2), S. 115–158.

Vishnevskaya, A. B.; Kushnirov, V. V.; Ter-Avanesyan, M. D. (2007): Neurodegenerative amyloidoses: Yeast model. In: *Mol Biol* 41 (2), S. 308–315.

Walker, N. I.; Harmon, B. V.; Gobé, G. C.; Kerr, J. F. (1988): Patterns of cell death. In: *Methods Achiev Exp Pathol* 13, S. 18–54.

Walsh, Dominic M.; Klyubin, Igor; Fadeeva, Julia V.; Cullen, William K.; Anwyl, Roger; Wolfe, Michael S. et al. (2002): Naturally secreted oligomers of amyloid beta protein potently inhibit hippocampal long-term potentiation in vivo. In: *Nature* 416 (6880), S. 535–539.

Willingham, S. (2003): Yeast Genes That Enhance the Toxicity of a Mutant Huntingtin Fragment or -Synuclein. In: *Science* 302 (5651), S. 1769–1772.

Winderickx, Joris; Delay, Charlotte; Vos, Ann de; Klinger, Harald; Pellens, Klaartje; Vanhelmont, Thomas et al. (2008): Protein folding diseases and neurodegeneration: Lessons learned from yeast. In: *Biochimica et Biophysica Acta (BBA) – Molecular Cell Research* 1783 (7), S. 1381–1395.

Wloch-Salamon, D. M.; Bem, A. E. (2013): Types of cell death and methods of their detection in yeast Saccharomyces cerevisiae. In: *J. Appl. Microbiol* 114 (2), S. 287–298.

Woodle, E. S.; Kulkarni, S. (1998): Programmed cell death. In: *Transplantation* 66 (6), S. 681–691.

Wu, Yunkun; Sha, Bingdong (2006): Crystal structure of yeast mitochondrial outer membrane translocon member Tom70p. In: *Nat. Struct. Mol. Biol* 13 (7), S. 589–593.

Yang, H. W.; Hwang, K. J.; Kwon, H. C.; Kim, H. S.; Choi, K. W.; Oh, K. S. (1998): Detection of reactive oxygen species (ROS) and apoptosis in human fragmented embryos. In: *Hum. Reprod* 13 (4), S. 998–1002.

Yip, C. M.; McLaurin, J. (2001): Amyloid-beta peptide assembly: a critical step in fibrillogenesis and membrane disruption. In: *Biophys. J* 80 (3), S. 1359–1371.

Zahs, Kathleen R.; Ashe, Karen H. (2013): β-Amyloid oligomers in aging and Alzheimer's disease. In: *Front Aging Neurosci* 5, S. 28.

Zhang, W.; Espinoza, D.; Hines, V.; Innis, M.; Mehta, P.; Miller, D. L. (1997): Characterization of beta-amyloid peptide precursor processing by the yeast Yap3 and Mkc7 proteases. In: *Biochim. Biophys. Acta* 1359 (2), S. 110–122.

Zhang, Yun-wu; Thompson, Robert; Zhang, Han; Xu, Huaxi (2011): APP processing in Alzheimer's disease. In: *Mol Brain* 4, S. 3.

Abbreviations

Aβ	Amyloid-β peptides
AD	Alzheimer's disease
APP	Amyloid precursor protein
ATP	Adenosine triphosphate
BBB	Blood-brain-barrier
DHE	Dihydroethidium
DNA	Desoxyribonucleic acid
DTT	Dithiothreitol
E. coli	*Escherichia coli*
Early-onset AD	EOAD
ev	Empty vector
ER	Endoplasmic reticulum
FACS	Fluorescence activating cell sorting
FITC	Fluorescein isothiocyanate
EGFP	Enhanced Green fluorescence protein
HCl	Hydroclorid acid
HIS	Histidine
HSR	Heat shock response
LB	Luria Bertani
LiAc	Lithiumacetat
mA	Miliamper
mM	Milimolar
ml	Mililiter
µl	Microliter
µg	Microgram
MA	Morbus Alzheimer

MOMP	Mitochondrial outer membrane permeabilization
NaCl	Sodium chloride
NaOH	Sodium hydroxid
ND	Neurodegeneration disease
NCCD	Nomenclature Committee on Cell Death
OD_{600}	Extinction at 600nm
ONC	Overnight culure
P100	Microsome and ER fraction
P13	Mitochondrial fraction
PBS	Phosphate buffered saline
PCD	Programmed cell death
PCR	Polymerase chain reaction
PDVF	Polyvinylidendifluorid
PEG	Polyethylen glycol
PI	Propidiumiodid
PMSF	phenylmethylsulfonyl fluoride
PNS	Post nuclear supernatant
ROS	Reactive oxygen species
RT	Room temperature
rpm	Rotations per minutes
S100	Cytosol fraction
S. cerevisiae	Saccharomyces cerevisiae
SDS	Sodium dodecyl sulfate
SMD	Synthetic medium with glucose
SMG	Synthetic medium with galactose
TAE	Tris acetate EDTA buffer
TE	Tris EDTA buffer
URA	Uracil
WCE	Whole yeast extract
WT	Wild type
YPD	Yeast Peptone Dextrose